OXYGENATION FOR FISH FARMS

THESIS

Submitted for the degree of

Doctor of Philosophy

to

The University of Aston in Birmingham

by

BARRY JAMES SOWERBUTTS

November 1981

OXYGENATION FOR FISH FARMS

BARRY JAMES SOWERBUTTS PhD 1981

This thesis provides a detailed study of methods for dissolving oxygen in water to reduce water requirements for fish farming. The principal sources of oxygen are air or pure oxygen gas. Aeration methods have the distinct advantage of the universal availability of air. However, the effectiveness of such methods is diminished by the presence of nitrogen in the air and, in general, the maintenance of dissolved oxygen levels above 70% saturation is likely to result in excessive power requirements. Pure oxygen has five times the solubility of oxygen in air and it is possible, therefore to achieve much higher transfer rates. However, oxygen is expensive and its economic use is essential: it is important, therefore, to dissolve a high proportion of the oxygen.

Four distinct oxygenation systems were evaluated by the author. A detailed analysis of a column oxygenator is given first. The column was designed so that the oxygen bubbles generated are trapped within the column until dissolved. In seawater, much smaller bubbles are formed and this led to the development of a jet oxygenator which disperses gas bubbles within the rearing tank. Both the above systems were designed primarily for oxygenating recycled tank water. For oxygenating a primary water source, a U-tube device was evaluated. Lastly, the possibility of supporting fish stocks without any external power source, other than a pressured supply of oxygen from a liquid oxygen store, was considered.

Experience of running commercial-scale oxygenation systems in high-intensity fish farms has made it possible to estimate operating costs of both aeration and oxygenation systems. The significance of these costs is discussed.

Keywords: fish farming oxygenation aeration costs

i PREFACE

Preface

Oxygenation can significantly reduce the water requirements necessary for fish farming and the development of such water-saving techniques is an important contribution to the development of the industry. In 1974 Shearwater Fish Farming Ltd., then part of the B.O.C.I. Group, constructed a farm in Cumbria which was designed to investigate intensive fish farming on a commercial scale. A fundamental part of the programme was to reduce water requirements to a minimum and this was achieved by using pure oxygen gas to artificially replenish the oxygen consumed by the fish. However, following previous postgraduate research undertaken by Harman (1978), it was concluded that the oxygenation equipment in use up to 1977 was in need of major re-design. At the same time, a new marine farm was being completed in S.W. Scotland which would also require oxygenation technology. It was the need to develop efficient oxygenation equipment for these two farms which led to the initiation of the author's project. However, apart from the specific requirements of the farms in Cumbria and Scotland, it was also recognized that there was considerable potential in the fish farm industry generally for using oxygenation methods.

The Total Technology (T. T.) Scheme at the University of Aston in Birmingham encourages a multidisciplinary approach to the solution of problems with an engineering bias through post-graduate study. The T. T. Scheme was seen as an ideal system for initiating research into the problem. A T. T. project is set up on the basis of collaboration between a commercial sponsor, in this case Shearwater Fish Farming Ltd., and the University. Shearwater Fish Farming Ltd. provided the facilities for practical investigation, including the use of production rearing tanks, and necessary technical assistance and training was provided by the University. The supervisory team consisted of Dr E. L. Smith (Main Supervisor), Dr J.R.M Forster (Industrial Supervisor) and Dr N. Bromage (Associate Supervisor), and the project was coordinated by Dr D. J van Rest (Tutor). Financial support was provided jointly by the Science Research Council and Shearwater Fish Farming Ltd.

In Chapter 1 of this thesis, water-use in fish farming is considered and the potential for reoxygenation is discussed. Chapter 2 focuses on the use of air as a source of oxygen and the application of aeration methods in fish farming, whereas Chapter 3 describes some of the basic design requirements for the efficient use of pure oxygen gas and the application of oxygenation methods.

The next four chapters describe the various types of oxygenation equipment studied by the author. Chapter 4 is a detailed evaluation of the column oxygenator, designed to support stocks at the Low Plains site. In Chapter 5, the development of a jet oxygenator for supporting fish stocks at the Finnarts Bay site is described. Work with a U-tube system is covered in Chapter 6, and this is followed in Chapter 7 by an assessment of the possibility of achieving efficient oxygen dissolution using the energy created as pressure from the liquid oxygen store.

Chapter 8 provides some estimates of operating costs of oxygenation systems and these are compared with those for aeration systems.

Finally Chapter 9 contains the general conclusions and summary.

SUMMARY

PREFACE

TABLES AND FIGURES

CHAPTER 1

TECHNICAL BACKGROUND

1.1 Introduction

A fundamental requirement for fish farming is the maintenance of an adequate supply of dissolved oxygen which fish require for respiration. Many farm systems have been devised to meet the fishes' requirements which utilise the oxygen dissolved in natural waters. However, the quantities of dissolved oxygen which occur naturally are very small and large volumes of water are therefore required for fish farming. This represents a major constraint to the development of the industry.

Water requirements can be considerably reduced by artificially replenishing the oxygen which the fish take out. The process is called reoxygenation and the source of oxygen can be air, pure oxygen gas or a mixture of the two.

1.2 Fish Farm Systems

1.2.1 Species Reared

Rainbow trout (*Salmo gairdneri*) are the most common finfish grown in freshwater farms in the U.K. although some carp (*Cyprinus sp.*) and eels (*Anguilla anguilla*) are also reared. Abroad, catfish (*Ictalurus punctatus*) are produced in the U.S.A., while tilapia (*Tilapia sp.*) are reared in the Middle and Far East.

In marine farming, interest is growing in a variety of species including turbot (Scophthalmus maximus), sole (Solea solea), bream (Sparus aurata) and bass (Dicentrarchus labrax).

Species such as Atlantic salmon (Salmo salar) require mixed salinities; eggs are hatched in freshwater and the larger fry are slowly acclimated to seawater.

1.2.2 Water Use in Fish Farming

The primary requirement of all fish farming methods is the need to ensure sufficient water exchange to meet the fishes' oxygen requirements. A secondary function of the water exchange is to remove the waste products of metabolism (Fig. 1.2.1).

In most land-based farms water flows from the source through various types of enclosure such as ponds, tanks or raceways and then to waste (Fig. 1.2.2). This approach is often referred to as a "once-through" system. An alternative approach is to locate fish cages or net pens in open water where there is sufficient natural water exchange to meet the fishes' requirements.

1.3 Factors Affecting the Fish Farm System

1.3.1 Oxygen Requirements

Most species of fish can survive in dissolved oxygen levels of less than 3 ppm. However, under fish farming

Fig. 1.2.1 Exchange of Soluble and Solid Products

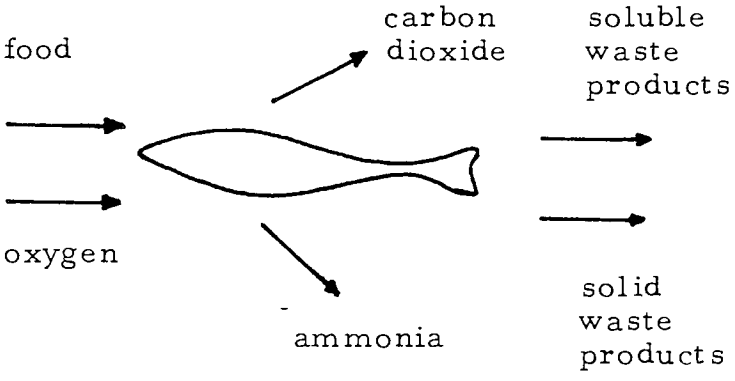

Fig. 1.2.2 Typical Farm Systems

Pond System

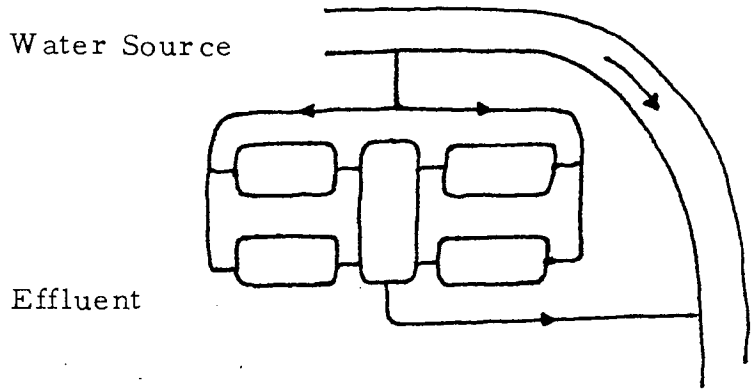

Tank System

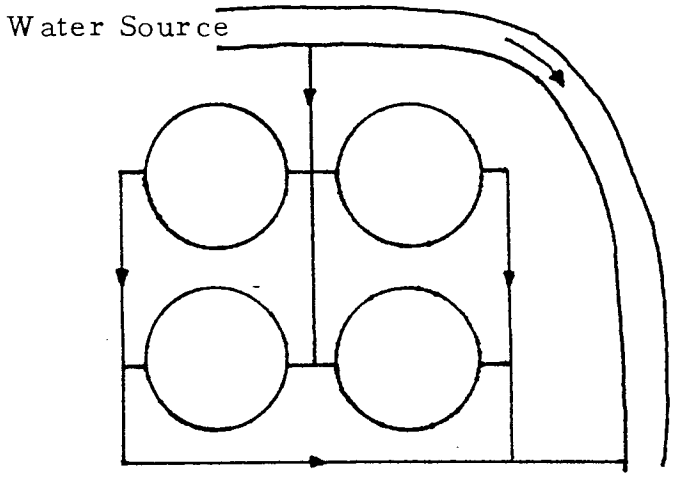

Raceway System

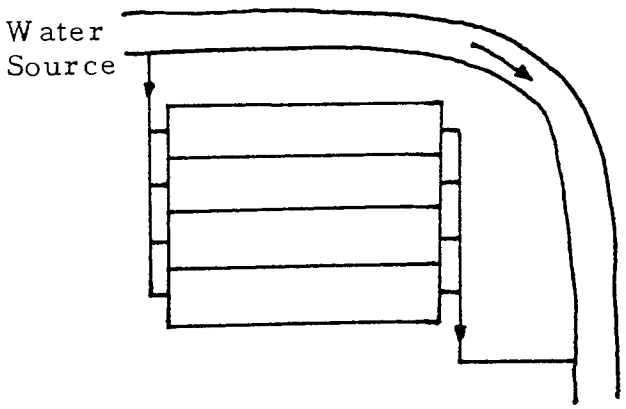

conditions where conversion and mortality rate are important factors, higher levels are generally maintained (Jones, 1964). Minimum dissolved oxygen levels of 5 ppm are recommended for salmonids, for example (Larmoyeux and Piper, 1973; Warren et al, 1973). At oxygen levels above these minima the fish can use food for both energy production and growth.

Oxygen consumption varies with temperature and for trout, oxygen requirements at 20° C are three times greater than at 5° C (Liao, 1971). Requirements also vary diurnally, with peaks at dawn, dusk and during feeding. Overnight oxygen consumption is relatively low (Harman, 1978).

1.3.2 Water Requirements

Oxygen is relatively insoluble and air contains only 21% oxygen so natural air-saturated waters contain little oxygen. In addition the dissolved oxygen level in the water is influenced by several factors. Firstly, the saturation concentration falls as the temperature increases, for example, from 12.8 ppm dO_2 at 5° C to 9.2 ppm dO_2 at 20° C. Secondly, dissolved oxygen concentrations are reduced if there are impurities in the water and typical values in seawater are 10 ppm dO_2 at 5° C and 7.4 ppm dO_2 at 20° C. Thirdly, pressure affects oxygen solubility and saturation concentrations are lower by about 15% at an

altitude of 1500 m (APHA, 1971).

An example of the effects of temperature on the water requirements for fish farming due to the changes in fish oxygen consumption and oxygen solubility is given in Table 1.3.1 which shows the oxygen consumption of rainbow trout at different water temperatures and estimates of the volumes of water required to support one tonne of fish assuming a minimum dissolved oxygen concentration in the discharge water of 5 ppm dO_2.

TABLE 1.3.1 The Effect of Temperature on Oxygen Consumption and Water Requirements for Rainbow Trout (200 gms av. wt.) (Forster and Smart, 1979)

The volumes are very large and yet are likely to be underestimates because:

(1) No account has been taken of diurnal variations in fish oxygen requirements. Variations in oxygen demand cause changes in the dissolved oxygen level. Maintaining levels at 5 ppm during peaks will lead to increased water requirements.

(2) It has been assumed that the incoming water is saturated. In many waters dissolved oxygen levels may fall well below saturation overnight when aquatic plant respiration continues but photosynthesis ceases (Mitchell and Kirby, 1976). Larger water volumes may be necessary if such variations are to be tolerated.

(3) It has also been assumed that the incoming water is freshwater at sea-level. The reduction in oxygen solubility with salinity or altitude necessitates even greater volumes of water.

Periods of temporary overstocking or exceptionally high temperatures will add further to water requirements. In addition, it is necessary to keep the fish at the minimum dissolved oxygen level they will tolerate to make optimum use of the water supply. For the fish this means that when water temperatures are highest and their growth rate is fastest there is least oxygen available to them in the water.

1.3.3 The Limitations of the Water Supply

The principal problem is that there are very few sites available where sufficient freshwater can be supplied under a natural head for the establishment of a very large fish farm. Cage farming practices combine the requirements of the necessary water exchange with the need to be sheltered and have reasonable access and are at a premium. Pumping can often provide access to larger volumes of freshwater and for any land-based marine operation pumping is nearly always essential. However, even where pumping is possible the large quantities of water necessary for fish farming can significantly increase production costs.

1.4 Potential for Reoxygenation

1.4.1 Aeration and Oxygenation: Some Definitions

There is, therefore, considerable incentive to try to reduce water requirements and this can be done by artificially replenishing the oxygen in the water which the fish take out. The oxygen may be supplied in one of three ways, namely as air, pure oxygen gas or as a mixture of the two, commonly referred to as oxygen enriched air. When air is used, the process is called aeration; when oxygen or oxygen-enriched air is used the term oxygenation is employed.

1.4.2 Reoxygenation for Improved Water Use

Both processes can be and are used at various levels of intensity. At the lowest level they are used during brief periods of oxygen shortage, such as may be caused by night-time oxygen depletion due to plant respiration, exceptionally high temperatures or temporary over-stocking. At the highest level the vast majority of the fishes' oxygen requirements are met artificially and the principle role of water exchange is then to remove waste products of metabolism. This can lead to increased levels of carbon dioxide, ammonia, suspended solids and other waste products in the rearing tanks. Unfortunately, most of these waste products are not easily removed without the use of expensive waste-water treatment plants although excess suspended solids may be removed despite low water flows by using self-cleaning tanks. Critical levels of these waste products limit the degree of water economy which can be achieved, therefore.

1.4.3 Reoxygenation to Raise Dissolved Oxygen Levels

Aeration and oxygenation may also be used to maintain higher dissolved oxygen concentrations in rearing enclosures than would otherwise be possible under natural conditions. This might be particularly important during periods of high temperatures or at times of intensive

feeding. In some circumstances using oxygenation methods, it is even possible to maintain dissolved oxygen levels above the equilibrium concentration for air-saturated waters, that is at supersaturated levels. There are reports claiming improved growth rates of trout when dissolved oxygen levels of up to 250% of air saturation are maintained but the possible advantages of such methods are unclear (Shabi and Hibberd, 1977; Sowerbutts and Forster, 1980).

1.5 Secondary Requirements

1.5.1 Bulk Mixing of Reoxygenated Water

Reoxygenation diminishes the role of the water source as a carrier of oxygen. Part of the requirement of any aeration or oxygenation process is, therefore, to distribute the artificially replenished water evenly throughout the rearing enclosure. Several considerations prevent the use of bulk agitation, which is a method used in other industries to provide liquid mixing (Uhl, 1966). Firstly, large-scale agitation would tend to disturb the gentle flow patterns required in tanks and raceways for self-cleaning or might stir up a pond bottom, many of which are unlined. Secondly, high levels of mechanical agitation might stress the fish or cause physical damage to them. Thirdly, high water velocities might cause excessive fish activity,

thereby reducing the growth rate and food conversion efficiency (Brett, 1970). The mixing ability of aerators and oxygenators is therefore an important consideration in equipment specification.

1.5.2 Other Dissolved Gases

So far, the discussion has been concerned with the dissolved oxygen requirements for fish farming. However, other gases may be present in natural waters or increase as a result of fish production, namely nitrogen, carbon dioxide and ammonia. Nitrogen supersaturation can occur in water sources where temperature or pressure conditions have changed rapidly, such as in geothermal or power station cooling waters (Aston, 1980). This may lead to gas bubble disease in fish (Rucher, 1972). Carbon dioxide can occur in some groundwater sources and will increase in a fish farm due to fish respiration (Reid, 1961; Forster and Smart, 1979). High levels of carbon dioxide may also be harmful to fish and can lead to a condition known as nephrocalcinosis in rainbow trout, for example (Smart et al 1978). Ammonia is also excreted by the fish as a waste product of metabilism and its toxic effects are well known (Smart, 1975).

The presence or absence of these gases and their effects on the fish can have important implications for the choice of reoxygenation equipment for fish farming.

1.5.3 Stand-by Facilities and Reliability of Equipment

All land-based farms are liable to drastic stock losses in the event of water failure. In farms supplied with water under a natural head the risks of such failure are slight but nevertheless exist due to a variety of hazards which may obstruct or pollute water channels. Farms which rely on pumped water incur the additional risk of pump failure and, if electrically driven, of power failure. In the evaluation of methods, consideration will be given to the facilities available for back-up in the event of water failure.

On the other hand, where aeration or oxygenation are used to economise on water use the supply of oxygen is then as dependent on these processes as it is on the water source in a once-through system. It is therefore self-evident that equipment must be reliable despite continuous use. In view of the location of many fish farms consideration must also be given to maintenance procedures and to the availability of spare parts.

1.6 Costs

There are therefore many requirements which may influence the choice of reoxygenation system and the costs of reoxygenation. In deciding which of the various methods to use it is most important to give detailed consideration to such factors as:

(1) Fish species

(2) Farm location

(3) Local costs of power and oxygen

(4) Nature of the farm water supply

(5) Existing farm layout and production facilities

(6) Level of management and technical competence

(7) Availability of stand-by services

(8) Future production objectives

In short a reoxygenation system should be tailored to the specific needs and dictates of the farm to achieve full cost-effectiveness.

1.7 Mass Transfer of Oxygen from the Gas into Water

1.7.1 Solubility and Saturation: Some Definitions

In order to appreciate the operation of aerators and oxygenators, it is necessary to consider the physico-chemical process involved in oxygen dissolution. One important aspect is the solubility or the equilibrium concentration of oxygen in water. This is the maximum concentration of oxygen which can be dissolved in the water relative to the concentration of oxygen in the gas under the prevailing conditions of temperature and pressure. When this concentration is reached, the oxygen in the gas and the dissolved oxygen in the water are in equilibrium and the water is saturated under the conditions.

If the gas is air at atmospheric pressure, then the water is saturated with respect to air. Air saturation is often used as a reference level for measuring dissolved oxygen concentrations. Levels above the equilibrium value with air are defined as supersaturated and those below are referred to as a percentage of saturation.

1.7.2 The Mass Transfer Equation

If the conditions of equilibrium are changed oxygen will be transported from one phase to the other by a process called mass transfer. The so-called "Two Film" theory to describe this mass transfer process was first developed by Lewis and Whitman (1924) and later adapted and revised by Ippen et al (1952) for oxygen absorption in water (Mavanic and Bewtra, 1974). According to this theory mass transfer is governed by the following equation (Fig. 1.7.1):

Fig. 1.7.1 Mass Transfer across the Interface

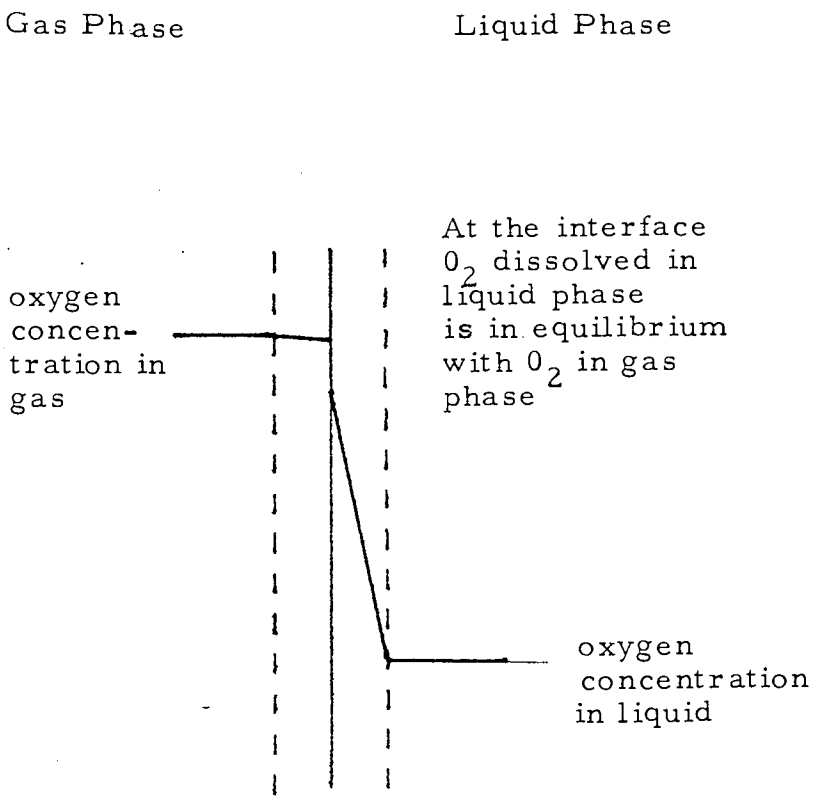

The main resistance to transfer is within the liquid "film" close to the interface

$$\varphi = k_L A (Co_2^* - Co_2)$$

The rate of mass transfer, φ,

$$= k_L A (Co_2^* - Co_2) \qquad (1.7.1)$$

where k_L is the liquid-film mass transfer coefficient,

A is the area of the gas liquid interface,

Co_2^* is the equilibrium oxygen concentration, and Co_2 is the dissolved oxygen concentration of the reoxygenated water. The oxygen gradient $(Co_2^* - Co_2)$ is often referred to as the driving force for transfer.

For a well-mixed flow system under steady-state conditions the overall mass-transfer rate can be related to the expression (Fig. 1.7.2):

$$Q_L (Co_2 - Co_{2,T}) \qquad (1.7.2)$$

where Q_L is the flow-rate of the reoxygenated water

and $Co_{2,T}$ is the dissolved oxygen concentration before reoxygenation.

Co_2^* in equation 1.7.1 is related to the partial pressure of oxygen in the gas phase by Henry's Law:

$$p = H\, Co_2^* \qquad (1.7.3)$$

where p is the partial pressure of oxygen and H is the Henry's Law constant. H depends on temperature and the presence of salts.

Fig. 1.7.2 Oxygen Balance in a Well-mixed System

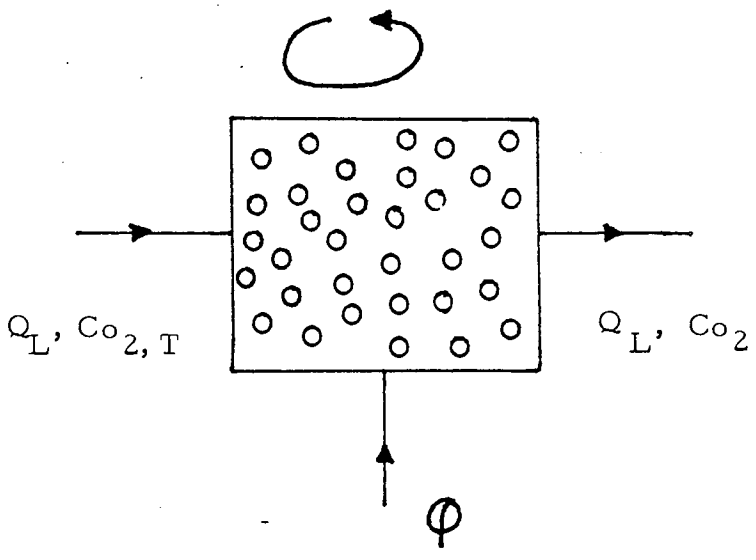

$$\varphi = Q_L \ (Co_2 - Co_{2,T})$$

$$\varphi = k_L A \ (Co_2^* - Co_2)$$

The term (k_L A) also depends on the physical properties of the water, such as density, viscosity and surface tension; gas density and diffusivity in the water are important as well. It should be noted that temperature has an effect on all the physical properties mentioned. (k_L A) also depends on the design and operating characteristics of the mass-transfer device.

p depends on the concentration of oxygen in the gas and the total system pressure. The latter operating parameter is usually fixed by the choice of reoxygenation system as is Q_L, the water flow-rate.

Finally, the dissolved oxygen concentration, $Co_{2,T}$ is pre-determined by the fish farm conditions, as are the temperature and the physical properties of the water.

From this discussion, it may be concluded that the only independent variables affecting mass transfer are the operating characteristics of the device and the concentration of oxygen in the gas.

Similar equations also apply for nitrogen and carbon dioxide and therefore mass-transfer processes may be used for gas desorption while simultaneously dissolving oxygen. However, because carbon dioxide is highly soluble it only exerts a low partial pressure in the gas phase and so it is difficult to strip from solution. By

contrast, nitrogen has a low solubility and will transfer until relatively high partial pressures are reached in the gas phase.

1.7.3 The Gas-Liquid Interface

All mass transfer devices exchange gas through the gas-liquid interface, A. There are three main types of interface created by mass transfer devices:

(1) gas dispersed in water - usually in the form of bubbles,

(2) water dispersed in the gas - usually as droplets or a spray,

(3) foam - can occur at an agitated gas - liquid surface.

Most mass transfer devices depend on a combination of these processes. For example in a waterfall, water falling through the air creates droplets in the gas phase, it forms a foam layer at the interface and it entrains bubbles into the water (Fig. 1.7.3). It should be noted that in the case of many proprietary devices there is one predominant process.

Mass transfer will also occur across a plane surface, for example the surface of a pond. However, unless the surface is agitated or very extensive the rate of transfer will be small compared with that of the mass-transfer device (Downing and Truesdale, 1955).

Fig. 1.7.3 The Waterfall: Gas - Liquid Interfaces

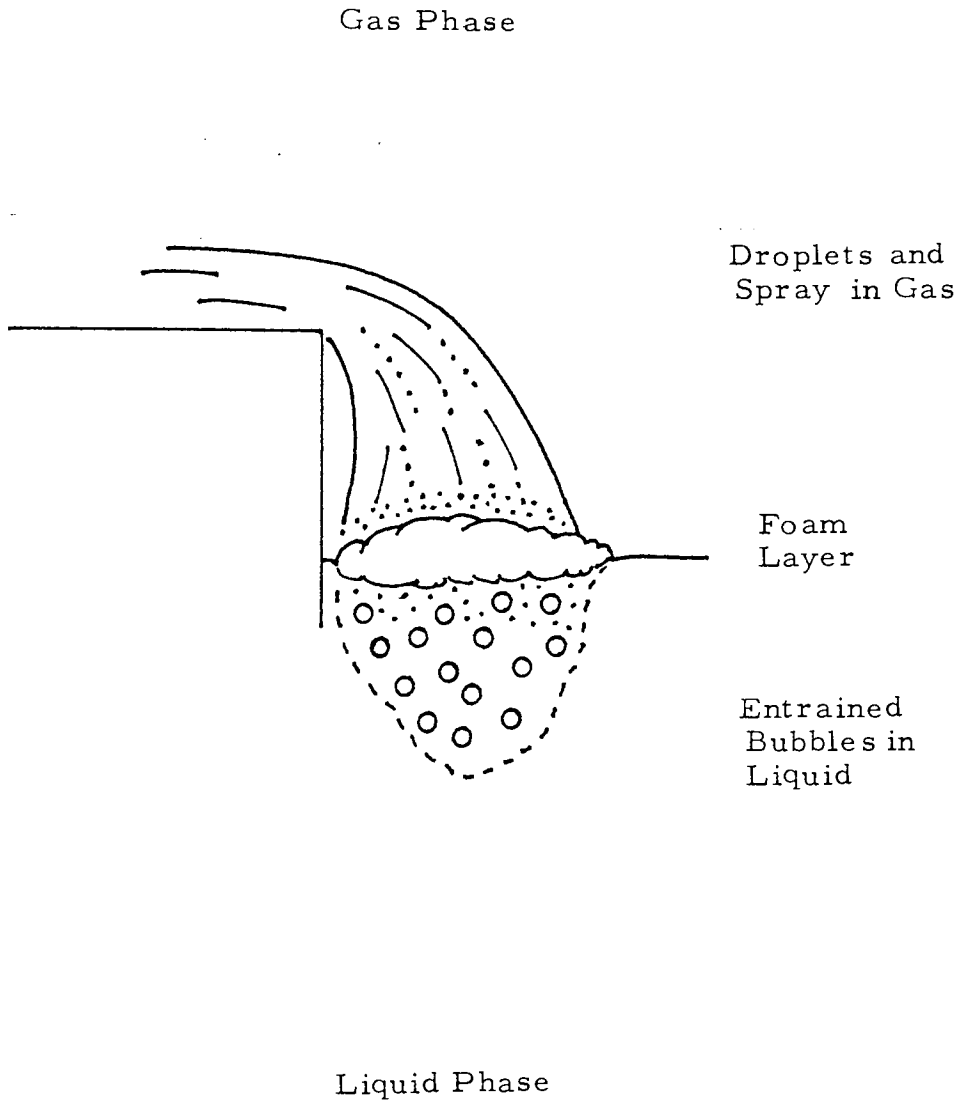

1.8 Bubble Sizes and Dissolution Times

1.8.1 Bubble Sizes

For many mass-transfer devices the interfacial area is created by generating bubbles in the water. A greater understanding of the operation of these systems is possible with a knowledge of bubble size, bubble dissolution time and bubble rise velocity. From the bubble size and the contact time the dissolution efficiency can be estimated. For design purposes, high dissolution efficiencies can be obtained if the gas-liquid contact time can be made comparable to the time required to completely dissolve the bubble, that is the bubble dissolution time. This is a particularly important consideration when either pure oxygen or oxygen-enriched air is used, due to the cost of producing these gases.

The rise velocity of bubbles of different sizes is well-documented (Motarjemi and Jameson, 1978). Unfortunately, there are very few data published on the sizesof bubbles produced by proprietary reoxygenation devices.

For bubbles generated from porous plates in water, the bubble size and bubble size distribution have been found to vary with gas flow-rate (Koide et al, 1968). The bubble size directly above the distributor is reported

to be very small, with coalescence of bubbles occuring above the plate. Thus the formation of large bubbles and bubble size distribution are dependent on gas flow-rate. In bubble columns, bubbles generated in water have been generally observed to be less than 10 mm (Yoshida, 1965). Motarjemi (1978) refers to fine bubble aeration systems with bubble sizes of 2 - 5 mm. The rise velocity of bubbles in this size range is around 0.25 m/s.

A marked change in bubble size and stability is found in seawater and intermediate salinities. Yoshida (1965) suggested that the occurrence of small bubbles in electrolyte solutions was due to electrostatic potential at the gas-liquid interface. Other workers have noticed the change in bubble size caused by the presence of electrolytes (Lee and Meyrick, 1970). A minimum bubble size has been associated with a maximum viscosity using water-alcohol solutions (Schnurmann, 1937), while the presence of electrolytes has been found to reduce coalescence by increasing viscosity (Zieminski and Whittmore, 1971). It is worth noting that an increase in the amount of solute causes a corresponding decrease in bubble size until a minimum is reached beyond which further addition of solute has no effect (Calderbank, 1958). Solution strengths of various electrolytes corresponding to minimum bubble sizes are shown in Table 1.8.1.

TABLE 1.8.1 Minimum Bubble Sizes in Various Electrolytes (Calderbank, 1958)

Bubble size has been found to fall from 2.5 mm in 0.01 M KCl and $Na_2 SO_4$ solutions to as low as 0.3 mm in 1 M KCl and $Na_2 SO_4$ solutions (Koide et al, 1968). A detailed analysis of the effects of varying concentrations of electrolytes is beyond the scope of this thesis, but the change in bubble size seems to be due to the effects of ionic strength and viscosity.

1.8.2 Dissolution Times

Dissolution times for bubbles of different sizes and at two different pressures have been calculated and are given below (Table 1.8.2). The assumptions made in performing the calculations were as follows:

(1) The water contains no dissolved nitrogen. Desorption of nitrogen would affect the oxygen partial pressure and hence the transfer rate. Motarjemi (1978) has allowed for this effect in his own calculations which are discussed later, and considered it relatively unimportant except for bubble diameters greater than 5 mm released at depths greater than 10 m (equivalent to 2 atm)

(2) Co_2 is constant at 10 ppm dO_2

(3) Co_2^* for pure oxygen at 1 atm is 55 ppm dO_2

(4) The variation of k_L with bubble size can be based on the data collected by Motarjemi (1978) in his own work and that of others.

TABLE 1.8.2 Dissolution Times of Bubbles

		Bubble Diameter (mm)					
Dissolution Time	(s)	0.5	1	2	3	4	5
Pressure (atm)	1	52	51	66	112	175	229
	2	47	47	59	101	155	205

Motarjemi's studies were made on bubbles rising in deoxygenated water. From the depths required for 95% dissolution of the bubble mass and bubble rise velocities the times required for 95% dissolution can be estimated (Table 1.8.3).

TABLE 1.8.3 Times for 95% Dissolution of Bubbles (Motarjemi, 1978)

The results are of the same magnitude as the author's but Motarjemi's results are lower by a factor of two. However, the results in Table 1.8.2 were for the case of complete dissolution. The following times were obtained on the basis of 95% dissolution (Table 1.8.4).

TABLE 1.8.4 Times for 95% Dissolution of Bubbles

Dissolution Time	(s)	0.5	1	2	3	4	5
Pressure (atm)	1	33	32	42	71	110	144
	2	30	30	37	64	98	130

These results show good agreement with those reported by Motarjemi (1978), and the combined results highlight several points. Firstly, considerable time is required to dissolve the last 5% of the gas in a bubble. Secondly, the calculations show a negligible effect due to pressure which may be explained in the following way. The mass of a bubble of given volume increases with pressure, whereas the interfacial area per unit mass decreases. However, because Co_2^* increases with pressure, this balances the loss of transfer area and the net effect is to slightly reduce bubble dissolution time. It should be noted of course, that despite the similar dissolution times considerably greater mass is transferred at the higher pressure.

Motarjemi (1978) was concerned with the depth needed to dissolve a single bubble rising in a stationary fluid. For many practical aeration or oxygenation devices, bubble path length or contact time are more meaningful concepts than the depth required for dissolution. It may be concluded that in freshwater, contact times of at least 120 seconds are required while in seawater, times over 30 seconds are necessary. These are the minimum times since in many reoxygenation systems Co_2 will increase as the bubble dissolves reducing the local concentration gradient.

1.9 Conclusions

In the case of once-through systems the limited availability of water for fish farming is a major constraint to the development of the industry. Pumping can often provide access to larger volumes of water but this can be expensive. In addition, it is often necessary to operate so that as much oxygen as possible is consumed by the fish and this can lead to low dissolved oxygen levels when higher levels might provide better conditions for growth. In such once-through systems there is no protection against water failure which may lead to partial or total loss of stock.

Reoxygenation can improve water use and raise dissolved oxygen levels but continuous, reliable operation is essential and so full consideration must be given to maintenance of equipment and stand-by facilities. However, the reoxygenation requirements and the costs of such a system can only be evaluated for each individual site. Even then, there may be additional benefits which are difficult to assess.

The mass-transfer equation explains the dissolution of oxygen in water through the gas-liquid interface created by the device. For processes generating gas bubbles in water bubble sizes of up to 5 mm may be expected in freshwater, but they may be as small as 0.5mm

in seawater. A minimum of 120 secs. is required for 95% dissolution in freshwater compared with 30 secs. in seawater.

CHAPTER 2

AERATION

2.1 Introduction

Aeration methods enhance natural rates of surface aeration through the creation and enlargement of an air-water surface and by agitation at the interface. They are widely used for the treatment of sewage by activated sludge processes and in biochemical engineering for fermentation (USEPA, 1974, Schügerl et al, 1977). Their application in fish farming has been recently reviewed by Colt and Tchobanoglous (1979).

The principal advantage of such methods is the universal availability of air. However, the nitrogen content in air restricts the potential for aeration in fish farming.

2.2 Mass Transfer

The important point regarding the use of air as a source of oxygen is that saturation concentrations are low because the oxygen solubility is low and because air contains only 21% oxygen (Table 2.2.1).

TABLE 2.2.1 Dissolved Oxygen Concentrations of Water in Equilibrium with Air at Atmospheric Pressure (APHA, 1971)

Since minimum dissolved oxygen levels of 3-5 ppm are usually required for the fish, both the terms $(Co_2^* - Co_2)$ and $(Co_2 - Co_{2,T})$ defined in equations 1.7.1 and 1.7.2 are small. It is possible to enhance Co_2^* by increasing the operating pressure of the aerator but the corresponding increase in the driving force for nitrogen transfer can lead to nitrogen supersaturation. Operating pressures are therefore generally kept near to atmospheric pressure.

$$\varphi = Q_L(Co_2 - Co_{2,T}) \qquad 1.7.2$$

Inspection of equation 1.7.2 shows that increasing Q_L offers a suitable way of overcoming the problems arising from the small difference between Co_2 and $Co_{2,T}$.

$$\varphi = k_L A(Co_2^* - Co_2) \qquad 1.7.1$$

Similarly, in equation 1.7.1, increasing the term ($k_L A$) is a suitable way of compensating for the small difference between Co_2^* and Co_2 and this may be achieved by bringing large volumes of air and water into contact with each other. Only a small proportion (typically 5-10%) of the oxygen in the air is dissolved which maintains an optimum driving force for oxygen transfer and the large volumes involved ensure adequate overall transfer rates (Leary et al, 1969).

Such devices are therefore characterised by a short contact time between large volumes of air and water producing high ($k_L A$) values.

2.3 Principles of Aeration

Aerators work on a variety of principles and can therefore be classified in many ways (Eckenfelder, 1956; WRC, 1977). In this review they are divided into two groups according to whether the interfacial area is created by (1) pumping water or (2) blowing air, although some operate using both principles. For aerators ($k_L A$) is the major determinant of transfer rate and for fish farmers the key comparative measure is the transfer efficiency, that is the quantity of oxygen dissolved per unit of energy supplied. Comparative performance is usually measured under standardised conditions, namely in clean freshwater at 10° C or 20° C containing no

dissolved oxygen. The transfer efficiency at a dissolved oxygen concentration $Co_{2,T}$ can be calculated from the following equation (Colt, 1979):

$$E = E_o \left\{ \frac{\beta C_{o_2}^* - C_{o_2,T}}{9.2} (1.024)^{\theta-20} \alpha \right\}$$

where E = transfer efficiency under field conditions

E_o = transfer efficiency under standard conditions

$C_{o_2}^*$ = equilibrium dissolved oxygen concentration

θ = field temperature

α, β are coefficients affected by the physical and chemical properties of the water but typical values are 0.85 and 0.9 respectively for freshwater fish farms (Colt, 1979).

Substantial corrections must therefore be made to estimate performance under farm conditions.

2.3.1 Pumped Water Aerators

(1) Surface Aerator (Fig. 2.3.1)

Water is drawn from below the aerator and discharged into the atmosphere as a spray. The spray is aerated in flight and as it splashes onto the water surface.

One such device is produced by Smiths Industries Ltd. and is available in 0.25 - 22 kW sizes pumping from 80 - 2500 m^3/h. Operating depths of 0.6 - 2 m are required and transfer efficiencies of 2.2 - 2.4 $kg O_2/kWh$

Fig. 2.3.1 Surface Aerator

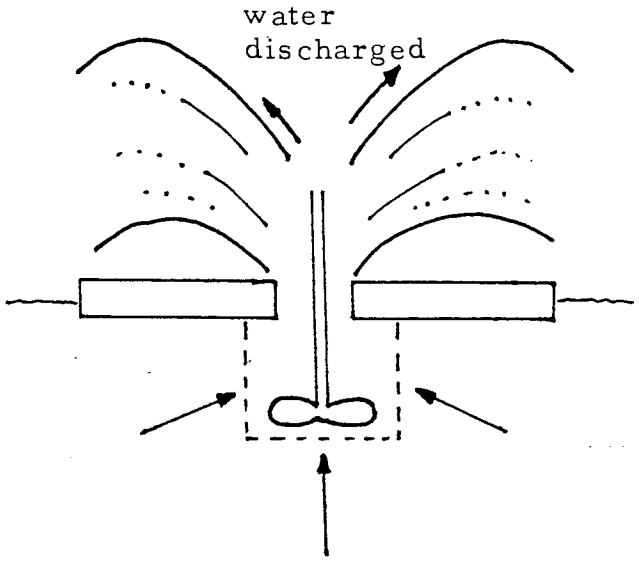

Fig. 2.3.2 Surface Agitator

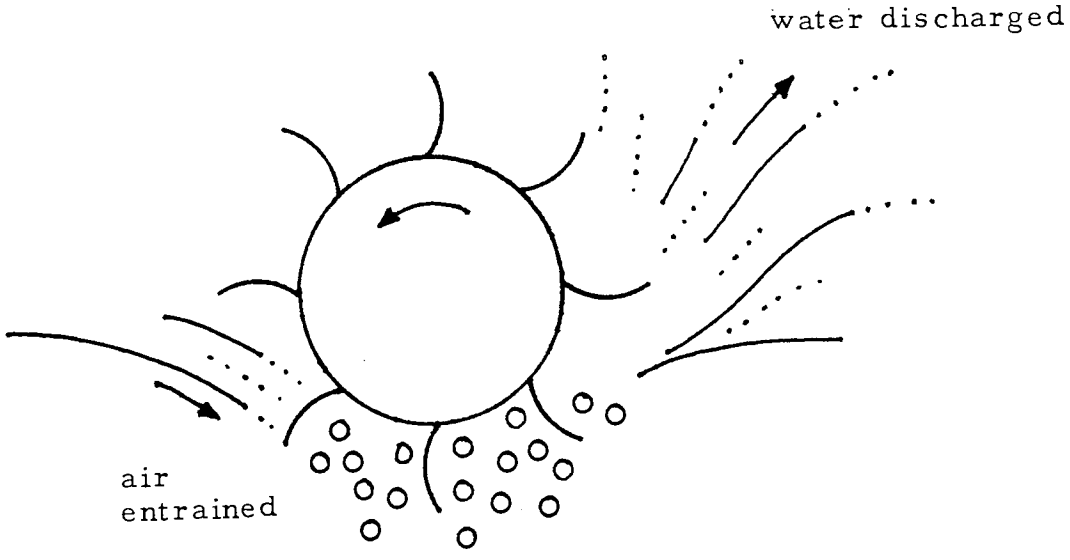

are achieved under standard conditions.

(2) Surface Agitator (Fig. 2.3.2)

There are various paddle type devices, some with axis horizontal, others with a vertical axis. They operate in a similar fashion to surface aerators but activity is principally at the pond surface.

One example of a proprietary device is the Yasuda Aquamill, manufactured in 0.4 and 2.2 kW sizes. A transfer efficiency of 2.3 kgO_2/kWh is given under standard conditions. It should be noted that surface agitators may require screens to prevent fish damage.

(3) Venturi (Fig. 2.3.3)

Water passing through a venturi draws air down into the throat of the venturi creating small bubbles which are dispersed horizontally in the water. The pressure drop across the venturi usually results in a high energy consumption. The air may be blown in as an alternative to create a larger interfacial area but at the expense of increased power requirements.

The ITT Flygt Ejectors are venturi aerators, pumping from 18 - 250 m^3/h water. Transfer efficiencies of about 1 kgO_2/kWh are estimated for this system when

operating under standard conditions. This figure only takes into account the pressure loss across the venturi, however.

(4) Submerged Pump (Fig. 2.3.4)

Air is drawn down a central shaft where it is broken into small bubbles by a rotating impeller, and violently mixed with the water. This type of aerator is similar in operation to the venturi but the process of bubble generation is more efficient. Again the air may be blown in as an alternative. Nitrogen supersaturation is a possibility with both the submerged pump and the venturi due to the water and air being subjected to rapid pressure changes.

One manufacturer of the submerged pump is ABS Pumps Ltd. Pumps are available in 3 - 22kW sizes. Transfer efficiencies of 2.3 kgO_2/kWh are achieved under standard conditions.

(5) Impinging Jet (Fig. 2.3.5)

This is a simple water jet directed down onto the water surface, forcing gas bubbles down into the water. Because of its simplicity it is commonly used in fish farming for solving oxygen problems, yet no proprietary devices are manufactured.

Fig. 2.3.3 Venturi

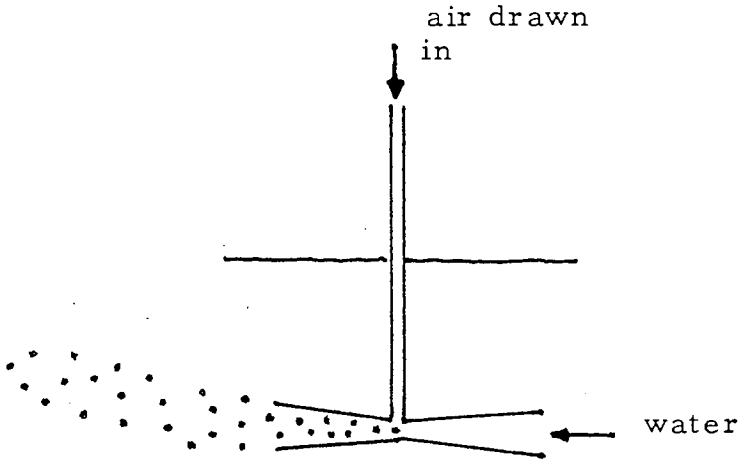

air bubbles dispersed

Fig. 2.3.4 Submerged Pump

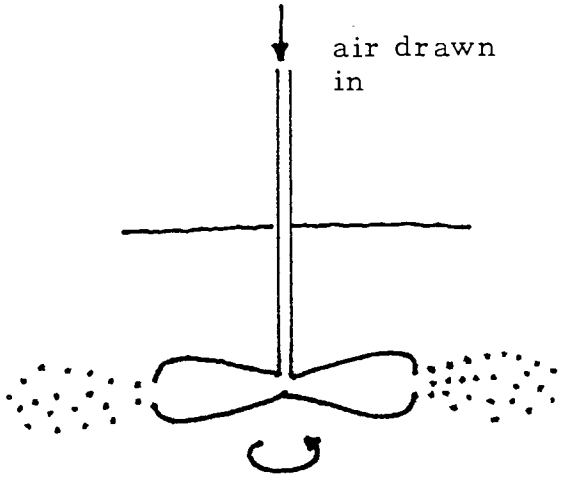

air bubbles dispersed

Typical transfer efficiencies of 1.3 - 2.4 kg/O_2/kWh may be expected.

(6) Cascade (Fig. 2.3.6)

A simple cascade may also be used for aeration. This is particularly useful if a natural head is available, for example between raceways.

2.3.2 Diffused Air Methods

Diffused air methods may be classified into those which operate at very low pressures (less than 0.2 atm), dependent on the water depth, and those which operate at higher pressure (0.5 - 1.0 atm) (Fig. 2.3.7). The first type rely on using very large volumes of air to create large ("coarse") bubbles and in the latter case smaller volumes are used to create smaller ("fine") bubbles.

(1) Coarse Bubble Aeration

These methods consist of a row of holes in plastic or rubber tubing. The hole size may vary from 0.1 mm up to several millimetres. They produce bubbles up to 10 mm in diameter. A refinement of this is to enclose the diffuser in a static tube open at the top and bottom (Fig. 2.3.8). Air, introduced through the diffuser at the bottom will draw water up through the tube and

Fig. 2.3.5 Impinging Jet

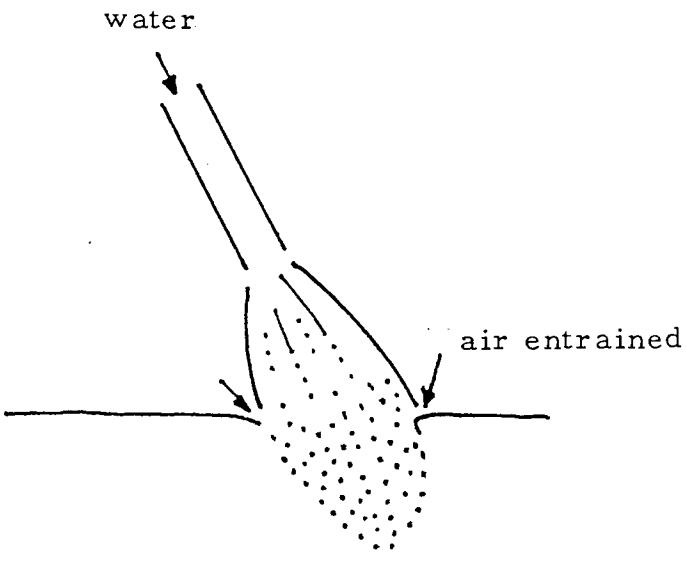

Fig. 2.3.6 Cascade

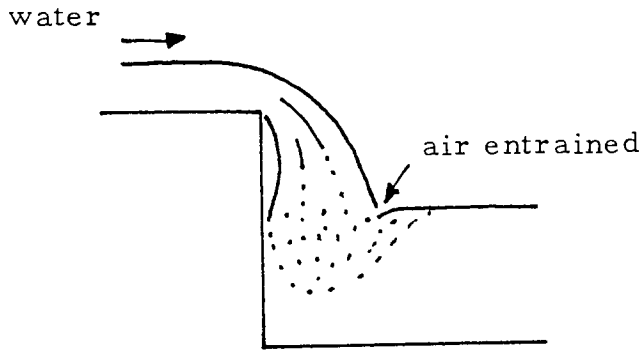

considerable mixing will occur: internal baffles may aid mixing. Aerated water is discharged at the top in a similar fashion to an air-lift pump.

One such manufactured unit is produced by Mixaerators Ltd. A liquid flow of 177 m^3/h is produced from an air flow of 120 m^3/h supplied at 0.06 atm pressure. The diffuser is arranged such that water flows past the diffuser and shears off the air bubbles. A transfer efficiency of 4.3 kg O_2/kWh is achieved under standard conditions.

(2) Fine Bubble Aeration

At the expense of higher pressures, the air may be broken up into smaller bubbles, typically 2 - 5 mm, through a variety of proprietary diffuser elements. These elements may be constructed of porous rubber, syntered ceramic, metal or glass. The pressure required is dependent on the pore size (typically 10 - 50 microns) and the air flow-rate. It is important to realise that high pressures are used to create small bubbles by a large pressure drop across the diffuser. The bubbles will be formed at a pressure equal to the diffuser depth and therefore in fish ponds and tanks nitrogen supersaturation is unlikely.

There are a variety of diffuser elements marketed by Ramot Plastics Ltd., Ames Crosta Ltd., and

Fig. 2.3.7 Diffused Air Methods

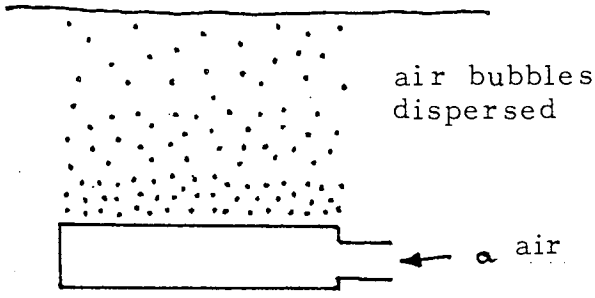

Fig. 2.3.8 Static Tube Mixers

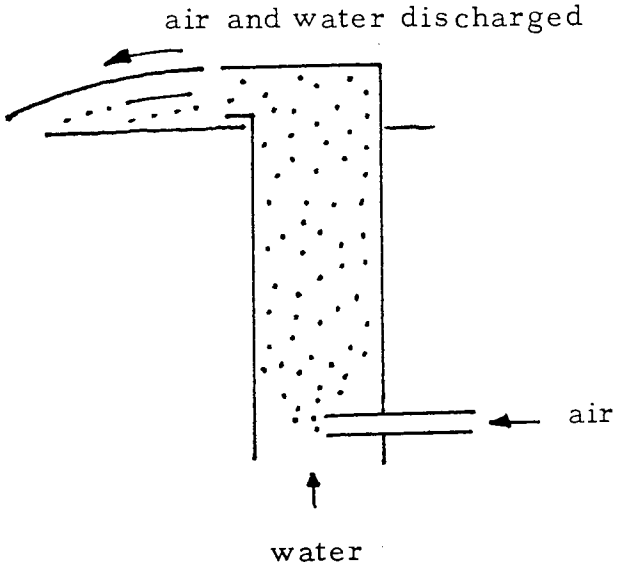

ITT Flygt Ltd., for example. Transfer efficiencies of up to 8 kgO_2/kwh have been estimated. However, high efficiencies are only achieved at very low air flow-rates and high rates of transfer may only be achieved with large areas of diffuser element.

The other important point to consider in evaluating air-powered systems is that transfer efficiencies of proprietary diffused air systems are usually based solely on the pressure loss across the diffuser.

2.3.3 U-tube (Fig. 2.3.9)

One method which does not readily fit into the classification given above is the U-tube. This consists of two vertical tubes sunk below ground and connected at the bottom to form a "U". Water flows down one tube and back up the other. Air is introduced near the top of the "down" pipe and is carried to the bottom of the U by the velocity of the water. As the air descends it is subjected to an increasing hydrostatic head which raises the equilibrium concentration above that of saturation with air at atmospheric pressure, so Co_2^* is enhanced and high transfer rates are possible. In addition, the U-tube can be driven by a low liquid head or by injecting air several feet along the "down" pipe, with the difference in density between the two "legs" providing the driving force (Hemming et al, 1977).

Fig. 2.3.9 U-tube Aeration

Water Powered U-tube

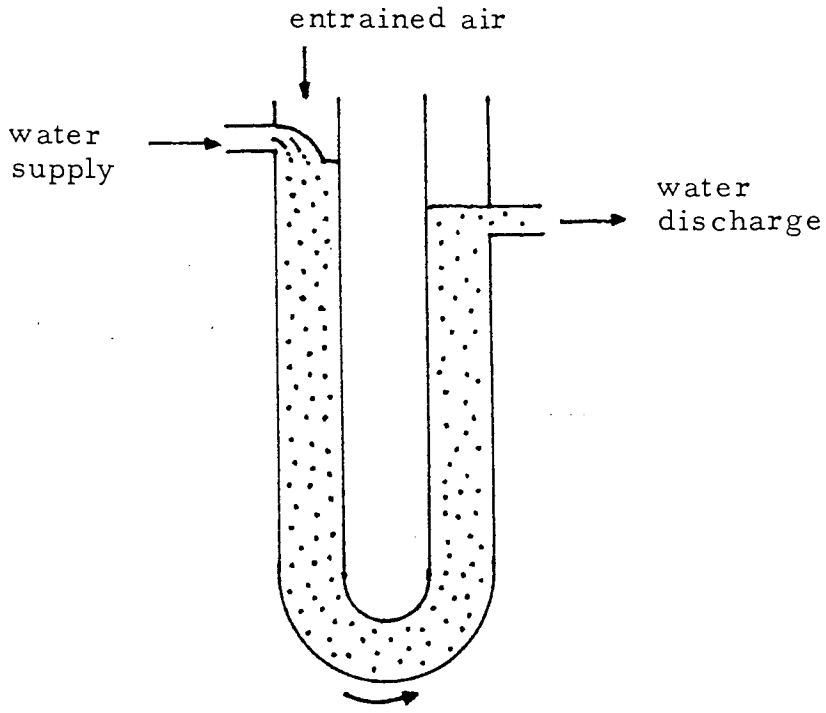

Air Powered U-tube

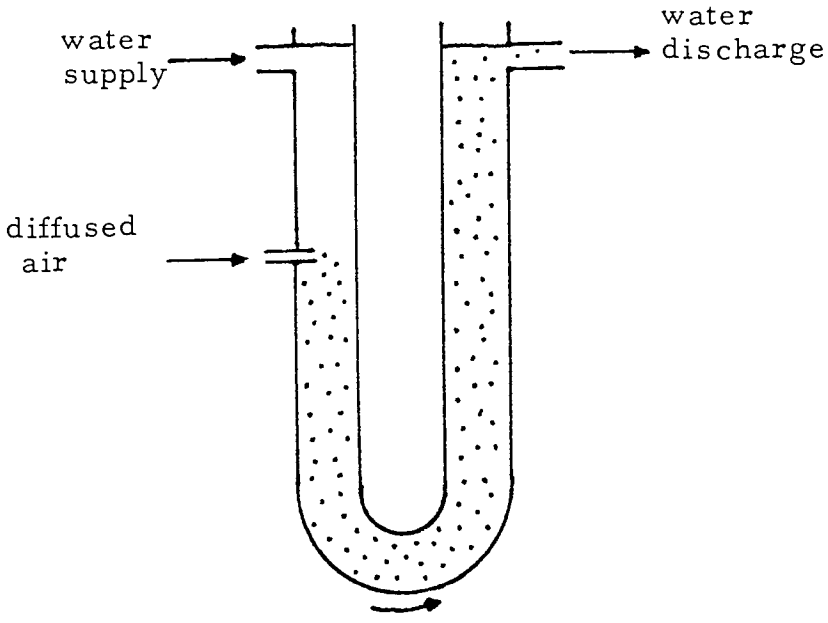

The combination of high transfer rate and low energy requirement leads to high transfer efficiencies.

The principal problem concerning U-tube aeration is nitrogen supersaturation. The increased hydrostatic head is also available to the nitrogen in air and contact under these conditions can supersaturate the water with nitrogen. For water saturated with nitrogen outlet dissolved nitrogen levels of 110% and 120% saturation have been predicted for 6 m and 12 m U-tubes (Speece, 1970).

It is generally accepted that levels over 110% saturation will present problems in fish farming applications yet the method is still used (Speece, 1969, Petit, 1980, pers. comm.). In such applications, stripping of nitrogen through cascades is therefore an important consideration and indeed, the subsequent head loss through the falls should really be included in the assessment of transfer efficiency.

2.4 Comparison of Techniques for Fish Farming

The majority of data published on aerator performance has been concerned with operation under standard conditions. The results are summarised in Table 2.4.1.

TABLE 2.4.1 Comparison of Aerator Performance

Aerator Type	Transfer Efficiency (kgO_2 /kWh)	Reference
Surface Aerator	1.2 - 2.4	Colt 1979
Surface Agitator	1.2 - 2.4	Colt, USEPA, WRC 1977
Venturi	0.6 - 0.9	Eckenfelder '56 Bayley & Wyatt '61, WPRL '74
Submerged Pump (with air)	1.3 - 1.4	Eckenfelder, USEPA 1974
Water Jet	1.3 - 2.4	Chessness '73, Sneath '78
Cascade	1.2 - 2.3	Chessness '71, Petit '75
Coarse Bubble Diffused Air	0.9 - 1.0	USEPA, Eckenfelder
Static Tube	1.2 - 1.8	Colt, Campbell & Rocheleau '76
Fine Bubble Diffused Air	1.5 - 5.5	Eckenfelder, USEPA, Lister & Boon '77, WRC 1977
U-tube	1.8 - 4.0	Speece 1973

Most results are in reasonable agreement for a particular type of aerator. The differences in results for fine bubble diffusers may be due to a number of factors. Firstly, it has been found that aerator performance in flat-bottomed tanks is different from that in furrow-bottomed tanks and so it may be concluded that tank shape affects mixing patterns and hence transfer efficiency (Lister and Boon, 1977). Secondly, changes in air flow-rate through a

diffuser can affect the transfer efficiency, since the air flow-rate influences both bubble size and the degree of "gulf streaming", (Koide et al, 1968, Motarjemi and Jameson, 1978). The variability in U-tube results may be due to the range of possible methods for operation.

Some of the more recent comparative studies have been undertaken under fish farming conditions (Rappaport et al, 1976, Busch et al, 1974). Mitchell and Kirby (1976) have produced the most systematic evaluation of aeration methods. In their studies, aerators were divided into three groups, (1) diffused air systems (2) venturi units and (3) surface aerators or agitators. Initial tests of diffused air systems and venturi aerators were conducted under laboratory conditions in clean water and results were corrected to 25° C and 50% saturation. Comparisons were made on the basis of (k_L A), oxygen absorption efficiency and transfer efficiency.

Porous plastic tube was chosen for pond evaluation because of its low cost and high transfer efficiency. Various combinations of venturi were tested because of their high (k_LA) and mixing ability. Surface aerators were included in pond tests. Table 2.4.2 summarises the transfer efficiencies recorded in each group, corrected to 50% saturation and 25° C (equivalent to 4.2 ppm dO_2), and compares them with values predicted

by Colt (1979) for aerators operating at a dissolved oxygen concentration of 6.0 ppm at 20° C. The results show that under farm conditions transfer efficiencies are likely to be 20 - 30% of those measured under standard conditions.

TABLE 2.4.2 Aerator Performance Under Pond Conditions

	Transfer Efficiency (kgO_2/kWh)	
	Mitchell & Kirby (1976)	Colt (1979)
Surface Aerators	0.24 - 0.48	0.25 - 0.5
Fine Bubble Diffused Air	0.96	0.25 - 0.42
Venturi Aerators	0.16 - 0.35	0.25 - 0.5

2.5 Application of Aeration in Fish Farming

Aeration systems for fish farming are likely to require significant amounts of power. Power requirements will obviously depend on the overall efficiency of the method selected but will also be substantially affected by the level of dissolved oxygen it is necessary to maintain.
Fig. 2.5.1 is a graph of the power requirements to support one tonne of rainbow trout taking a typical transfer efficiency of 2 kgO_2/kWh achieved under standard conditions corrected for temperature and dissolved oxygen level

using equation 2.3.1. The air volumes given are for fine bubble diffused aeration also assuming 2 kgO_2/kWh transfer efficiency.

As an approximate guide maintenance of dissolved oxygen levels above 70% saturation is likely to result in unacceptably high power requirements. This can have important implications where saturated dissolved oxygen levels are naturally low such as at high temperatures, high altitudes or in seawater (Table 2.5.1). For example, 70% saturation at 20° C in seawater is only 5.2 ppm dO_2 which is close to the minimum acceptable dissolved oxygen level for salmonids.

TABLE 2.5.1 Dissolved Oxygen Concentrations at 70% Saturation (APHA, 1971)

Another important factor tending to reduce efficiency, as well as increasing capital costs, is the variable nature of oxygen demand on fish farms. Variations due

Fig. 2.5.1 Aeration Requirements to Support One Tonne Rainbow Trout (200 g ave)

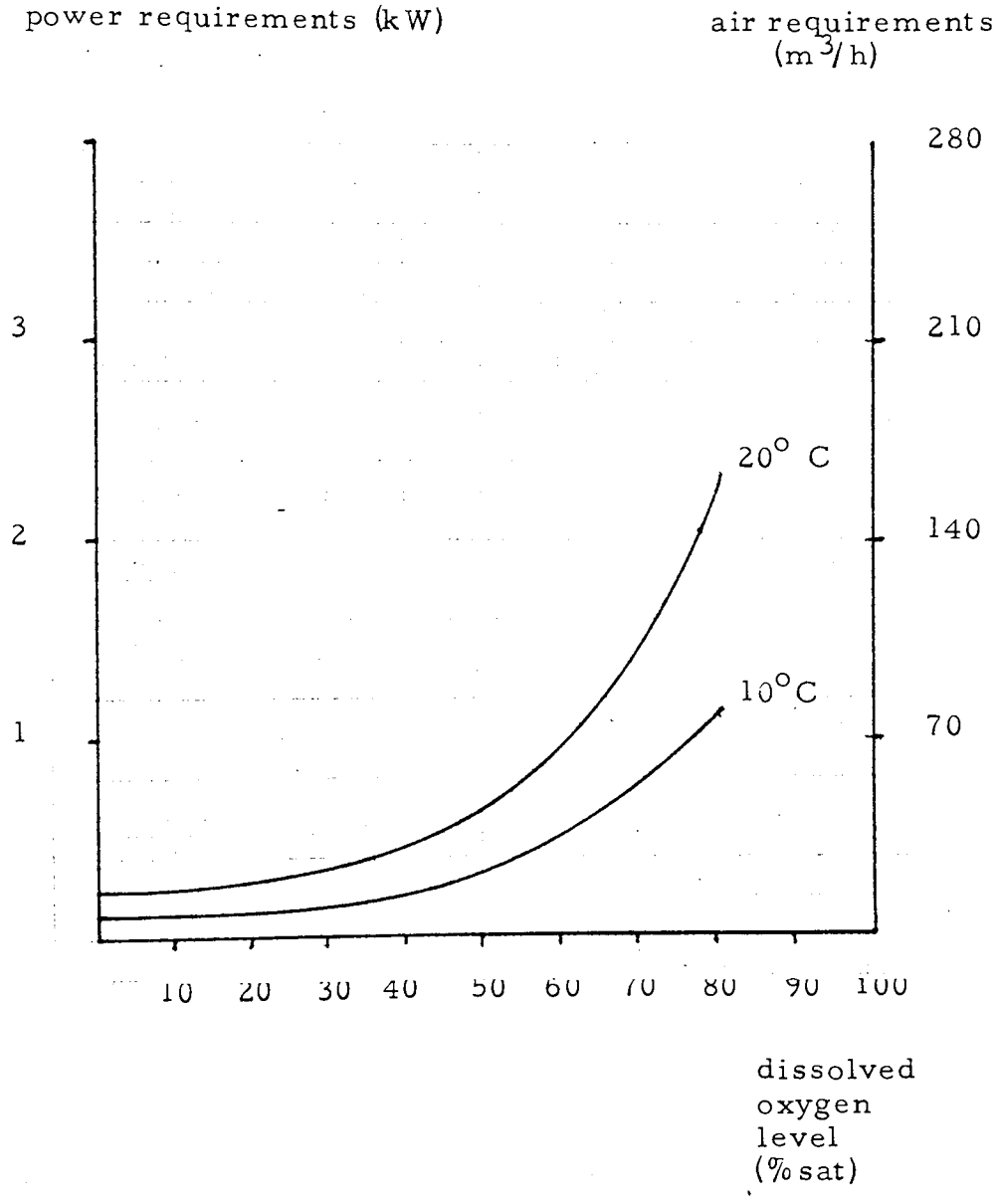

to temperature changes, water availability or stocking levels will be superimposed on normal diurnal rhythms to give very wide fluctuations. An aeration system must obviously be designed to cope with the most extreme circumstances which means that under normal circumstances there will be excess capacity. The nature of many aeration systems is such that oxygen control is difficult and results in less than maximum efficiency.

The most appropriate type of aeration method for different farms will depend closely on the operating conditions, the layout of a particular farm and on the degree of water economy which it is required to achieve. Close attention must be given to accurate sizing which in turn depends on precise specification of requirements. For diffused air systems centralised production of pressurised air will usually be most efficient but in such cases detailed attention must be given to its subsequent distribution to minimise pressure losses. An appropriate source of power and back-up power must also be considered, and in selecting appropriate machinery account must also be taken of maintenance procedures and the availability of spare parts. This aspect is particularly important for the requirement of continuous, reliable operation.

In addition it should be remembered that the large turnover of water involved in aeration generally provides

good mixing resulting in even oxygen and temperature distributions, but this may become excessive if aeration requirements are high.

Finally, it is important to consider aeration as a means of dissolved gas removal. The mode of operation of aerators makes them suitable for gas desorption, the contacting of large volumes of air and water making it possible to remove both excess carbon dioxide (despite its high solubility) and excess nitrogen (even when the gradient is small). However, the efficiency of these processes will be reduced as the dissolved levels approach saturation figures. No matter how great the water saving, the oxygen requirements of the fish will dictate a degree of aeration sufficient to remove metabdically produced carbon dioxide (Speece, 1973). Ammonia, however, can only be effectively removed when the pH is in excess of 10 (Short, 1973). Little ammonia will therefore be stripped from fish rearing enclosures using aeration.

2.6 Conclusions

The limitations on the use of air as a source of oxygen are due to the low solubility of oxygen in air.

Transfer efficiencies of aeration devices range from 0.6 - 5.5 kgO_2/kWh under standard conditions but these will be considerably reduced under fish farming

conditions. In addition, there is an effective upper limit of 70% saturation on dissolved oxygen levels which can be economically maintained. The capital and running costs of using aeration to save water will be magnified by the need to specify a system which can cope with the most extreme conditions of oxygen demand. In the system design close attention must be paid to the operating conditions, the duty specification and to the power supply and back-up requirements.

Aerators are suitable for gas desorption, however, which can have particular merit in removing the carbon dioxide produced from fish respiration.

CHAPTER 3

OXYGENATION

3.1 Introduction

The solubility of pure oxygen is approximately five times that of oxygen in air and its use can therefore greatly increase oxygen dissolution rates. In fish farming the main benefit of using pure oxygen is that high transfer rates can be achieved without risk of nitrogen super-saturation. Oxygen-enriched air has similar advantages but its use is always less effective due to the presence of some nitrogen.

The main disadvantage is the cost of these gases and because of this efficient dissolution is essential. In addition to transfer efficiency, therefore, a second measure of performance is dissolution efficiency, that is the percentage of oxygen supplied which is dissolved.

3.2 Gas Production

3.2.1 Oxygen-Enriched Air

Oxygen-enriched air is produced by the removal of nitrogen from air using a nitrogen adsorber, such as zeolite (Boon, 1976). The pressure swing adsorption (PSA) plant is one method of achieving this. Air is passed through a cylinder containing zeolite and the nitrogen is adsorbed, producing oxygen-enriched air. The nitrogen is then removed under vacuum. Two

Missing page(s) from the bound copy

zeolite cylinders are used, working in alternate cycles. Oxygen purities of up to 90% are possible. Energy requirements amount to about 1 kW/m^3 oxygen produced (700 kW/tonne).

3.2.2 Pure Oxygen

Pure oxygen is produced by cryogenic separation (Boon, 1976). Air is liquified by cooling, and because all its constituents evaporate at different temperatures, each can be distilled individually. The oxygen produced is over 99% pure and is stored at -183° C in a vacuum-insulated container. Liquid is evaporated for use, the gas being available at a pressure of 10 atm.

3.3 Design Considerations

3.3.1 Gas-Liquid Contact Time

The primary consideration in the design of an oxygenator is the need to achieve high dissolution efficiencies because of the costs of the gas. Table 3.3.1 is a summary of times for 95% dissolution of bubbles of various sizes.

TABLE 3.3.1 Times for 95% Dissolution of Bubbles(s)

Bubble Size (mm)		0.5	1	2	3	4	5	
Pressure (atm)	1	33	32	42	71	110	144	(s)
	2	30	30	37	64	98	130	

In freshwater bubble sizes are generally found to be 2 - 5 mm diameter and these require long contact times for dissolution. The basic contacting principles of bubbles in water or sprays in gas generally only produce a short contact time, so the use of pure oxygen under these conditions will therefore result in low dissolution efficiencies. In addition, nitrogen will readily transfer to the gas phase, since there is no nitrogen in the gas initially, and hence will be stripped from solution (Fig. 3.3.1).

Various methods have been adopted in oxygenator design to create sufficiently long contact times for efficient dissolution. These techniques have been developed for oxygenating waste water and are now applied in fish farming (Boon, 1976). The methods apply to the use of pure oxygen but are followed by a consideration of the implications of using oxygen-enriched air.

Fig. 3.3.1 Open Continuous System

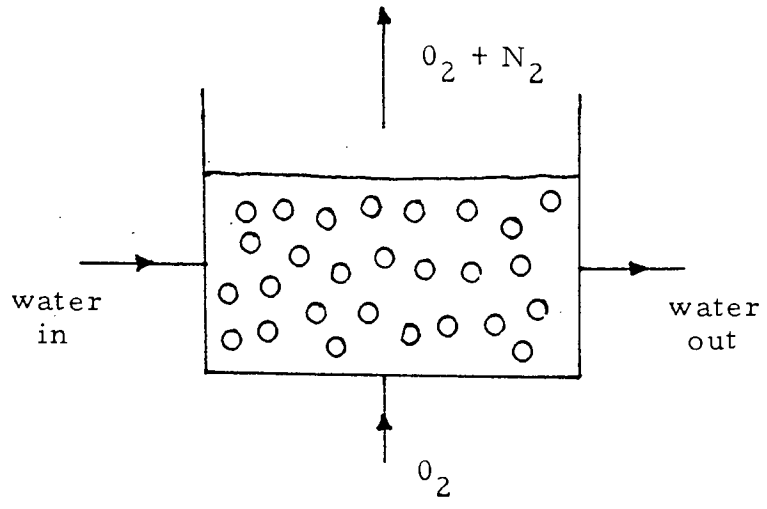

low dissolution efficiencies are achieved since the gas-liquid contact time is short. Nitrogen is stripped from solution and lost to the atmosphere

3.3.2 Methods for Achieving Long Contact Times

(1) Recycling - undissolved gas from an oxygenator is collected and fed back into the oxygen supply (Fig. 3.3.2). In this way gas is continuously recycled until dissolved.

(2) Enclosing the Device - so that oxygen is trapped within the oxygenator and continuously mixed with the water until dissolved (Fig. 3.3.3).

One feature of these methods is that, if no gas is lost from the oxygenator, nitrogen which is stripped from solution by the oxygen will accumulate in the oxygenator until equilibrium is reached between the nitrogen in the gas and liquid phases. So for air-saturated waters the nitrogen partial pressure in these systems will be 0.8 atm. Therefore, at atmospheric pressure the oxygen partial pressure can only be 0.2 atm despite the use of pure oxygen. However, the low oxygen partial pressure can be overcome by pressurisation or, at low pressures, by replacing the nitrogen with oxygen as it is stripped from solution.

The use of high pressures produces a large driving force which allows high transfer rates and highly super-saturated solutions despite the accumulation of nitrogen in the gas phase. Both oxygen and nitrogen are trapped in

Fig. 3.3.2. Continous System with Gas Recycle

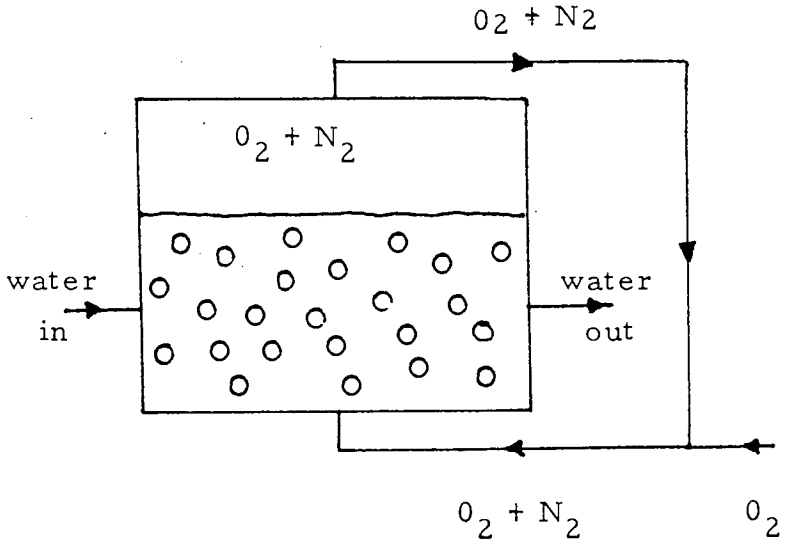

Nitrogen will accumulate until equilibrium is reached between nitrogen in gas and liquid phases. No gas is lost so high dissolution efficiencies are achieved.

Fig. 3.3.3 Closed Continuous System

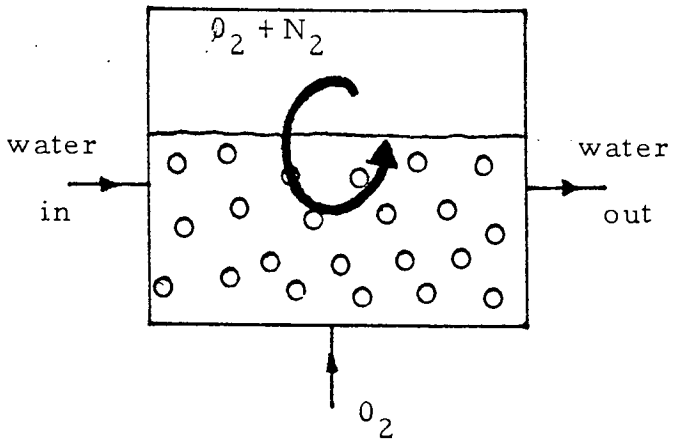

Again nitrogen accumulates until equilibrium is reached and no gas is lost. Continuous mixing of the gas and liquid phases ensures oxygen transfer. Pressure may be used to enhance transfer rate.

the oxygenator so very high dissolution efficiencies are achieved. Nitrogen supersaturation cannot occur since there is no additional nitrogen to dissolve. Super-saturated solutions are therefore produced at the expense of increased energy requirements.

At atmospheric pressure or just above, high oxygen gradients and therefore increased transfer rates are maintained by continuously removing nitrogen from the oxygenator and replacing it with oxygen, thereby effectively controlling the rate of nitrogen accumulation (Fig. 3.3.4). The gas can be removed using either an intermittent or continuous purging system but some oxygen is lost, mixed with the nitrogen purged from the oxygenator. At low pressures, therefore, supersaturated solutions are produced at the expense of lower dissolution efficiencies.

(3) Long Path Length Design - If the oxygenator can be designed such that gas bubbles travel on a sufficiently long path length then efficient dissolution is possible without nitrogen accumulating in the oxygenator (Fig. 3.3.5). A natural purge of replaced nitrogen and wasted oxygen is then achieved through allowing gas to escape directly to the atmosphere, avoiding the sophistication of enclosing the device or recycling gas. However, for 2 - 5 mm diameter

Fig. 3.3.4 Semi-Closed Continuous System

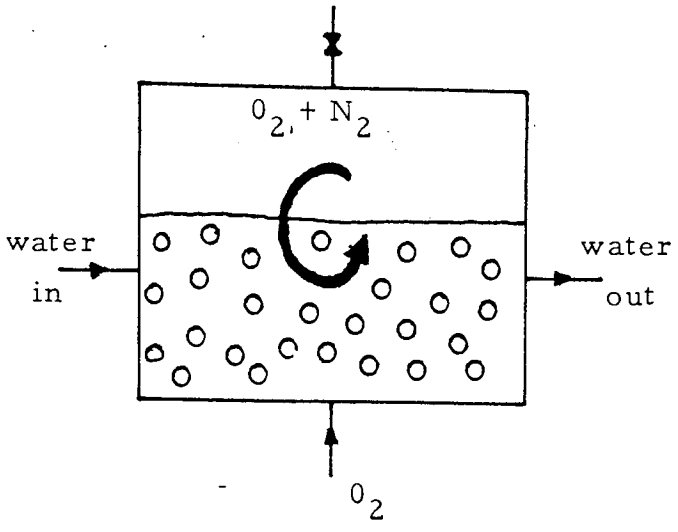

Nitrogen accumulates but equilibrium between gas and liquid phases is never reached since some nitrogen is purged. Nitrogen is therefore continuously removed from the liquid phase and replenished with oxygen.

Fig. 3.3.5 Open Continuous System with Long Contact Time

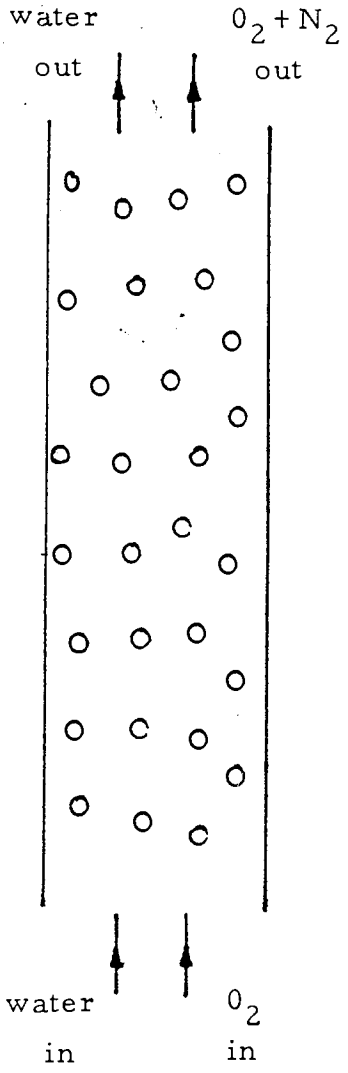

Nitrogen does not accumulate but efficient dissolution is ensured by long contact time. Purged gas escapes to atmosphere.

bubbles formed in freshwater this technique involves a large oxygenator design.

(4) Formation of Small Bubbles - The formation of small bubbles reduces the contact time required for dissolution and oxygenation, using the principle outlined in (3) above, can therefore be made much more compact. However, considerable energy is required to generate small bubbles in freshwater, which once formed, tend to coalesce to form much larger bubbles (Motarjemi and Jameson, 1978, Koide et al, 1968). In seawater smaller bubbles are much more easily formed and this technique readily lends itself to oxygenation under these conditions.

3.3.3 Implications of Using Oxygen-Enriched Air

When using oxygen-enriched air there are two additional aspects of oxygenator design to be considered. Firstly, the nitrogen partial pressure in the oxygenator must always be less than 0.8 atm if nitrogen supersaturation is to be avoided, so the operating pressure of the oxygenator will be restricted by the concentration of nitrogen in the gas supply. For example, if the gas contains 20% nitrogen the pressurisation to 4 atm is possible whereas if the gas contains 40% nitrogen then 2 atm is the upper

limit. Secondly, since the nitrogen in the gas is not dissolved it must be removed from the oxygenator. This necessitates the use of a purge-stream and oxygen will naturally be lost in the waste gas.

3.4 Examples of Proprietary Devices

Various proprietary devices are produced which use the techniques described above. Performance data is taken principally from trade literature.

3.4.1 Air Products and Chemicals Ltd - Diffuser and Hood (Fig. 3.4.1)

Oxygen is diffused through the water and undissolved gas is collected in a hood placed over the diffuser at the surface of the water. The gas in the hood is fed into a compressor where it is pressurised and delivered back into the diffuser, replenished with fresh oxygen from the feed gas (Shabi and Hibberd, 1977).

Provided the dissolved oxygen concentration in the water remains below saturation, complete dissolution is possible. If supersaturated water is required, then a natural purge of replaced nitrogen and waste oxygen is effected by gas not collected in the hood. This is also the case if the feed gas is oxygen-enriched air.

Transfer efficiency is not given but will be determined by the diffuser depth and the dissolved oxygen concentration

desired which will also affect the dissolution efficiency. However, 3 - 5 kg O_2/kWh is estimated under standard conditions when 100% dissolution should be achieved. The system is suitable for use in freshwater or saline water.

3.4.2 L'Air Liquide - Turboxal (Fig. 3.4.2)

This is a surface agitator operating in an oxygen enriched atmosphere. Water is driven through an enclosed chamber by a small head of water where it is mixed with oxygen using a turbine. The unit is designed for oxygenating 13 - 40 thousand m^3 water/day. The change in dissolved oxygen concentration is given as 10 ppm, but the outlet concentration is not given. It may be assumed that the data are based on measurements taken under standard conditions.

The unit should be capable of operating in freshwater or saline water. It would not be suitable for use with oxygen-enriched air without a purging mechanism being installed.

3.4.3 Messer Griesheim GmbH - Oxidator (Fig. 3.4.3)

This is a high pressure counter current gas-liquid contactor. Gas is trapped in the vessel by a high water velocity at the inlet and a low velocity close to the outlet.

Fig. 3.4.1 Diffuser with Gas Recycle

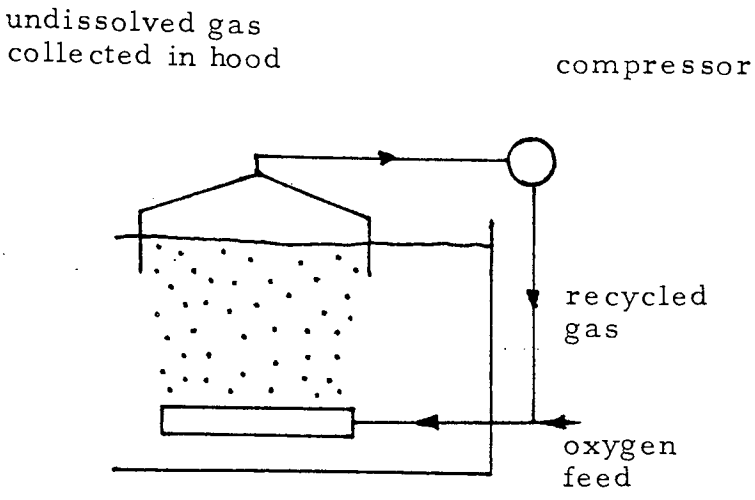

Fig. 3.4.2 Enclosed Surface Agitator

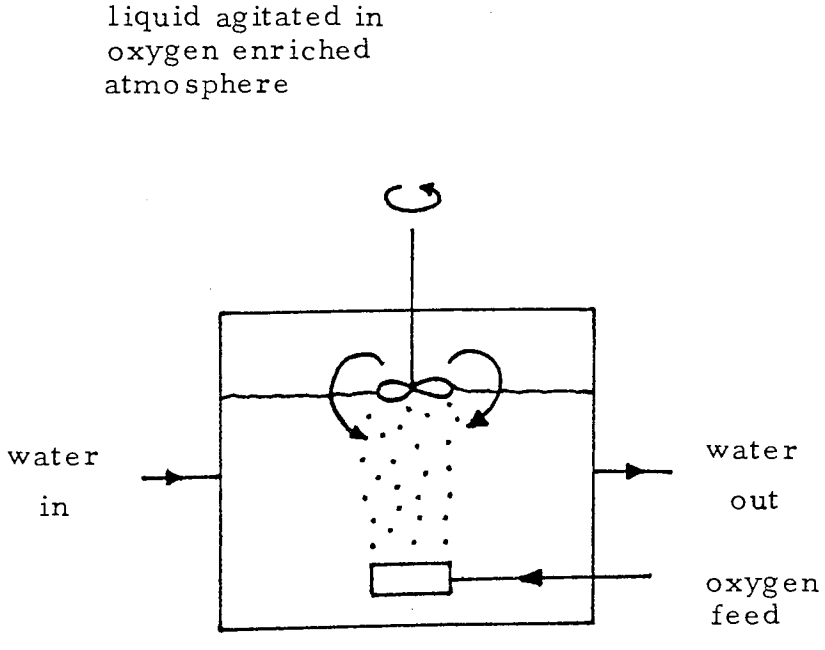

The unit operates at pressures between 0.5 and 2.5 atm gauge and outlet concentrations of 25 ppm dO_2 are available at very high dissolution efficiencies for an oxygen transfer efficiency of 3.22 kgO_2/kWh under standard conditions. It is claimed that dissolved oxygen concentrations of up to 100 ppm can be achieved.

Many of these high pressure devices contain packing which makes them only suitable for a clean water supply. If no packing is used then the device is suitable for saline water but water capacities may have to be changed in order to trap the smaller bubbles formed within the oxygenator. For oxygen-enriched air, the operating pressure will be limited by the oxygen purity; a purge of waste gas may occur in the out-flowing liquid.

3.4.4 Hede Neelson A/S - Down Flow Bubble Contactor (Fig. 3.4.4)

This is an example of a low pressure oxygenator. As with the high pressure contactor the gas is trapped in the device by a high inlet velocity and a low outlet velocity, but the device operates with only 0.5 m water head (Bruun de Neergaard, 1978).

At such low pressures the device will only re-saturate the water at very high efficiencies; supersaturated levels

Fig. 3.4.3 High Pressure Countercurrent Contactor

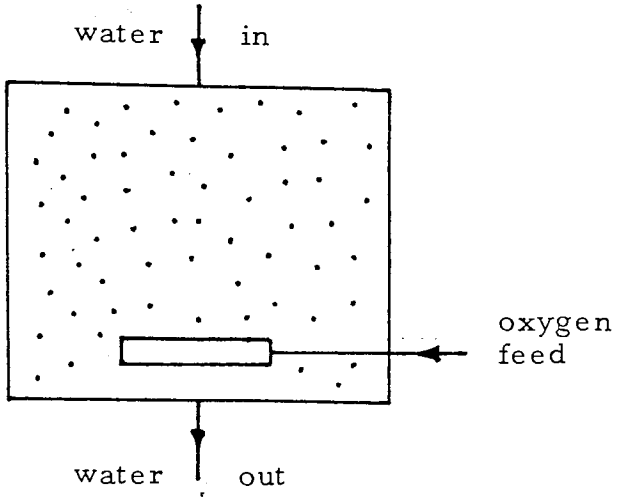

Fig. 3.4.4 Low Pressure Countercurrent Contactor

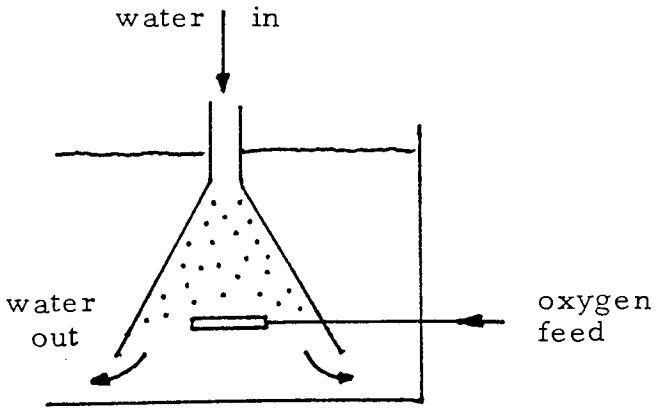

are achieved with a reduction in dissolution efficiency. Transfer efficiencies are not given since the device is designed to be driven by a natural head of water. However, a transfer efficiency of 3.3 kg O_2/kWh can be estimated from theoretical considerations, under standard conditions (Speece, 1971; Bruun de Neergaard, 1978).

This device may also be used for oxygenating saline water but the capacity of the unit may have to be altered to accommodate the smaller bubbles. It is also suitable for use with oxygen-enriched air, waste gas being purged in the outflow.

3.5 Techniques Developed by Shearwater Fish Farming Ltd.

The techniques developed by Shearwater are intended to cover the majority of situations which may arise in fish farm systems. The performance figures are based on equipment used in their own farms but these figures will be generally applicable to other fish farms. Actual equipment and capacities, however, must be selected and designed to suit the requirements set for individual farms.

3.5.1 Column Oxygenator (Fig. 3.5.1)

This is a low pressure counter-current gas-liquid contactor designed for use in freshwater utilising

operating pressures of less than 0.5 atm gauge. Outlet concentrations of up to 30 ppm dO_2 are possible at 10^{o} C with an inlet concentration of 10 ppm dO_2, and transfer efficiencies of around 1 kg O_2/kWh are achieved under these conditions. Dissolution efficiencies of 70-100% are possible depending on the desired outlet concentration.

The device is suitable for use with oxygen-enriched air as waste gas can be purged in the outflow. The unit may also be used in saline water but at a reduced oxygenation capacity.

3.5.2 Jet Oxygenator (Fig. 3.5.2)

The jet absorber is a far simpler device than the column for oxygenating seawater and water of high salinities. The jet produces a stream of bubbles which are dispersed in the water. The contact time is such that with the small bubbles formed, high dissolution efficiencies can be achieved.

Operating pressures of 0.5 - 1.0 atm gauge are employed and transfer efficiencies of 2-3 kg O_2/kWh have been obtained in seawater (34 ppt salinity) at 8.5 ppm dO_2 and 13^{o} C. Dissolution efficiencies of 60-100% are possible depending on operating pressure.

The device is not suitable for freshwater or water of low salinities. It is however suitable for use with

Fig. 3. 5. 1 Column Oxygenator

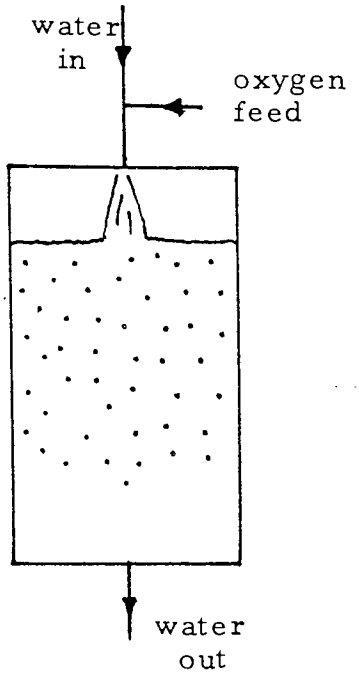

Fig. 3. 5. 2 Jet Oxygenator

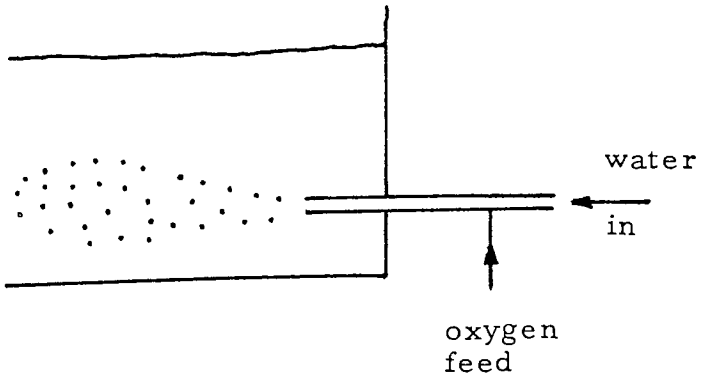

oxygen-enriched air though this may limit the operating pressure.

3.5.3 U-tube Oxygenator (Fig. 3.5.3)

This system was originally developed for aeration but the characteristics of U-tube operation make it suitable for oxygenation. It is one of the few techniques which can provide gas bubbles with a sufficiently long path length for efficient dissolution in freshwater, as the path length and hence oxygen dissolution efficiency are dependent on U-tube depth. In addition, the method has the virtues associated with U-tube aeration, namely an increasing hydrostatic head for enhanced Co_2^* values and a low driving force, enabling high rates of transfer for low cost.

For a 6m deep U-tube a change in dissolved oxygen concentration from 10 ppm to 15 ppm is possible at 75% dissolution efficiency and from 10 ppm to 20 ppm at 65% dissolution efficiency. Transfer efficiencies depend on the capacity of the unit but for a typical driving force of 0.2 m head of water 9 kg0_2/kWh may be calculated from theoretical considerations for an outlet concentration of 15 ppm d0_2(Speece, 1969).

The system was developed for use in freshwater but it may also be suitable for saline water, if a sufficient contact time can be achieved. It is also suitable for oxygen-

enriched air provided the depth of the U is not sufficient to cause nitrogen supersaturation.

3.5.4 Diffuser Elements (Fig. 3.5.4)

Using the energy stored in the oxygen due to its pressurisation on evaporation, oxygen bubbles can be created through a diffuser element.

In freshwater, small bubbles are generated which very quickly coalesce to form bubbles 2 - 5 mm in diameter which require long path lengths for dissolution, the minimum being about 10m. In rearing enclosures with a typical depth of 1 m, they are at best about 15% efficient. Therefore,they are not recommended as a means for oxygen dissolution although they are an effective st nd-by measure.

In seawater, the smaller bubbles formed require much shorter path lengths and under limited conditions they are a suitable method of oxygenation as dissolution efficiencies of 60-65% can be achieved in 1.5 m of water provided the oxygen flow-rate is low enough to avoid bubble coalescence.

For porous plastic tube used in tests an oxygen flow-rate of 0.18 m^3/h per metre length of diffuser was found to be acceptable although this will vary with diffuser type.

Diffusers are suitable for use with oxygen-enriched air.

Fig. 3.5.3 U-tube Oxygenator

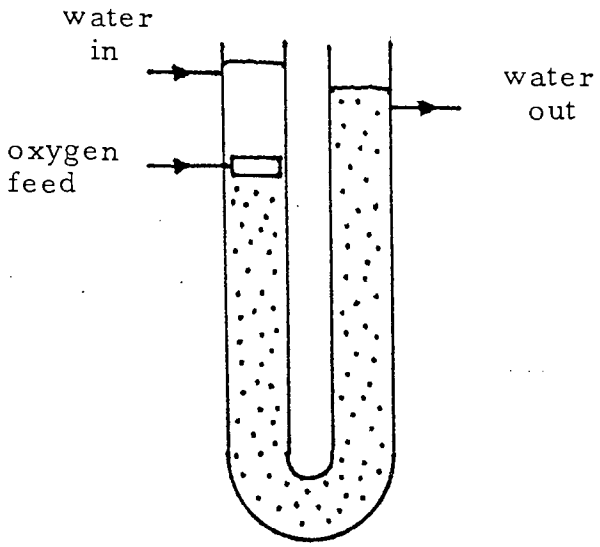

Fig. 3.5.4 Diffuser Element

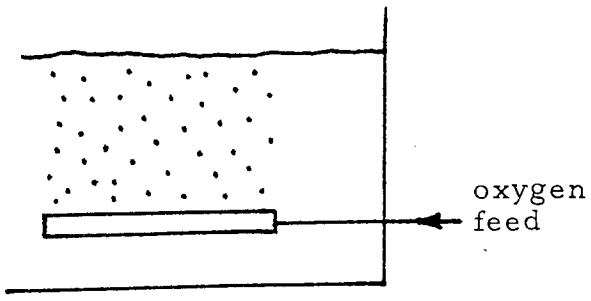

3.6 Application of Oxygenation to Fish Farming

The various approaches to oxygenation given above may be used to improve water economy in the majority of fish farms. However, certain advantages may be gained from the way in which these methods are used on the farm. These will now be discussed, followed by a general review of oxygenation for fish farming.

Although it is somewhat over simplifying the situation, there are basically two points at which oxygenation can be undertaken in a fish farm. These are (1) into the primary water source and (2) into individual production units.

3.6.1 Oxygenation of the Primary Water Source

Introduction of oxygen into the primary water supply has the substantial advantage of requiring only one point of oxygenation and is, therefore, simple. Its effectiveness is derived from the fact that, with pure oxygen, high oxygen gradients ($Co_2^* - Co_2$) and ($Co_2 - Co_{2,T}$) are produced in the oxygenator and, hence, high rates of transfer are possible even if the primary water source is already saturated. It is therefore relatively easy to raise the dissolved oxygen concentration, Co_2, of the water source to supersaturated levels, thereby increasing the amount of oxygen available to the fish.

For example, a typical situation in many trout farms would be that where the primary water source naturally contains 10 ppm dO_2 and, during passage through the farm, this is reduced to 5 ppm dO_2; thus, there is 5 ppm dO_2 available for the fish. By increasing the dissolved oxygen level in the water supply to, say, 15 ppm, twice as much oxygen is available and a two-fold saving in water use is achieved.

Higher levels of supersaturation may be achieved either by accepting lower dissolution efficiencies or by increasing the operating pressure. The cost of increasing oxygen addition will be a trade-off between power requirements and dissolution efficiency, therefore. If high pressures are considered, however, the oxygenator may need to be designed to pressure-vessel safety standards, thereby increasing capital expenditure.

In addition two potential problems can arise through increased water use, if achieved in this way. Firstly, if high levels of supersaturation are achieved through the use of high pressures then a reduction to atmospheric pressure en route to the rearing tank may cause "degassing", that is oxygen may come out of solution and escape to atmosphere. Secondly, as a result of high water utilisation the water flow to each production unit may be very low. Since this water will contain oxygen dissolved

to very high levels, poor mixing of the oxygenated water within the production unit may result. Just how far supersaturation of the water source can be taken depends very much on a particular application.

3.6.2 Oxygenation of Individual Production Units

Introduction of oxygen into individual fish production units is more complex because individual supply points and oxygenators are required. Dissolution is most commonly achieved by a sidestream system, whereby a quantity of tank water is withdrawn from the tank and oxygenated, frequently to supersaturated levels in the oxygenation device and then returned to the tank. The main advantage of oxygenation by this method is that individual oxygen control in production units is possible and in general, higher levels of water economy, up to 15 times, can be achieved without excessive pressurisation or a reduction in dissolution efficiency. In addition the quantities of water involved in a sidestream system are generally sufficient to provide good mixing of the oxygenated water. Control of the dissolved oxygen level can be precisely adjusted to the fishes' variable demand and optimum requirements, merely by linking the output from a meter monitoring tank dissolved oxygen levels to a regulator on the oxygen gas supply.

3.6.3 Raised Dissolved Oxygen Levels

Using either technique for oxygenation, one particular benefit resulting from the ability to super-saturate the water is the facility to maintain dissolved oxygen levels in the production units at, or even above, that of saturation. This may be of considerable importance in maintaining optimum conditions for fish growth when oxygen requirements are high and saturation dissolved oxygen levels are naturally low.

3.6.4 Oxygen for Stand-by

The use of pure oxygen can also be extremely effective as a stand-by measure. The risk of stock losses can be greatly reduced if a reasonable quantity of oxygen is stored on site. Since such a store provides its own pressure supply, oxygen gas can be piped to individual production units independently of any external power source and can be simply diffused into the water. Such diffusion is a very inefficient way to dissolve the gas but this is acceptable for a back-up system and the method readily lends itself to automatic control.

3.6.5 Gas Desorption

High dissolution efficiencies are necessary in oxygen-ation devices, so there is little scope for stripping of other

gases. This is most important in the case of carbon dioxide which is produced by fish respiration. A consequence of using oxygenation methods to save water, therefore, can be an increase in dissolved levels of carbon dioxide. The significance of this, however,will depend on the degree of water economy to be achieved, the nature of the water source and the species of fish being farmed.

3.6.6 The Cost of Oxygen and Reliability of Supply

The cost of oxygen will be a major factor in assessing the merits of an oxygenation system. The cost is made up from three components namely manufacturing, distribution and storage. Manufacturing costs are related to the cost of energy and to the capital equipment required for the separation process. Distribution costs are a function of distance from the source of manufacture and for some farms located in remote areas are prohibitive. Storage in any quantity is almost always undertaken in vacuum-insulated containers in which oxygen is held in liquid form at -183^{o} C. Such storage is both routine and reliable but the storage tanks are expensive.

Reliability of supply must be guaranteed and in situations where there is any uncertainty, for example in locations which may be isolated by adverse weather

conditions, adequate storage capacity must be specified and stocks well maintained.

The alternative to liquid oxygen is of course the PSA plant, although as yet it is untested in fish farm conditions. However, it is becoming more widely used in sewage treatment processes despite the fact that it is a highly-sophisticated piece of equipment. The capital cost of a PSA plant is extremely high, especially for a high-purity gas. The plant is also electrically powered so a stand-by system must be considered in case of power failure.

3.7 Conclusions

The cost of oxygen is a principal factor in determining the viability of oxygenation, and a major consideration in equipment design is the need to achieve high dissolution efficiencies. The specification of an oxygenation system must be considered in conjunction with many factors concerning the way the farm operates. Where this results in a cost-effective solution, the use of oxygen can have some significant advantages.

Firstly, improved water use may be achieved either by oxygenating the primary water source for simplicity, or by oxygenating tank water for closer individual control. Secondly, dissolved oxygen levels can be maintained up to or even above saturation levels, where this may achieve optimum conditions for fish growth. Thirdly, oxygen can

be used as an effective stand-by system independently of any external power source.

However, as a result of the high dissolution efficiencies necessary, oxygenation methods will remove little metabolically produced carbon dioxide and increased dissolved levels of this gas may be expected.

CHAPTER 4

THE COLUMN OXYGENATOR

4.1 Introduction

A low pressure column oxygenator has been developed to support individual rearing tanks at the Low Plains site. The maximum oxygen demand was estimated to be 600 g/h, which had to be met at high dissolution efficiencies, and the liquid flow-rate had to be sufficient to create an even oxygen distribution throughout the tank without causing excessive turbulence.

The Low Plains site was originally designed to produce around 80 tonnes of 250g trout per year in 20 production tanks. The water supply is abstracted from three boreholes and a total of 200m^3/h water is pumped to site. The water temperature is nearly constant at 9°C.

Preliminary ideas for modelling column operation are introduced: these are based on experimental work and additional material relating to the theory of plunging jets.

4.2 Equipment and Experimental Programme

4.2.1 Equipment

The design of the prototype column was based on a high pressure bubble column evaluated by the University of Birmingham (Hood, 1976). Hood concluded that the bubble column approach was an effective method of dissolving pure oxygen but that a reduction in operating pressure could significantly reduce running costs.

A prototype low pressure column was constructed from clear PVC tube, 0.3m in diameter 1.2m in length. A sheet steel cone, fitted to one end of the column, was connected to a pump via 75mm diameter flexible pipe, and a 75mm diameter outlet pipe was attached to the side of the column, close to the flat base (see Fig. 4.2.1). A valve was connected between the pump and the column to control the water flow-rate, and a second valve was connected to the column outlet pipe to vary the pressure, which was monitored with a pressure gauge. A sample point was fitted to the outlet pipe, near to the tank, to monitor dissolved oxygen concentrations.

Water was pumped from the tank, mixed with oxygen in the column, and returned to the tank carrying some undissolved gas with it. Oxygen flow-rate was controlled with a flow-meter, valve and pressure gauge. The general equipment layout is shown in Fig. 4.2.2.

4.2.2 Experimental Programme

The parameters investigated in the first phase of the experimental work were liquid flow-rate, oxygen flow-rate and operating pressure. Two values of each parameter were chosen, making a total of eight tests.

Fig. 4.2.1 The Prototype Column Oxygenator

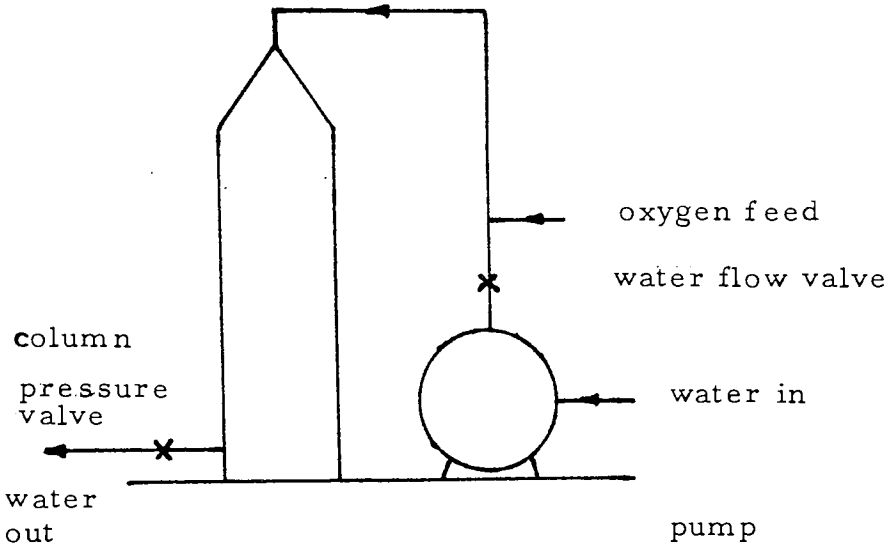

Fig. 4.2.2 The General Layout of Prototype Equipment

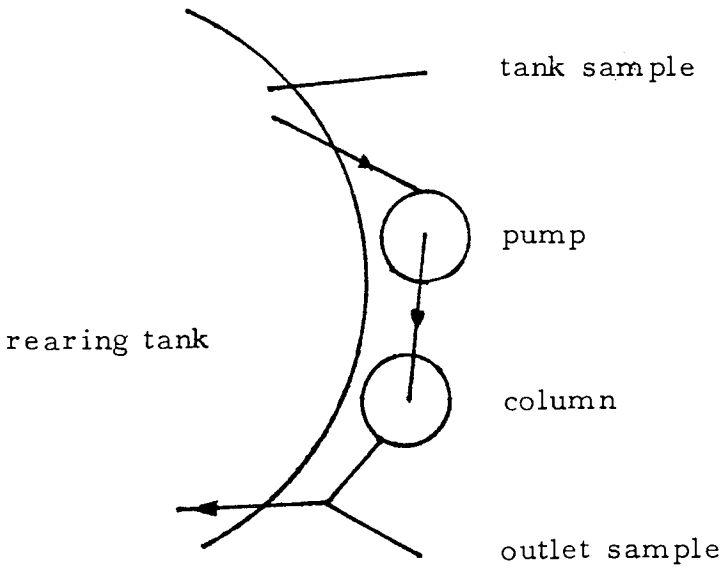

The liquid flow-rates used were:

30 m^3/h - an upper limit placed on the recirculation rate, to avoid excessive turbulence in the rearing tank, and

10 m^3/h - to measure the variation in performance with liquid flow-rate.

The oxygen flow-rates selected were:

600 g/h - the maximum required, assuming complete dissolution, and

200 g/h - to measure the variation in performance with oxygen flow-rate.

The pressures* employed were:

1.48 atm - the maximum safe working pressure of the column, and

1.14 atm - the lowest pressure, at which the column would operate due to internal pressure losses.

For each test the liquid flow-rate, operating pressure and oxygen flow-rate were set and the system left for 30 minutes to stabilise. Samples were then taken from the column outlet pipe and from the tank near the pump inlet. A second set of samples was taken after one hour to check that steady-state conditions had been reached. Dissolved oxygen concentrations of the samples were determined by the Winkler method (APHA, 1971).

* Pressures given in this chapter are absolute pressures.

A similar series of tests were conducted at the Finnarts Bay site using 16ppt salinity water. Dissolved oxygen concentrations were measured there using a Phox portable dissolved oxygen meter with a Mackereth-type probe: a single set of samples was taken after 30 minutes, as the results at Low Plains suggested that the column had stabilised within this period. The water temperature was also recorded since variations were to be expected.

Both series of tests were designed for factorial analysis, and Yates' method of analysis was used to determine the importance of the liquid flow-rate, oxygen flow-rate and pressure on the response variables - oxygen dissolution rate and oxygen dissolution efficiency. The method of analysis is given in Appendix 1.

4.3 Results and Observations

4.3.1 Results Summary

Untreated data and the results of the analysis are given in Tables 4.3.1 to 4.3.4. Results based on samples taken at 30 mins. and one hour have been combined since there was little difference between them.

TABLE 4.3.1 Untreated Data - Fresh Water at Low Plains

Absolute Pressure (atm)	Oxygen Flow-rate (g/h)	Liquid Flow-rate (m^3/h)	Oxygen Dissolved (g/h)	Oxygen Dissolution Efficiency (%)
1.48	592	30	573	97
1.14	600	30	461	77
1.48	225	30	221	98
1.14	248	30	236	95
1.48	616	10	238	39
1.14	600	10	210	35
1.48	224	10	194	87
1.14	216	10	87	41

Water temperature - 9°C

TABLE 4.3.2 Untreated Data - 16 ppt Salinity Water at Finnarts Bay

Absolute Pressure (atm)	Oxygen Flow-rate (g/h)	Liquid Flow-rate (m^3/h)	Oxygen Dissolved (g/h)	Oxygen Dissolution Efficiency (%)
1.48	596	30	346	58
1.14	604	30	296	49
1.48	200	30	177	88
1.14	198	30	147	74
1.48	600	10	192	32
1.14	600	10	174	29
1.48	200	10	142	71
1.14	200	10	120	58

Water temperature - 7°C

TABLE 4.3.3 Results of Analysis - Fresh Water at Low Plains

	Oxygen Dissolved (g/h)	Dissolution Efficiency (%)
Average Effect	278	71
Pressure	29	9
Oxygen	93	-9
Pressure/Oxygen	6	-3
Liquid	95	21
Liquid/Pressure	-6	3
Liquid/Oxygen	51	4
L/P/O	26	7

TABLE 4.3.4 Results of Analysis - 16 ppt Salinity Water at Finnarts Bay

	Oxygen Dissolved (g/h)	Dissolution Efficiency (%)
Average Effect	199	58
Pressure	15	5
Oxygen	53	-15
Pressure/Oxygen	2	-2
Liquid	42	10
Liquid/Pressure	5	1
Liquid/Oxygen	27	2
L/P/O	3	1

L/P/O is the Liquid/Pressure/Oxygen interaction

Low Plains Site - Fresh Water

Both the oxygen dissolution efficiency and the absorption rate increased with the liquid flow-rate, and both parameters were further improved with an increase in pressure. However, the dissolution efficiency was reduced as the oxygen flow-rate was increased. Although the target figure of 600 g/h oxygen absorbed was not achieved, it was considered that a further increase in oxygen flow-rate at the higher pressure and liquid flow-rate might be sufficient to dissolve 600 gO_2/h at an acceptable dissolution efficiency.

Results at 1.48 atm are given in Fig. 4.3.1 in the form of a contour plot. Assymptotes have been used to assist in the construction of the graph since (1) dissolution efficiency tended to 100% as the liquid flow-rate was increased at a constant oxygen-input, and (2), experimentally, outlet concentrations of 35 ppm dO_2 were never exceeded so this was taken to be an upper limit at the operating pressure of the column.

The contour plot shows that with a liquid flow-rate of 30 m^3/h and an operating pressure of 1.48 atm, the required absorption rate of 600 g/h is close to the efficient operating limit of the column. It also indicates that efficient dissolution can be achieved when the required absorption rates are below the maximum.

Fig. 4. 3. 1 Oxygen Absorption Rate Contour Plot For the Prototype Column - 1.48 atm

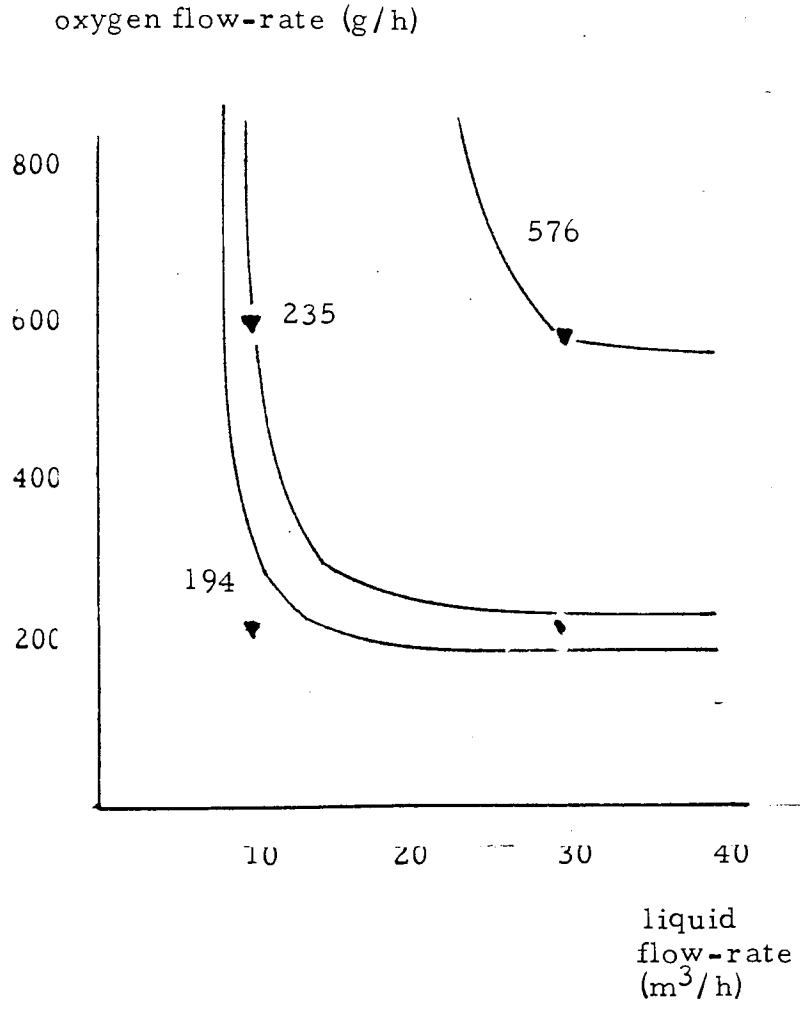

Finnarts Bay - Saline Water

Analysis of the results showed similar trends to those obtained during operation in fresh water, but lower overall dissolution efficiencies and absorption rates were found.

4.3.2 Visual Observations

Estimates of bubble diameter and the height of the different zones were made by eye (see Figs. 4.3.2 to 4.3.5).

(1) Low Plains Site - Fresh Water

At 10 m^3/h there were two distinct zones in the column (see Fig. 4.3.2). A gas space occupied about 75% of the total column volume through which the inlet water flowed in the form of a vertical jet. The jet impinged on the liquid surface, maintaining a dense bubble regime in the liquid. Bubbles of 2-5 mm diameter were observed, some of which were swept from the column along the outlet pipe.

When the liquid flow-rate was increased to 30 m^3/h there were three zones in the column volume; the bubble regime became deeper, although the bubble size remained constant at 2-5 mm diameter; and a third region was observed containing mostly liquid together with a few very small bubbles about 1 mm in diameter. These small bubbles were slowly carried out of the column but none of the larger bubbles escaped (see Fig. 4.3.3).

Fig. 4.3.2 Observed Flow in the Column

(Freshwater; Flow - 10 m^3/h)

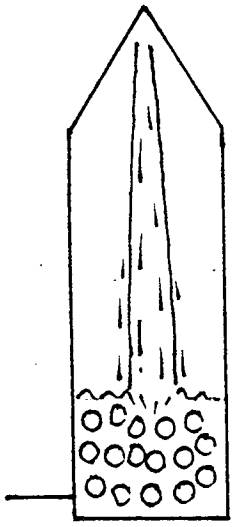

Large gas space occurs with liquid jet flowing through it

dense bubble regime:
2-5 mm diameter bubbles observed

Fig. 4.3.3 Observed Flow in the Column

(Freshwater; Flow - 30 m^3/h)

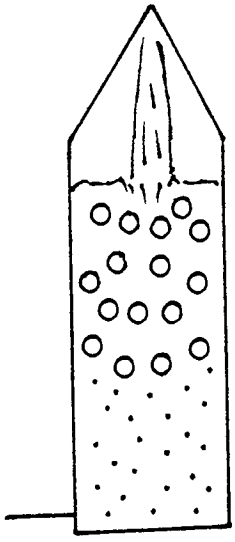

gas space reduced

bubble regime deepens:

2-5 mm diameter bubbles observed

a few small 1 mm diameter bubbles observed in a region containing mostly liquid

In general, as the oxygen flow-rate was increased, the volume of the gas space increased, the depth of the bubble regime increased slightly and more gas bubbles escaped through the outlet.

Increasing the operating pressure caused a reduction in the size of the gas space.

(2) Finnarts Bay - 16 ppt Salinity Water

In saline water there were two zones in the column (see Fig. 4.3.4). The gas space occurred, occupying 50-70% of the total volume, with the jet of inlet water flowing through it, but the bubble regime consisted of densely packed, 1 mm diameter bubbles. These small bubbles were continuously swept from the outlet.

Increasing the liquid flow-rate made little difference to the appearance of the column but the size of the gas space was reduced and the foam layer at the interface between the two zones became enlarged (see Fig. 4.3.5).

As the oxygen flow-rate was increased the gas space increased and the bubble regime became more dense.

As the pressure was increased the volume of the gas space reduced slightly.

4.4 Final Design of the Production Unit

The production column, 1.2 m high and 0.3 m in diameter, is constructed from glass fibre, with PVC pipe fittings

Fig. 4.3.4 Observed Flow in the Column

(Salinity - 16 ppt; Flow - 10 m^3/h)

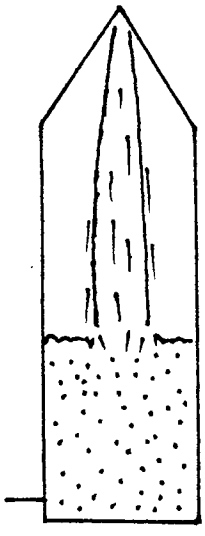

large gas space with liquid jet flowing through it

dense bubble regime:
1 mm diameter bubbles observed

Fig. 4.3.5 Observed Flow in the Column

(Salinity - 16 ppt; Flow 30 m^3/h)

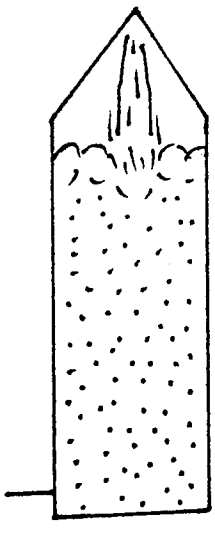

gas space reduced

bubble regime deepens:
1 mm diameter bubbles observed

moulded into the top and bottom (see Fig. 4.4.1). The column has a flat top, since it is considered unlikely that any advantage would be gained by having a conical top, due to the presence of the gas space during operation. The column also has a flat base so as to be self-supporting. The inlet pipe is 75 mm in diameter and the outlet pipe is 50 mm in diameter. A reducer is inserted in the outlet pipe to maintain the operating pressure. The general equipment layout is shown in Fig. 4.4.2.

The pump, specified as part of the oxygenation system, is manufactured by Worthington-Simpson Ltd, and the required performance is obtained with a 0.75 kW motor. The power consumed is estimated to be 0.7 kW, based on manufacturer's data and this corresponds to a transfer efficiency of 0.9 kgO_2/kWh at the maximum oxygen demand. Unfortunately, the net positive suction head (NPSH) requirement of the pump is greater than the head available from the tank water, and so the required liquid flow-rate is only attained at a pressure of 1.41 atm. The results obtained from the production unit operating at 1.41 atm are given in Fig. 4.4.3. The purged gas content was determined using a Beckman oxygen gas analyser and the rates of oxygen and nitrogen purged are also given.

The capital and operating costs for oxygenating the tanks at the Low Plains site are given in Chapter 8.

Fig. 4.4.1 The Production Column

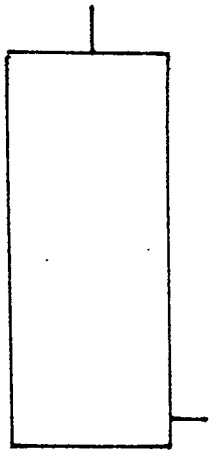

Inlet diameter - 75 mm

Column dimensions:

1.2 m high; 0.3 m diameter

Outlet diameter - 50 mm

Fig. 4.4.2 General Layout of Production Equipment

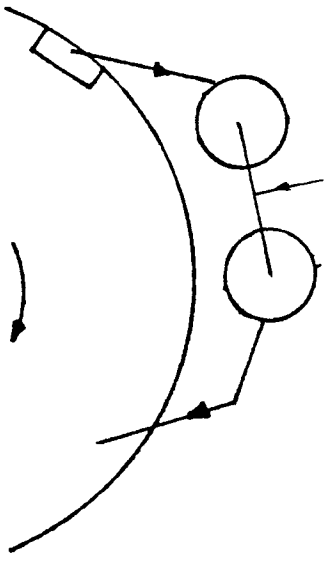

rearing tank

Inlet screen

pump

O_2 injection point

column

outlet pipe directed such that water flow creates circulation in rearing tank

Fig. 4.4.3 Oxygen Absorption and Purged Gas Data For the Production Column - 1.41 atm

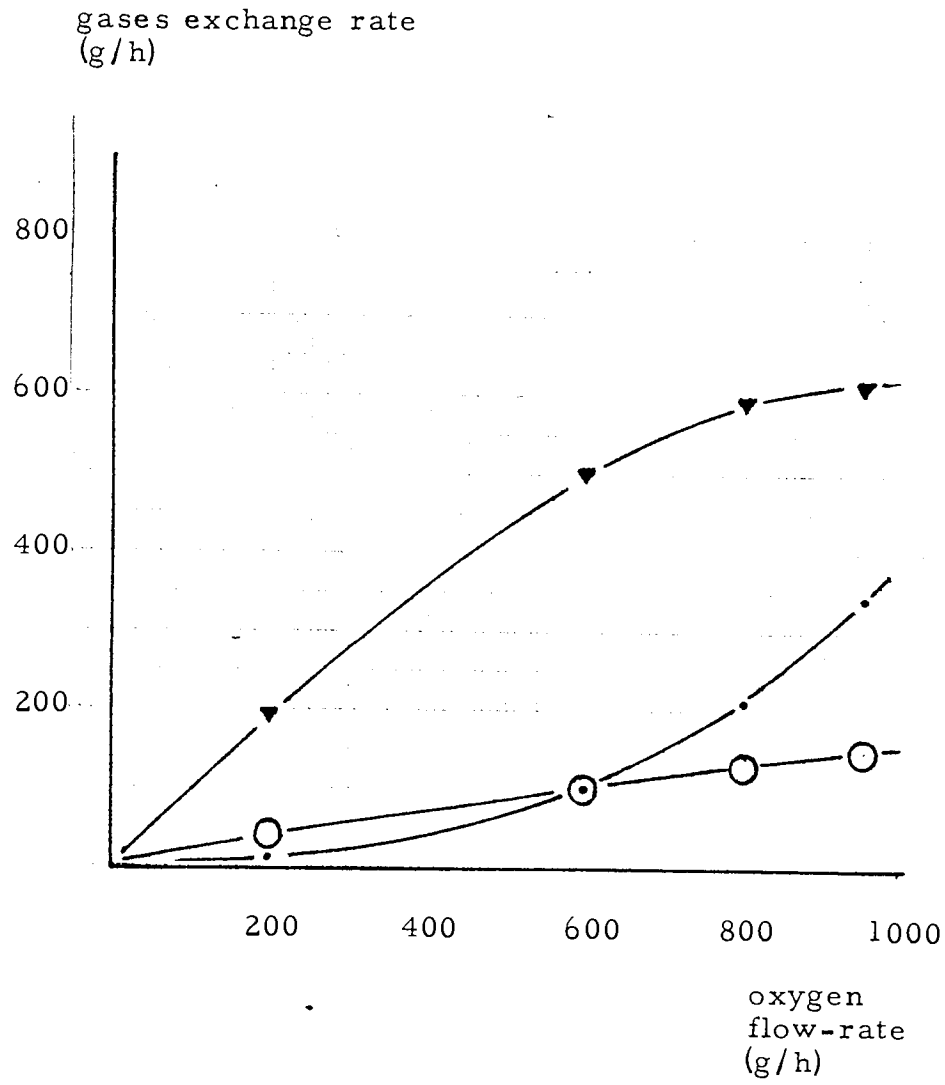

▼ - oxygen absorbed

• - oxygen purged at outlet to tank

o - nitrogen purged at outlet to tank

4.5 Theory of the Column Oxygenator

4.5.1 Modelling of Column Operation

Gas introduced into the column is trapped by the high inlet and low outlet superficial liquid velocities. A gas space accumulates at the top of the column and the incoming liquid forms a jet flowing through the gas space. The jet entrains gas bubbles into the liquid in the column which maintains a two-phase region (see Fig. 4.5.1). The size of the gas space varies with the oxygen flow-rate.

The aeration effects of the plunging jet were first realised over fifty years ago (Mertes, 1938). More recently, various studies have been undertaken with small diameter, high-velocity jets aerating open pools (Burgess et al, 1972; Smith and van de Sande, 1973). Plunging jets have been considered also in more practical situations, and the overall mass transfer coefficient has been estimated for jets up to 68 mm in diameter (Sneath, 1976); in the system studied by Sneath, the volume of the aerated liquid was also large compared with the liquid flow-rate through the jet. Bin (1979) has commented on the relatively high oxygen transfer efficiency of such aeration devices due to the large specific gas-liquid interface which can be generated.

Bubble sizes of 1.3-4 mm have been observed in plunging jets (Bin, 1979). In the column oxygenator the liquid flow-rate was relatively large compared with the volume of the column

Fig. 4.5.1 Column Operation

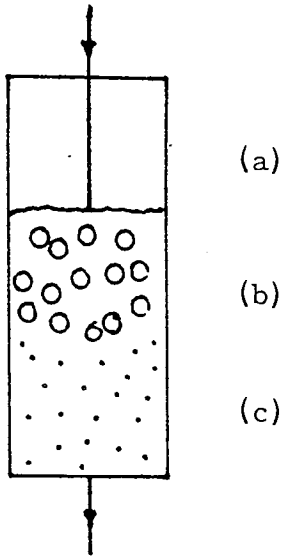

The jet plunging through the gas space (a) entrains gas bubbles into the liquid which maintains a two-phase region (b).
Some smaller bubbles are swept from the column by the superficial liquid velocity (c).

and some smaller bubbles were swept out of the column by the superficial liquid velocity. For this reason, the overall oxygen dissolution efficiency was slightly reduced (see Fig. 4.5.1).

4.5.2 Column Operation Using Pure Oxygen

In developing a model of oxygen transfer in the column oxygenator, the case of complete oxygen absorption is considered first. Oxygen transfer rates can be estimated using the following principles and assumptions.

(1) Let the operating pressure in the column be P_B. Initially, nitrogen will desorb into the gas phase since the gas contains only oxygen. As all the oxygen is absorbed, no gas is purged, and so nitrogen will accumulate in the gas phase until equilibrium is reached between the gas and liquid phases (see Fig. 4.5.2). At equilibrium, for air-saturated water, the nitrogen partial pressure, P_{N_2}, equals 0.8 atm, and the oxygen partial pressure, P_{O_2}, is given by

$$P_{O_2} = P_B - P_{N_2} \qquad 4.5.1$$

Also,
$$C^*_{O_2,B} = P_{O_2} C^*_{O_2} \qquad 4.5.2$$

and
$$C^*_{N_2,B} = P_{N_2} C^*_{N_2} \qquad 4.5.3$$

Fig. 4.5.2 Steady-state Conditions for Modelling Column Operation - No Gas Purged

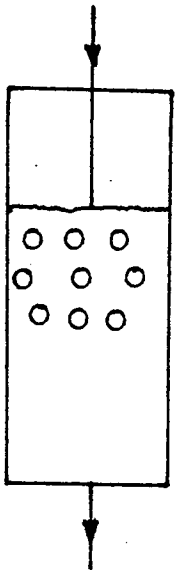

Operating Pressure, P_8

No gas is purged so nitrogen will accumulate in the gas phase, when

$$P_{N_2} = 0.8 \text{ atm}$$

$$P_{O_2} = P_o - P_{N_2} \text{ atm}$$

where $C^*_{O_2,B}$ and $C^*_{N_2,B}$ are the equilibrium concentrations of dissolved oxygen and dissolved nitrogen for the gas bubbles in the column, and $C^*_{O_2}$, $C^*_{N_2}$ are the equivalent values for oxygen and nitrogen respectively at a pressure of 1 atm.

(2) The liquid velocity at the nozzle,

$$v_n = \frac{4 Q_L}{\pi d_n^2} \qquad 4.5.4$$

where d_n is the nozzle diameter and Q_L is the liquid flow-rate.

An estimate of the head loss at the nozzle, h, can be obtained from

$$v_n = k\sqrt{(2gh)} \qquad 4.5.5$$

where $k = 0.8$ (Degrémont, 1979)

It should be remembered, however, that h is the head loss across the nozzle due to the change in liquid velocity through the nozzle and does not include the head which must be overcome due to the operating pressure, P_B.

The jet power, W_n, is given by

$$W_n = \frac{\rho g Q_L h}{1000} \qquad 4.5.6$$

where ρ is the liquid density (kg/m^3)

and g is gravitational acceleration (m/s^2)

(3) The overall mass transfer coefficient, K, can be predicted from the jet power, W_n (Sneath, 1976):

$$\frac{K}{d_n} = 5.134\ W_n + 0.59$$

In this empirical equation, the overall mass transfer coefficient is expressed in units of $(\text{minute})^{-1}$ with the jet power measured in kilowatts and the nozzle diameter in metres. Values of $k_L A$ (with units of m^3/s) can be derived with the use of the multiplication factor $\left(\frac{V}{60}\right)$, where V is the tank volume used by Sneath,

since $\frac{K}{60} = \frac{k_L A}{V}$

Hence $k_L A = 0.2\ (5.134\ W_n + 0.59)\ d_n \qquad 4.5.7$

It should be noted that this estimate does not include any term accounting explicitly for the oxygen flow-rate.

(4) Oxygen mass transfer is governed by the relationship

$$\varphi_{O_2} = k_L A \left(C^*_{O_2,B} - C_{O_2}\right) \qquad 4.5.8$$

Because of the observed flow patterns in the column the system will be assumed to be well-mixed.

An overall mass balance on oxygen leads to the relationship

$$\varphi_{O_2} = Q_L \left(C_{O_2} - C_{O_2,T}\right) \qquad 4.5.9$$

where C_{O_2} is the outlet dissolved oxygen concentration

and $C_{O_2,T}$ is the inlet dissolved oxygen concentration.

Similarly, nitrogen transfer is determined by

$$\varphi_{N_2} = k_{L,N_2} A \left(C_{N_2} - C^*_{N_2,B}\right) \qquad 4.5.10$$

and

$$\varphi_{N_2} = Q_L \left(C_{N_2,T} - C_{N_2}\right) \qquad 4.5.12$$

Since $k_L \propto \sqrt{\text{diffusivity}}$,

$$\frac{k_L}{k_{L,N_2}} = \frac{\sqrt{(O_2 \text{ diffusivity})}}{\sqrt{(N_2 \text{ diffusivity})}} \qquad 4.5.13$$

4.5.3 Sample Calculation based on Experimental Data

The following data, based on experimental results, are used to predict oxygen transfer assuming complete oxygen dissolution. The effect of operating pressure is easily incorporated and is also explored.

Data

(1) Liquid flow-rate, $Q_L = 30 m^3/h = 8.3 \times 10^{-3}\ m^3/s$

(2) Jet nozzle diameter, $d_n = 0.076$ m

(3) Operating pressure P_B = (a) 1.14 atm.
(b) 1.48 atm

(4) $C_{O_2}^* = 54$ ppm dO_2 at 1 atm and 10^oC; $C_{O_2,T} = 10$ ppm dO_2
$C_{N_2}^* = 24$ ppm dN_2 at 1 atm and 10^oC; $C_{N_2,T} = 19$ ppm dN_2

(5) Liquid density $\rho = 1000\ kg/m^3$
$g = 10\ m/s^2$

(6) $P_{N_2} = 0.8$ atm

Calculation

Then (a)	P_{O_2}	= 0.34 atm	from equ. 4.5.1
and	$C_{O_2}^*$	= 18.7 ppm dO_2.	from equ. 4.5.2
Now	v_n	= 1.83 m/s	from equ. 4.5.4
	h	= 0.26 m	from equ. 4.5.5
and	W_n	= 0.022 kW;	from equ. 4.5.6
therefore	$k_L A$	= 0.01 m^3/s	from equ. 4.5.7

Solving equations 4.5.8 and 4.5.9 simultaneously,

$$C_{O_2} = 14.8 \text{ ppm } dO_2$$

and

$$\varphi_{O_2} = 143 \text{ g/h}$$

Since there is no nitrogen purged the nitrogen is in equilibrium between the gas and liquid phases and no net nitrogen transfer occurs.

(b) $P_{O_2} = 0.68$ atm when $P_B = 1.48$ atm

so $C_{O_2}^* = 37$ ppm dO_2. from equ. 4.5.2

$k_L A = 0.01 \text{ m}^3/\text{s}$ as before.

Again solving equations 4.5.8 and 4.5.9 simultaneously,

$$C_{O_2} = 24.8 \text{ ppm } dO_2$$

and

$$\varphi_{O_2} = 443 \text{ g/h}$$

4.6 Discussion

The results predicted using the model suggest that, with an operating pressure of 1.14 atm, up to about 140 g/h can be dissolved at 100% dissolution efficiency, and at 1.48 atm, this is increased to 440 g/h. Complete dissolution was never achieved in tests due to the presence of the microbubbles which were swept out of the column, reducing the overall dissolution efficiency. Observed results,

which were achieved at about 95% dissolution efficiency, are compared with the predicted results in Table 4.6.1. The observed results are higher than predicted values, although this is explained in part by the lower dissolution efficiency achieved in the observed results. This aspect is considered more fully in section 4.6.1.

TABLE 4.6.1 Comparison of Predicted and Observed Transfer Rates for the Prototype Column

Operating Pressure (atm)	Observed Dissolution Rate (95% Dissolution) (g/h)	Predicted Dissolution Rate (100% Dissolution) (g/h)
1.14	190	143
1.48	576	443

The predicted ($k_L A$) values are based on an empirical relationship involving the liquid velocity at the nozzle and the nozzle diameter (Sneath, 1971). Other workers have also found similar relationships (Bin, 1979). In the column oxygenator, the gas space increases as the oxygen flow-rate increases and, as a result, the jet length, that is the distance from the nozzle to the liquid surface, is dependent on the oxygen flow-rate. Bin (1979) concludes that the effect of jet length on ($k_L A$) is small for high-velocity jets and consideration of the action of gravitational acceleration on high velocity jets over relatively small jet lengths would

tend to confirm this. On the other hand, Barret et al (1960) found that oxygen transfer in waterfalls was dependent on the height of fall. Jet length may therefore influence ($k_L A$) values generated by the low-velocity jets, produced in the column oxygenator. The dependence of ($k_L A$) on jet length implies that the gas-liquid interfacial area and, hence, gas hold-up in the two-phase region are dependent on the oxygen flow-rate, which was observed in tests. A more detailed analysis of the independent variables affecting ($k_L A$) generation is, therefore, required.

4.6.1 Effects of Phase Flow-rates

Oxygen Flow-rate

If the oxygen flow-rate is increased beyond that where 100% dissolution can be achieved under the prevailing operating conditions, then oxygen will begin to accumulate in the gas phase and the equilibrium concentration will increase (see Fig. 4.6.1). However, the nitrogen concentration will decrease, assuming the operating pressure is unchanged, so nitrogen will no longer be in equilibrium between the phases and hence will be desorbed. By removing nitrogen gas from the column, therefore, the nitrogen equilibrium concentration, $C^*_{N_2,s}$ will always be less than the dissolved nitrogen concentration, C_{N_2}, in the column; as a result, higher values of the oxygen equilibrium

Fig. 4.6.1 Steady-state Conditions for Modelling Column Operation - Small Gas Bubbles Purged.

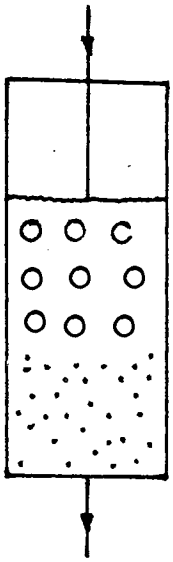

Small gas bubbles purge column of some nitrogen. The nitrogen partial pressure is reduced which allows higher oxygen partial pressure to exist in the column, so higher oxygen transfer rate is achieved. Small gas bubbles also contain oxygen so oxygen dissolution efficiency is reduced.

concentration, $C^*_{O_2,B}$, can be maintained in the oxygenator, and so higher oxygen transfer rates can be achieved. Nitrogen can be purged from the column in the microbubbles swept out by the superficial liquid velocity. Oxygen will also be contained in the microbubbles, so the greater the oxygen flow-rate, the higher the oxygen concentration in the gas bubbles and, hence, the lower the oxygen dissolution efficiency. In addition, as the oxygen flow-rate is increased, more nitrogen must be purged to allow higher values of $C^*_{O_2}$ to exist in the column, and since the nitrogen concentration in each bubble is reduced, more bubbles must be purged from the column. Eventually, if the oxygen flow-rate is high enough, sufficient nitrogen is only purged when large gas bubbles are swept from the column. In this condition, the gas space is very large to allow sufficient gas loss and the dissolution efficiency falls more rapidly (see Fig. 4.6.2). It is important to realise that column operation is self-regulating and depends directly on the oxygen flow-rate.

For any oxygen flow-rate, a steady-state condition will exist in the column oxygenator with

$$O_2 \text{ input} = O_2 \text{ absorbed} + O_2 \text{ purged}$$

and N_2 desorbed = N_2 purged.

Gas will therefore accumulate in the gas space until sufficient nitrogen is purged to reach the steady-state condition.

Fig. 4.6.2 Steady-state Conditions for Modelling Column Operation - Large Gas Bubbles Purged.

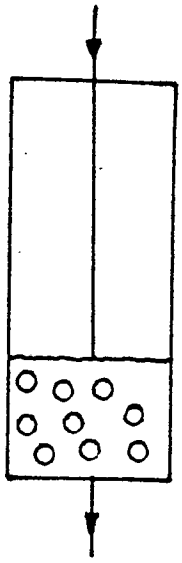

At high oxygen transfer rates, high oxygen partial pressures are necessary and much nitrogen must be purged. This is only achieved when large gas bubbles are purged from the column. Much oxygen is lost in the gas bubbles and the oxygen dissolution efficiency falls rapidly.

This particular aspect of the mass transfer process within the oxygenator is important since column operation can be studied by considering the rate of nitrogen purged from the system. Predicted and observed transfer rates are given in Table 4.6.2 for the production column when 50, 100 and 150 g/h are purged respectively. Comparison of results suggests that the predicted transfer rates are optimistic. This is most likely due to the assumptions made in estimating ($k_L A$) values.

TABLE 4.6.2 Comparison of Predicted and Observed Transfer Rates for the Production Column

	φ_{N_2} (g/h)	C_{N_2} (ppm)	$C^*_{N_2,B}$ (ppm)	$C^*_{O_2,B}$ (ppm)	C_{O_2} (ppm)	φ_{O_2} (g/h)
Predicted	0	19	19	32.9	22.5	375
	50	17.3	15.7	40.9	26.9	506
	100	15.7	12.5	47.9	30.7	622
	150	14.0	9.3	55.0	34.6	737
Observed	50	17.3	17.7	36.5	22.6	380
	100	15.7	15.8	40.6	26.6	498
	150	14.0	12.7	47.6	29.0	570

Observed equilibrium concentrations in the column are based on the gas concentrations measured in the purged gas, and this is justified since the system is well-mixed. However, inspection of the nitrogen mass transfer rates, taken from experimental observations, shows that at the lower oxygen transfer rates, the dissolved nitrogen concentration, C_{N_2}, is extremely close to the equilibrium concentration, $C^*_{N_2,B}$, and is, therefore, unlikely to yield the assumed nitrogen desorption rate.

This may be due entirely to assumptions made in estimating $C_{N_2,T}$ and $C^*_{N_2,B}$, but, if valid, the values suggest that the gas residence time in the column is long enough for the nitrogen to approach a new equilibrium condition between the gas and liquid phases with the superficial liquid velocity

purging sufficient nitrogen to allow increased oxygen transfer rates. However, at the highest oxygen transfer rate, sufficient nitrogen is only purged when the nitrogen equilibrium concentration, $C^{*}_{N_2,B}$, deviates from the dissolved nitrogen concentration, C_{N_2} . The existence of nitrogen, therefore, at, or near, equilibrium between the two phases may well determine the limits of acceptable dissolution efficiency.

The above may be, in turn, linked to one of the limitations of the model. Using the model, increased dissolved oxygen concentrations are always predicted by assuming more purged nitrogen and by accepting a lower dissolution efficiency, whereas experimental analysis suggests that an upper limit exists for the dissolved oxygen concentration, for any operating pressure. This limit may be caused by many factors which change as the gas space increases, such as (1) the respective oxygen and nitrogen gas residence times in the column, (2) a reduction in ($k_L A$) as the jet impinges on the base of the column, or (3) the reduction in liquid residence time. Table 4.6.3, which provides estimates of the relative gas and liquid residence times, shows that the oxygen gas residence time remains roughly constant, despite an increasing oxygen transfer rate; the nitrogen gas residence time reduces as more nitrogen is purged to allow the increased oxygen transfer rate; and the liquid residence time is almost halved as the gas space increases. It is

important for design purposes both to define the operating limit in relation to the pressure, and to determine how closely this upper limit can be approached whilst maintaining an acceptable dissolution efficiency.

TABLE 4.6.3 Estimates of Gas and Liquid Residence Time in the Column

Oxygen Flow-rate (g/h)	Jet Length (m)	Gas Residence Times (s)		Liquid Residence Time (s)
		O_2	N_2	
200	0.1	278	∞	8.3
400	0.3	288	2200	6.6
600	0.5	302	1400	4.8

Liquid Flow-rate

There are several aspects of the liquid flow-rate which are important in oxygenator design. Of these, the most important is the effect of the liquid flow-rate on ($k_L A$). Increasing the liquid flow-rate through the nozzle produces increased ($k_L A$) values. However, if the liquid flow-rate is doubled (and the nozzle diameter remains constant), examination of equations 4.6.4 - 4.6.7 shows that the head loss across the nozzle is increased by a factor of four. The jet power is increased by a factor of eight, and as a result, ($k_L A$) is doubled. Alternatively, if the nozzle diameter is increased but the liquid velocity at the nozzle is kept constant,

($k_L A$) is increased by about 60% but the jet power is doubled (see Table 4.6.4).

TABLE 4.6.4 Effect of Liquid Flow-rate on ($k_L A$)

Liquid flow-rate, (m^3/s)	8.3×10^{-3}	16.7×10^{-3}	16.7×10^{-3}
Nozzle diameter, (m)	0.076	0.076	0.107
Nozzle velocity, (m/s)	1.83	3.66	1.83
Head loss, (m)	0.26	1.04	0.26
Jet power, (kW)	0.022	0.173	0.044
$k_L A$ (m^3/s)	0.011	0.022	0.017

In either case, therefore, oxygenation using larger liquid flow-rates is likely to be less efficient. It should be noted, however, that the head loss across the nozzle is small compared with the total operating head, and so there may be scope for improving performance by optimising both generated ($k_L A$) values and operating pressures.

Two other effects of the liquid flow-rate are also important: these are the depth of jet penetration and the superficial liquid velocity in the column. The depth of penetration is an important consideration when estimating the design height of the column: the height must be such that the jet does not impinge on the bottom of the column or force gas bubbles out of the column prematurely. An

estimate of the depth of jet penetration, H_p , can be derived from

$$H_p = 1.75\ v_n^{0.85} d_n^{0.65} \qquad \text{(van de Sande \& Smith, '74)}$$

The superficial liquid velocity in the column must be fixed so that only the microbubbles are purged and that the larger bubbles are maintained in the bubble regime. The superficial liquid velocity of 0.114 m/s used in the 0.3 m diameter prototype column, was not found to be satisfactory when employed in larger columns. In bubble columns the velocity of liquid circulation has been found to depend on gas hold-up and column diameter (Joshi and Sharma, 1979). A similar relationship between superficial liquid velocity and column diameter is anticipated for the column oxygenator.

There are, then, many aspects of the liquid flow-rate, both at the nozzle and through the column which need to be quantified.

4.6.2 Effects of Salinity

The reduction in performance with salinity is also considered to occur as a result of the effects of the superficial liquid velocity. Assuming a reduction in mean bubble size from 2 mm to 1 mm diameter as the salinity is increased from 0 to 15 ppt, k_L is reduced by about 50% but the gas-liquid interfacial area is increased by about 400%. $(k_L A)$ values

should be approximately doubled, therefore. The reduction in Co_2^* with salinity will reduce this benefit slightly, but, since an overall reduction in transfer rate was found, the most likely conclusion is that gas bubbles are swept out of the column more readily. It would seem possible to overcome this by decreasing the superficial liquid velocity: however, further development work was not continued due to the potential of the jet oxygenator in seawater.

4.6.3 Tank Mixing of Oxygenated Water

One other criterion for oxygenator design is the effect of liquid mixing within the rearing tank. Mixing in tanks using submerged jets is considered more fully in section 5.6.3 but, using the data collected, a mean circulation velocity of 0.3 m/s appears to satisfy operating requirements. Under these conditions the estimated mixing time is about 14 minutes in the tanks at Low Plains.

4.7 Conclusions

The column oxygenator is an effective freshwater oxygenation device. A unit has been designed to support Low Plains rearing tanks up to the maximum requirement of 600 gO_2/h, with dissolution efficiencies generally close to 100%. With a liquid flow-rate of 30 m^3/h and an operating

pressure of 1.4 atm, a transfer efficiency of about 1kgO_2/kWh is achieved at the maximum oxygen demand.

A model has been developed to analyse column operation. The model is in the early stages of development since present understanding of many aspects of the column oxygenator is limited.

CHAPTER 5

THE SUBMERGED JET OXYGENATOR

5.1 Introduction

This chapter describes the development of a low pressure jet to support Finnarts Bay tanks. The maximum oxygen demand is estimated to be 2 kg/h which must be met at high dissolution efficiencies. Oxygenation must also maintain adequate water circulation without causing excessive turbulence.

The Finnarts Bay site is capable of producing in excess of 250 tonnes of 250 g trout in 30 production tanks. Individual oxygenators are required for each tank. The farm operates on mixed salinities: eggs are hatched in freshwater and the larger fry are slowly acclimated to seawater. The majority of fish are kept in water of 20 - 30 ppt salinity.

Column oxygenators do not perform particularly well in saline water, but high pressure jet oxygenators are known to be capable of achieving high oxygen dissolution efficiencies (Harman, 1975; Jones, 1976). They are, however, mechanically unreliable and have high running costs. By reducing operating pressures, greater reliability and lower running costs were anticipated.

A low pressure unit was built and tested to determine its acceptable operating range. From the results a second prototype was designed to meet the oxygen requirements of rearing tanks. This led to the specifi-

cation of production oxygenators for the Finnarts Bay site.

Information gained from experimental work and additional material relating to the theory of jet flow is then used to model jet oxygenator performance.

5.2 Evaluation of the First Prototype

5.2.1 Equipment and Experimental Programme

Equipment

The jet oxygenator was constructed from a length of 50 mm diameter PVC pressure pipe, with a sweep bend attached to it. The end of the bend was then heated and squashed to make a narrow slot, approximately 75 mm by 3 mm. Operating pressure was adjusted by varying the size of the slot. The nozzle arrangement is illustrated in Fig. 5.2.1.

During operation, water was pumped from the tank through the oxygenator, where it was mixed with oxygen, discharged from the nozzle and dispersed in the tank. Oxygen flow-rate was controlled with a flow-meter, valve and pressure gauge. Water flow-rate varied with operating pressure and was measured at each pressure. Pressure was monitored with a pressure gauge. The general equipment layout is shown in Fig. 5.2.2.

Fig. 5.2.1 Nozzle Arrangement of the Jet Oxygenator

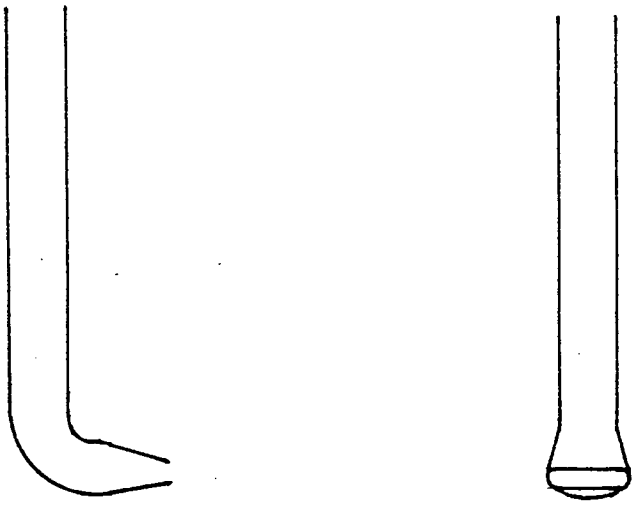

(1) Side View (2) Front View

Fig. 5.2.2 General Equipment Layout of the Jet Oxygenator

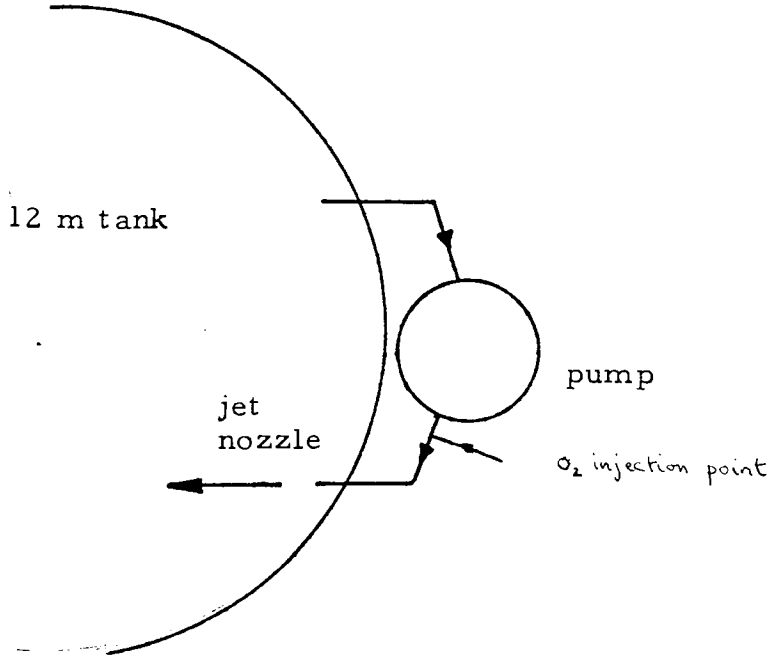

Experimental Programme

For the experimental runs three values were chosen for both the oxygen flow-rate and the operating pressure to explore performance up to the maximum requirement of 2 kgO_2/h. The three operating pressures were 1.34 atm, 1.82 atm and 2.90 atm*, and the oxygen flow-rates were 0.2 kg/h, 1.0 kg/h and 2.0 kg/h. The nine tests were conducted in freshwater initially, and were then repeated in 16 ppt salinity water to measure the anticipated change in performance. Water temperatures were measured daily. The method of determination of the oxygen dissolution rate and dissolution efficiency are given in Appendix 2.

5.2.2 Results and Observations

Results Summary

The results are summarised in tables 5.2.1 and 5.2.2. Water flow-rates for the oxygenators were 15.5, 13.0 and 12.6 m^3/h at operating pressures of 1.34, 1.82 and 2.90 atm respectively. Freshwater temperatures varied between 3 and 10°C during tests and the temperature of the 16 ppt salinity water was nearly constant at 7°C.

*Pressures given in this chapter are absolute pressures

TABLE 5.2.1 Experimental Data - Freshwater

Absolute Pressure (atm)	Oxygen Flow-rate (kg/h)	Oxygen Dissolved (g/h)	Dissolution Efficiency (%)
2.90	2.0	520	26
1.82	2.0	560	28
1.34	2.0	40	2
2.90	1.0	455	46
1.82	1.0	350	35
1.34	1.0	140	14
2.90	0.2	432	216
1.82	0.2	99	50
1.34	0.2	37	19

TABLE 5.2.2 Experimental Data - 16ppt Salinity Water

Absolute Pressure (atm)	Oxygen Flow-rate (kg/h)	Oxygen Dissolved (g/h)	Dissolution Efficiency (%)
2.90	2.0	720	36
1.82	2.0	790	40
1.34	2.0	490	25
2.90	1.0	545	55
1.82	1.0	585	59
1.34	1.0	325	33
2.90	0.2	304	152
1.82	0.2	288	144
1.34	0.2	116	58

Several large errors appeared in the results with dissolution efficiencies of up to 200% being recorded at low oxygen flow-rates. However, in other Shearwater tests, using high pressure jet oxygenators which have an operating pressure of 4 atm and a liquid flow-rate of 4.5 m^3/h, dissolution efficiencies of up to 150% have been found (Harman, 1975; Jones, 1976). Since the method used to calculate dissolution rates relies on perfect mixing within the tank (see Appendix 2), it is possible that this condition was not achieved in tests.

All tests show a reduction in dissolution efficiency with increased oxygen flow-rate. At the lowest pressure, dissolution rates were reduced when the oxygen flow-rate was increased from 1 kg/h to 2 kg/h. It is considered that the gas flow-rate might have been sufficient to cause slug formation thereby reducing the dissolution rate.

In freshwater, pressure has a significant effect on dissolution efficiency at low oxygen flow-rates, but this effect is reduced with increasing gas flow-rate. None of the devices performed particularly well, with the best, operating at 2.9 atm, dissolving less than 50% of an oxygen input of 1 kg/h.

Slightly higher dissolution rates were achieved, overall, using 16 ppt salinity water. The prototype operating

at 1.82 atm produced marginally higher dissolution rates than when operating at 2.9 atm. Even so, the best performance achieved was only 60% dissolution efficiency, using a 1 kg/h oxygen input.

Visual Observations

All measurements of bubble size were made by eye.

In freshwater, large bubbles of 2-5 mm diameter were seen at the water surface (see Fig. 5.2.3). The number of undissolved bubbles increased with oxygen flow-rate.

In 16 ppt salinity water, a cloud of small bubbles about 0.5 mm in diameter was observed, some of which reached the water surface (see Fig. 5.2.4). As the oxygen flow-rate was increased, the cloud became more dense.

In all cases, the oxygen did not appear to be dispersing well within the tank. No effects due to changes in operating pressure were observed.

5.2.3 Discussion and Conclusions Leading to the Design of the Second Prototype

Pressure has a major effect on oxygenator performance in freshwater, primarily due to the size of bubble generated. However, there was little difference in performance between the prototype operated at 2.9 atm pressure and a

Fig. 5.2.3 Observed Bubble Pattern at the Tank Surface

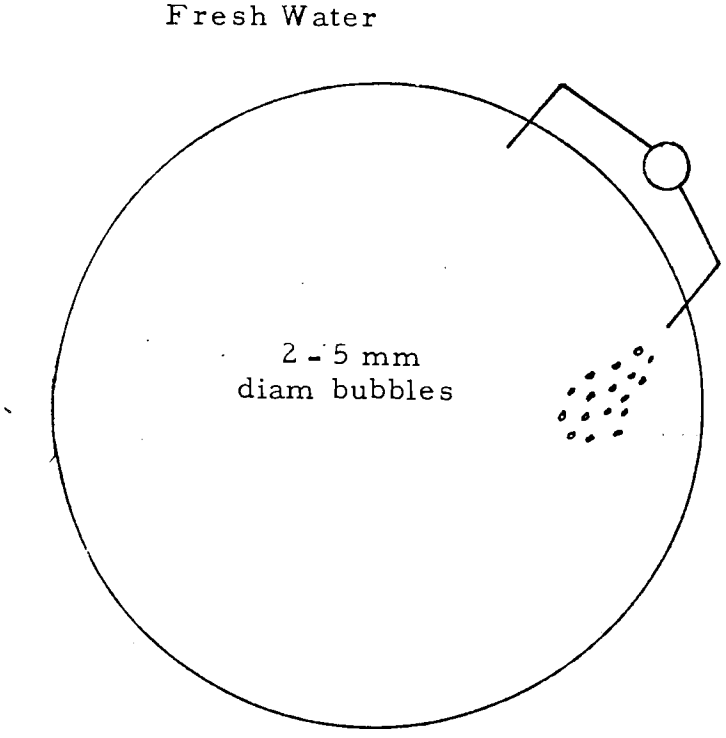

Fig. 5.2.4 Observed Bubble Pattern at the Tank Surface

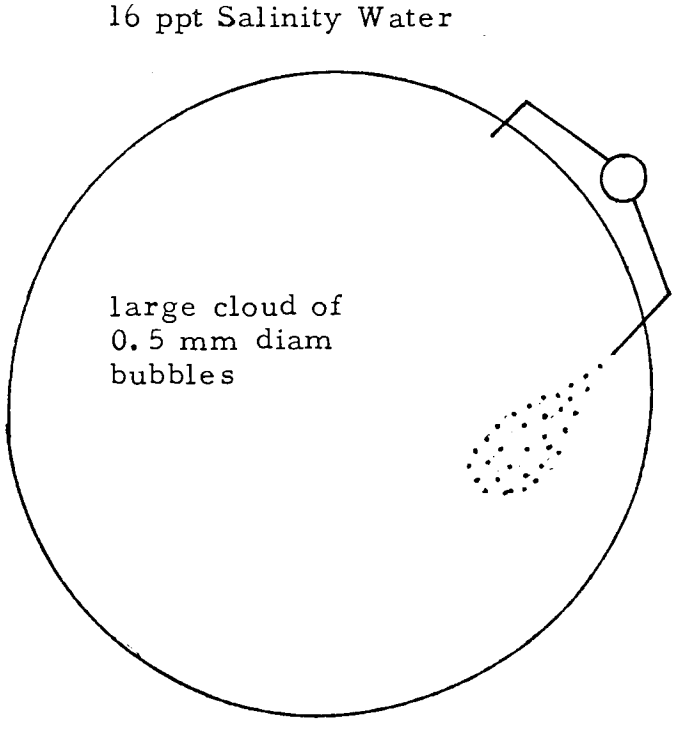

high pressure jet oxygenator, despite the differences in liquid flow-rate and operating pressure (see Fig. 5.2.5). In 16 ppt salinity water, the effects of pressure were far less dominant, but again comparative performance between the prototype operated at 2.9 atm and a high pressure jet oxygenator was similar (see Fig. 5.2.6). A further reduction in operating pressure to 1.82 atm actually improved performance.

This suggests that the operating pressure of this type of oxygenator can be reduced significantly, without affecting performance, provided the water flow-rate is increased simultaneously, although there would appear to be more scope for pressure reductions using saline water than freshwater. This may not reduce power requirements but it would allow the use of more reliable low pressure pumps.

In 16 ppt salinity water, a jet operating at 1.82 atm was found to give the best performance, but even so, the dissolution efficiency was only 60% with a 1 kg/h oxygen flow-rate. Four such devices would be necessary, therefore, to meet the peak oxygen requirements of the rearing tanks. Alternatively, it may be worthwhile specifying one large device with four times the liquid flow-rate of the prototype. In either case, the power consumption would be about 3 kW per tank.

At this operating pressure a jet oxygenator achieved only about 35% dissolution efficiency in freshwater using a 1 kg/h oxygen flow-rate and so it is not considered suitable as an efficient freshwater oxygenation device.

Fig. 5.2.5 Comparison of Jet Oxygenator Results - Freshwater

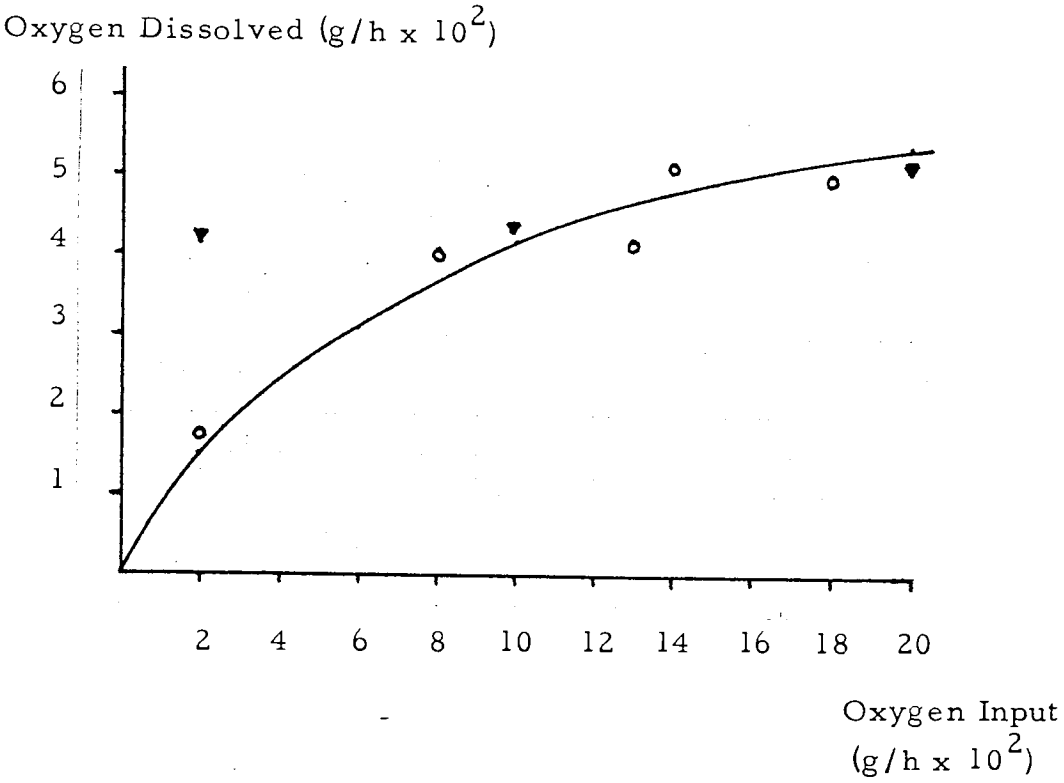

▼ - Author's present results (40 m^3/h, 2.9 atm)

o - Harman 1979 (4.5 m^3/h, 5.3 atm)

Fig. 5.2.6 Comparison of Jet Oxygenator Results - 16 ppt Salinity

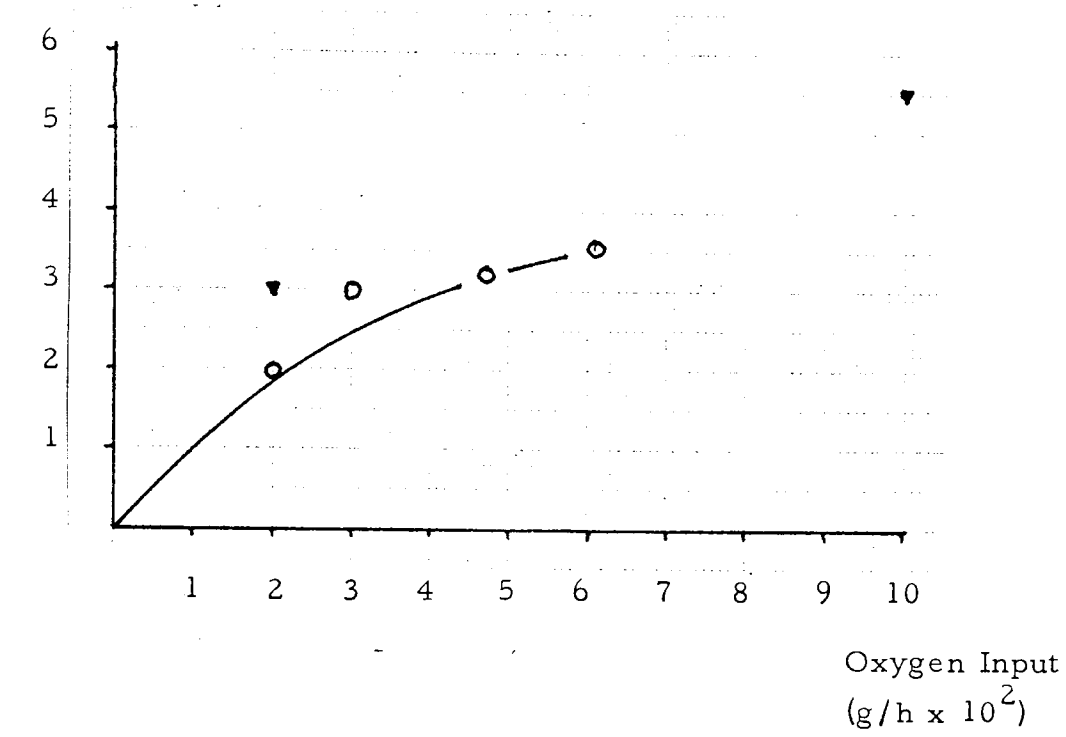

▼ - Author's present results (40 m^3/h, 2.9 atm)

o - Harman 1975 (4.5 m^3/h, 5.3 atm)

5.3 Evaluation of the Second Prototype

5.3.1 Equipment and Experimental Programme

A second prototype was designed to operate with four times the liquid flow-rate of the original, that is to say 60 m^3/h, and at a working pressure of 1.82 atm. It was hoped that tests on this unit would enable a final design for an oxygenation system at the Finnarts Bay site to be produced. The design was identical to that of the first prototype except that it was constructed in 75 mm diameter PVC pipe. A valve was added between the pump and the nozzle to control the liquid flow-rate.

Two values were chosen for each of the liquid flow-rate, oxygen flow-rate and operating pressure, making eight tests in all. The upper values of each parameter were those considered necessary to dissolve 2 kg O_2/h, based on the results of the original prototype, and the lower values were chosen to measure the change in performance due to each parameter.

The liquid flow-rates chosen were: 60 m^3/h and 40 m^3/h,
the oxygen flow-rates were: 3 kg/h and 1 kg/h,
and the operating pressures were : 1.82 atm and 1.41 atm.
Tests were conducted in 20 ppt salinity water.

The experimental procedure was identical to that used previously, except that the water flow-rate was set before each test. The dissolution rates and dissolution efficiencies

were found by the method given in Appendix 2. Yates' method of analysis was used to assess the importance of the liquid flow-rate, oxygen flow-rate and operating pressure on the two response variables, oxygen dissolution rate and oxygen dissolution efficiency. The method of analysis is given in Appendix 1.

5.3.2 Results and Observations

Results Summary

Untreated data and the results of the analysis are given in Tables 5.3.1 and 5.3.2. The water temperature during tests was 13°C.

Overall, increasing the liquid flow-rate from 40 m^3/h to 60 m^3/h had a slightly detrimental effect on the oxygen dissolution rate and dissolution efficiency. Increasing the pressure improved performance but more so at the lower liquid flow-rate. However, the overall effect of pressure is small at high water salinities, which confirms the results of the first prototype. Overall, changes in the oxygen flow-rate had little effect on dissolution efficiency.

A combined contour plot of dissolution rate and dissolution efficiency has been constructed using results from both prototypes operated with a 1 kg/h oxygen flow-rate (see Fig. 5.3.1). Insufficient data has been collected to repeat the plot using an oxygen flow-rate of 3 kg/h, but similar trends are expected.

Fig. 5.3.1 Contour Plot of Dissolution Rate and Dissolution Efficiency

Oxygen Input 1kg/h; Water Salinity 16 - 20 ppt.

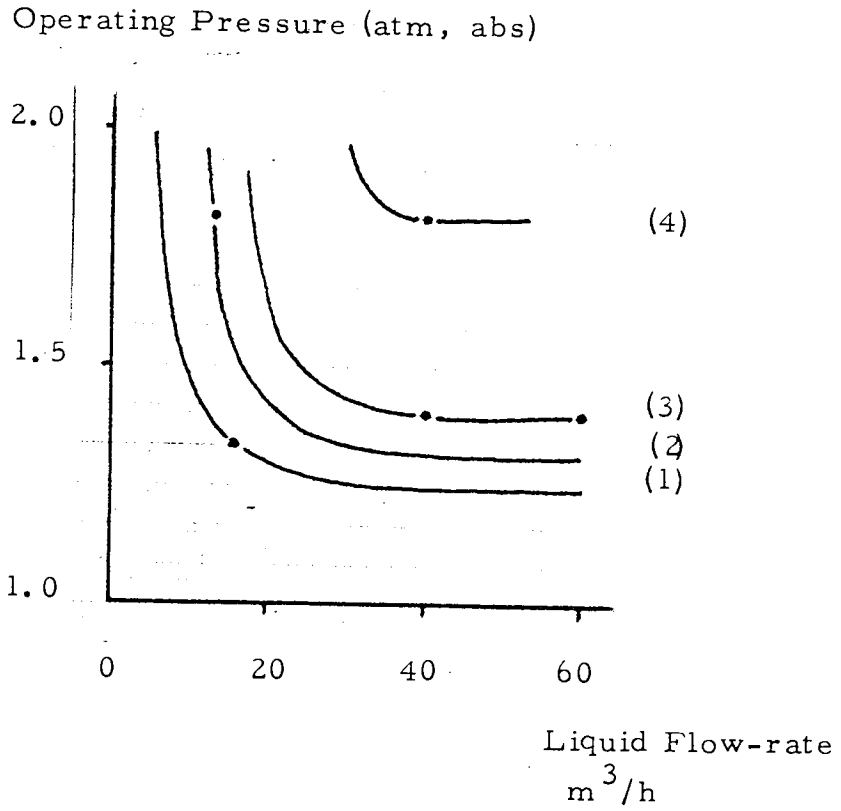

(1) - 325 g/h O_2 dissolved - 33% dissolution eficiency
(2) - 585 g/h O_2 dissolved - 59% dissolution efficiency
(3) - 675 g/h O_2 dissolved - 69% dissolution efficiency
(4) - 840 g/h O_2 dissolved - 84% dissolution efficiency

Additional data by Harman (1979) used to develop assymptotes for the construction of the contour plot (not shown).

TABLE 5.3.1 Experimental Data

Absolute Pressure (atm)	Oxygen Flow-rate (kg/h)	Liquid Flow-rate (m^3/h)	Oxygen Dissolved (g/h)	Dissolution Efficiency (%)
1.82	3	60	1758	59
1.41	3	60	1836	61
1.82	1	60	627	63
1.41	1	60	679	68
1.82	3	40	2754	92
1.41	3	40	1851	62
1.82	1	40	841	84
1.41	1	40	675	68

TABLE 5.3.2 Results of Analyses

	Oxygen Dissolution (g/h)	Dissolution Efficiency (%)
Ave. Effect	1378	69
Pressure	117	5
Oxygen	672	1
Pressure/Oxygen	89	2
Liquid	-153	-7
Liquid/Pressure	-150	-7
Liquid/Oxygen	-100	-2
L/P/O	-94	-1

Visual Observations

The operating pressure and the liquid flow-rate both affect the liquid velocity from the jet nozzle. At its lowest level (40 m^3/h, 1.41 atm), the velocity was such that some bubbles broke the surface about halfway across the tank (see Fig. 5.3.2). The bubbles were about 0.5 mm in diameter.

As the pressure and/or liquid flow-rate was increased, the jet penetration increased and the dispersion of bubbles improved so that no bubbles could be at the surface, or they were so widely dispersed as to be unnoticeable. At the highest liquid velocity (60 m^3/h, 1.82 atm), the jet stream could be seen bouncing off the far side of the tank, creating a "standing wave" which was observed at the surface (see Fig. 5.3.3). The appearance of this "standing wave" suggests that the jet penetration may have been excessive for the size of tank, which may explain the lower dissolution rates achieved when the liquid flow-rate was 60 m^3/h.

5.4 Final Design for the Production Unit

It was decided that there was no point in specifying a liquid flow-rate greater than 40 m^3/h for a jet oxygenator operating in Finnarts Bay tanks.

In the tests, increasing the pressure from 1.41 to 1.82 atm had improved the dissolution efficiency but in

Fig. 5.3.2 Jet Penetration (40 m^3/h, 1.41 atm)

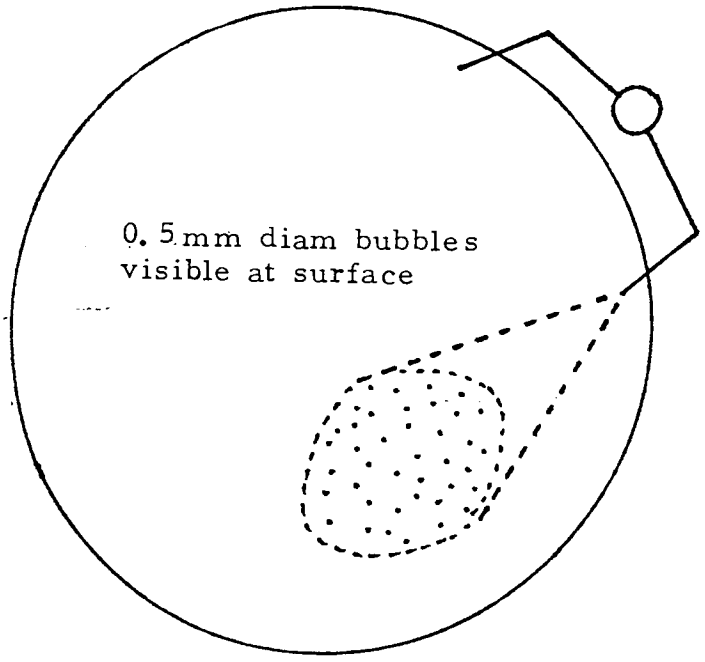

Fig. 5.3.3 Jet Penetration (60 m^3/h, 1.82 atm)

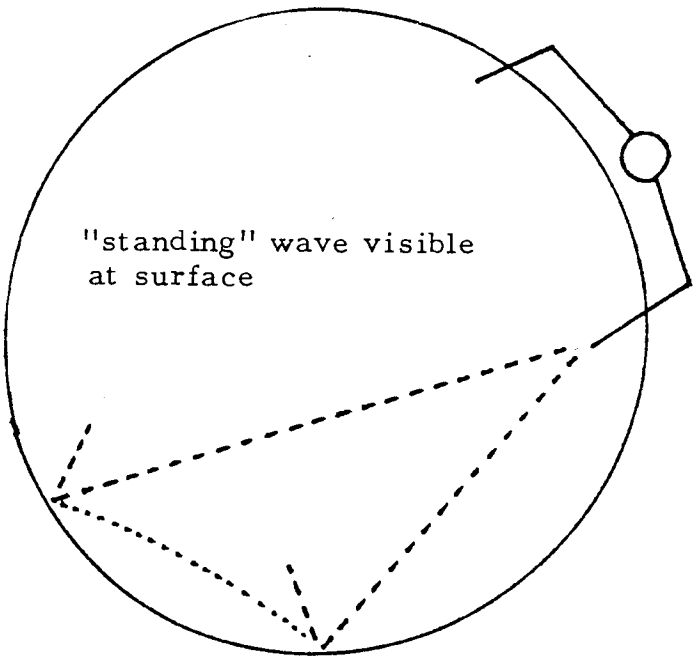

a production unit, this improvement would only be achieved with increased pumping costs. The operating pressure of the production unit was, therefore, chosen after considering estimates of the annual costs of oxygenating Finnarts Bay tanks.

Additional tests were conducted at intermediate pressures, corresponding to specific pump sizes, and the results are summarised in Table 5.4.1.

TABLE 5.4.1 Results of Tests at Intermediate Pressures

Absolute Pressure (atm)	Oxygen Flow-rate (kg/h)	Liquid Flow-rate m^3/h	Oxygen Dissolved g/h	Dissolution Efficiency (%)
1.68	3.0	40	2350	78
1.68	1.0	40	715	72
1.54	2.8	40	1890	68
1.54	1.0	40	725	73

Fig. 5.4.1, which shows the variation in performance with pressure when the liquid flow-rate was 40 m^3/h, was then used to estimate annual oxygenation costs at the Finnarts Bay site. These estimates suggested that an oxygenator pressure of 1.68 atm would result in lowest operating costs. Details of the costs are given in Chapter 8.

The final design for the jet oxygenator has a liquid flow-rate of 40 m^3/h and an operating pressure of 1.68 atm.

Fig. 5.4.1 The Variation in Oxygenator Performance with Pressure ($40m^3/h$, 20 ppt water salinity)

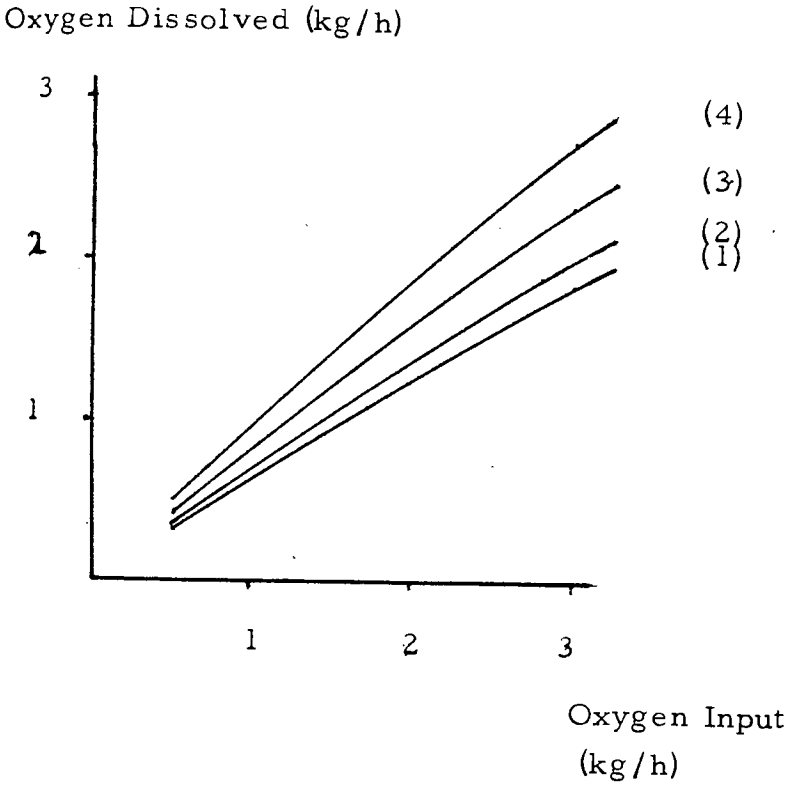

(1) 1.41 atm. abs.

(2) 1.54 atm. abs.

(3) 1.68 atm. abs.

(4) 1.82 atm. abs.

The jet nozzle is a slot, about 100 m long by 15 mm wide, cut in a length of PVC pipe. The pipe is placed vertically in the tank with the slot about 50 mm from the tank bottom (see Fig. 5.4.2). The jet formed by the water flow through the slot is directed at an angle of 45° to a tangent at the tank wall to promote good mixing.

The pump specified for the system is manufactured by Myson Pumps Ltd and the required performance is obtained using a nominal 1.5 kW motor. The manufacturer's data suggests that the power consumed will be 1.3 kW, which gives the jet oxygenator a transfer efficiency of 1.7 kg O_2/kWh. The dissolution efficiency is about 75% when operating at high water salinities. The variation in performance with salinity of the production unit is given in Fig. 5.4.3.

5.5 Theory of the Jet Oxygenator

5.5.1 Modelling of Jet Operation

The jet oxygenator operates, as an oxygen transfer device, by creating bubbles which are then dispersed in the tank by the flow of liquid from the jet nozzle. In the tank, bubbles rise to the surface and, in doing so, oxygen is absorbed and nitrogen desorbed.

Fig. 5.4.2 Nozzle Design for the Production Oxygenator

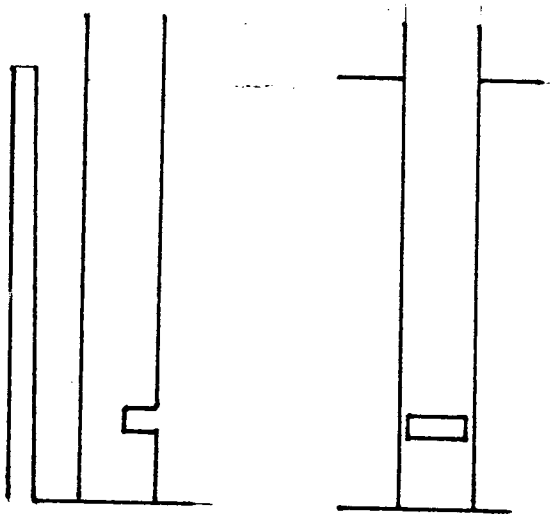

(a) Side View (b) Front View

Fig. 5.4.3 The Variation in Performance with Salinity of the Production Oxygenator - 3 kg/h oxygen input

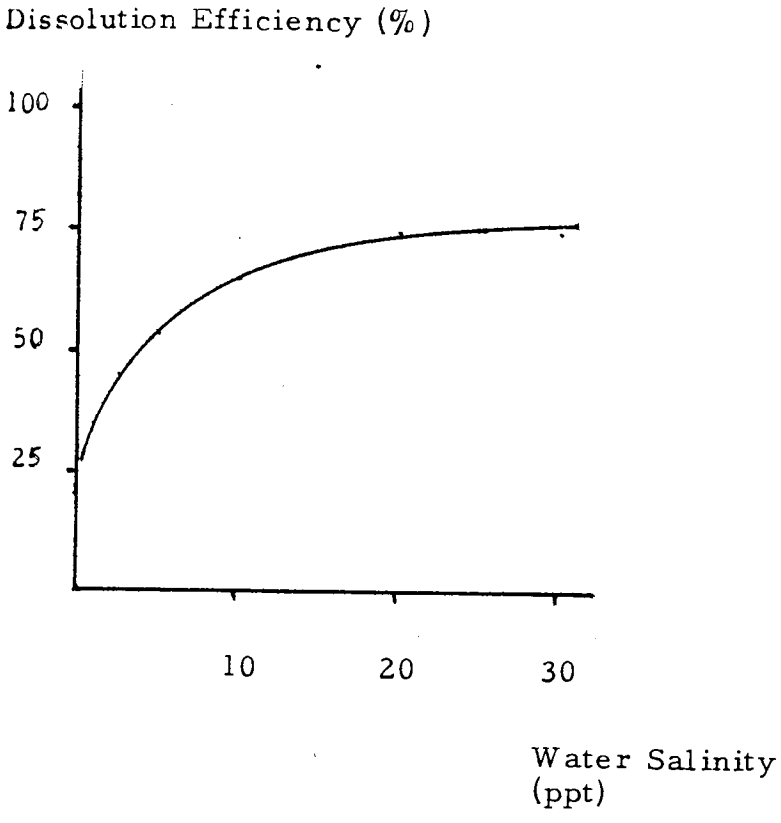

In developing a model of the behaviour of the system, two phase flow of the jet-stream has to be considered. The established jet theory is discussed and the conditions under which the theory is developed are compared to operation of the jet oxygenator in fish tanks. Results predicted by the model are then compared with the experimental observations.

5.5.2 Round Free Jet (following Davies, 1972)

The theory introduced here concerns the turbulent flow of a fluid through a second ambient fluid. This process has been covered in great detail by several authors (Ambromovich, 1963; Davies, 1972; Brodkey, 1975 and Hinze, 1975). Relatively straightforward modelling has been achieved by considering a round, free, turbulent jet of fluid issuing into the same still fluid. A free jet has a cross-sectional area of less than 20% of the total cross-sectional flow area of the region through which it is flowing. The flow is turbulent for $Re > 2500$. A free, turbulent jet is considered to comprise four flow regions as shown in Fig. 5.5.1. These are

(1) a region of flow establishment, extending to about 6.4 nozzle diameters (d_n) (the fluid in this region has a core velocity approximately equal to the mean discharge velocity, v_n),

Fig. 5.5.1 Flow Regimes in a Turbulent Jet

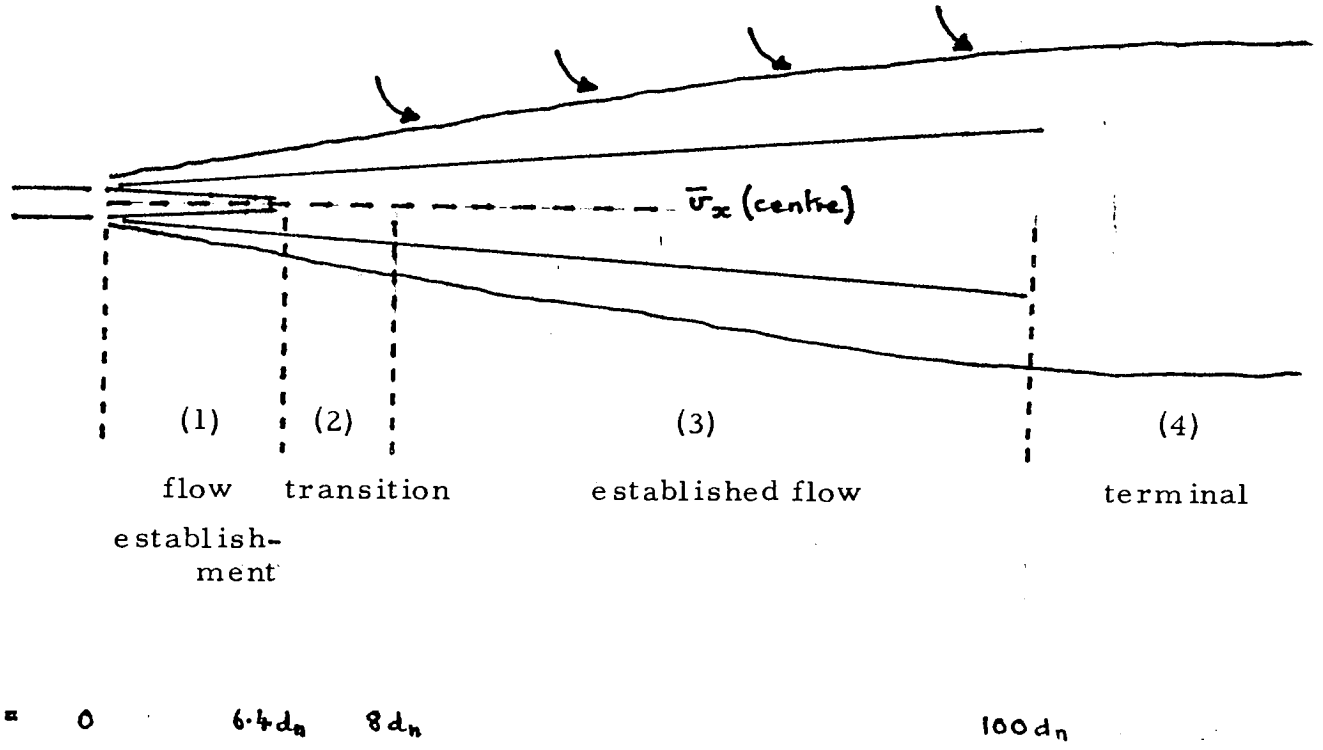

(2) a transition region from 6.4 - 8.0 d_n,

(3) a region of established flow extending to about 100 d_n,

(4) a terminal region where the centre line velocity decreases steeply to zero.

A virtual origin of the jet, x_{vo}, is taken at the end of the constant velocity core where $x_{vo} = 6.4\ d_n$. The axial velocity, $\bar{v}_x$(centre), is given by

$$\frac{\bar{v}_x\ (\text{centre})}{v_n} = \frac{x_{vo}}{x} \quad \text{for} \quad x > x_{vo}$$

where v_n is the axial velocity at the nozzle.

In and around the free turbulent jet, mixing occurs in three ways. Firstly, some of the surrounding fluid is entrained into the jet. Secondly, turbulent diffusion occurs within the jet and thirdly, general circulation is caused in the surrounding fluid. Entrainment occurs in relation to the spread of the jet which forms a cone of half angle 10 - 14°. Water jets, flowing into still water, entrain liquid such that

$$V_x = V_e + V_n = 0{\cdot}23 \frac{x}{d_n} V_n$$

where V_n = volumetric flow-rate at nozzle,

V_e = volumetric flow-rate entrained

and V_x = total volumetric flow-rate at x.

The constant 0.23 varies according to the half-angle of the cone and values as high as 0.34 have been recorded. The turbulent jet has no sharp boundary, the velocity

decaying gradually to zero near the boundary formed by the cone. An approximate Gaussian distribution is assumed for the velocity profile. Within the cone, a jet angle of about 5^{o} describes an inner cone formed by the locus of the half-centreline velocities; about 45% of the total volumetric flow occurs within this "half-speed" cone and about 55% outside.

5.5.3 Plane Jets (following Brodkey, 1975)

A plane jet is formed from a slot length, ℓ, and width, w. For $\frac{\ell}{w} > 20$, it exhibits approximately two-dimensional flow over the range $4 < \frac{x}{w} < 2\ell$, with rapid velocity decay from $\frac{x}{w} = 4$, according to the equation

$$\frac{\bar{v}_x\,(\text{centre})}{v_n} = 2.4\sqrt{\left(\frac{w}{x}\right)}$$

The virtual origin is given by $\frac{x_{vo}}{w} = 0.6$. Velocity distributions of different jets can differ in extent, despite constant jet Reynolds numbers, so flow conditions at the slot may play some part in jet behaviour.

Entrainment rate is given by the following equation:

$$\frac{V_{xs}}{V_{ns}} = 0.625\sqrt{\left(\frac{x}{w}\right)}$$

where V_{xs} is the total volumetric flow at

and V_{ns} is the volumetric flow at nozzle.

For $\frac{l}{w} < 20$, three-dimensional flow takes place and as $w \rightarrow d_n$ the flow regimes of the round, free jet predominate.

5.5.4 A Qualitative Comparison with the Experimental System

The submerged jet used in experimental runs, though simple in construction, is complex in its operation. Firstly, the fluid is a two-phase mixture of gas and water. Secondly, the buoyancy of the gas dictates that the jet of fluid must emerge as near to the bottom of the tank as is possible and, consequently, the jet is free on the upper side but restrained on the underside (see Fig. 5.5.2). Thirdly, because of the mixing requirements in the tank (see section 5.6.3), the jet is initially directed at 45° to the flow of the ambient liquid, and is then carried into the flow of the bulk liquid by the circular motion of the liquid in the tank. Finally, for ease of variation during experiments, the nozzle was formed by squashing a tube to make a slot with $3 < \frac{l}{w} < 10$. Such geometrics are likely to produce jets in the transition region between axisymmetric and plane jets.

These complexities have been neglected when attempting to model the system, and use has been made of theory describing the flow of an axisymmetric jet into still, ambient fluid. This approach can be justified on the following grounds. Firstly, the gas-liquid ratio in the jet

Fig. 5.5.2 Two-phase Submerged Jet in the Rearing Tank

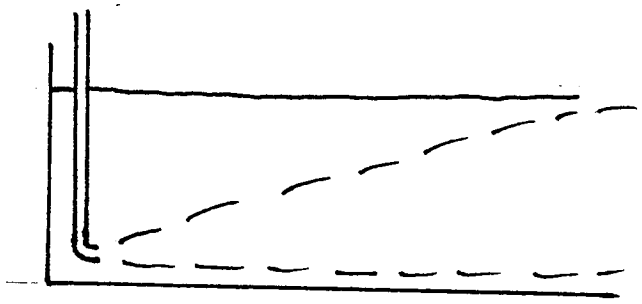

Jet must emerge as near the tank base as possible, due to the buoyancy of the gas. Jet is therefore restrained on the underside.

is low, at less than 5% by volume at atmospheric pressure, and the buoyancy of the gas is reflected in the bubble rise time. Secondly, compared with nozzle velocities of over 7 m/s, the velocity of the ambient fluid is relatively low, although it should be noted that the jet velocity will reduce to this value, rather than to zero as suggested by the general theory. Finally, with $\frac{l}{w} < 10$, flow will be predominantly three-dimensional and, therefore, will be more likely to conform to axisymmetric jet theory than to plane jet theory.

5.5.5 Two-Phase Submerged Jet Theory

In the two-phase flow of gas and liquid from an axisymmetric jet, produced from a nozzle, diameter d_n, into the surrounding liquid, the region of established flow is assumed to extend to a distance of 100 d_n, after which the centre-line velocity decreases steeply to $\bar{v}_c$, the mean tank circulation velocity. The liquid flow-rate increases with distance from the nozzle due to entrainment and the oxygen concentration in the gas reduces with distance as nitrogen is desorbed. The mass transfer rate from gas bubbles will therefore vary with distance from the nozzle, so a number of key assumptions and principles must be used to predict overall transfer rates.

(1) At the jet nozzle, the nozzle diameter, d_n, and the jet velocity at the nozzle, v_n, can be calculated from the volumetric flow-rate, V_n, and the operating pressure, h (expressed in metres of water head), by the following:

$$V_n = k(\pi d_n^2)\sqrt{(2gh)} \qquad 5.5.1$$

and

$$v_n = k\sqrt{(2gh)} \qquad 5.5.2$$

where $k = 0.62$ for an orifice (Degrémont, 1979).

(2) The cone of two-phase flow can be divided into regions ψ_i $(i = 1 \ldots m)$, where ψ_i is the volume of the region between x_i and x_{i-1} (see Fig. 5.5.3). x_i is the distance from the nozzle, with $x_0 = 0$ and $\sum_{i=1}^{m} (x_i - x_{i-1}) = 100\, d_n$. The liquid flow-rate, V_i, through each region, ψ_i, is taken to be the mean value and is assumed constant in each region (see Fig. 5.5.4). Then

$$V_i = 0{\cdot}23\, V_n \left(\frac{x_i + x_{i-1}}{2 d_n}\right) \qquad 5.5.3$$

(3) The initial oxygen flow-rate $R_{O_2,o}$ is broken down into bubbles, diameter d_B, at the nozzle, with the number of bubbles produced, N_o, being given by

$$N_o = \frac{R_{O_2,o}}{V_B\, \rho_{O_2}} \qquad 5.5.4$$

Fig. 5.5.3 The Cone of Two-phase Flow subdivided into Regions, ψ_i

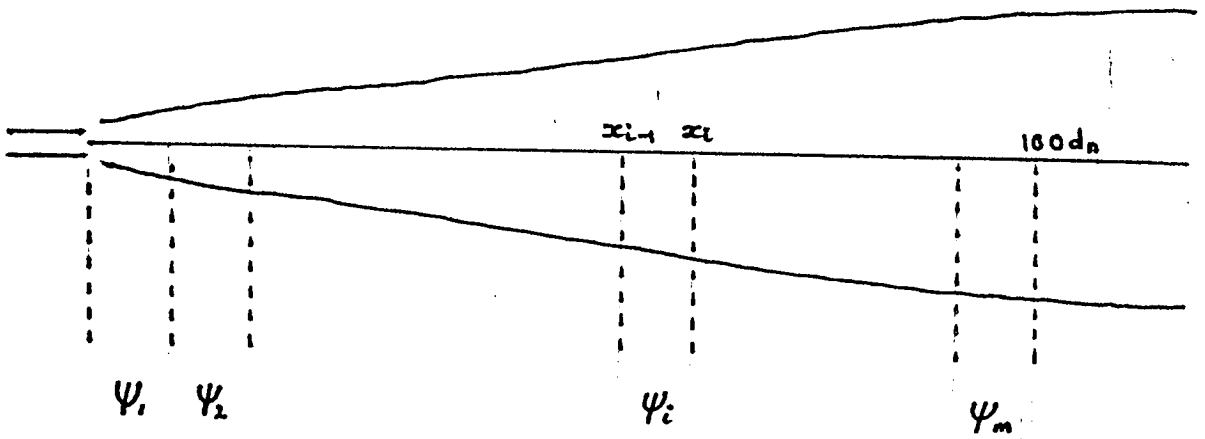

Fig. 5.5.4 Assumed Liquid Flow Through a Region, ψ_i

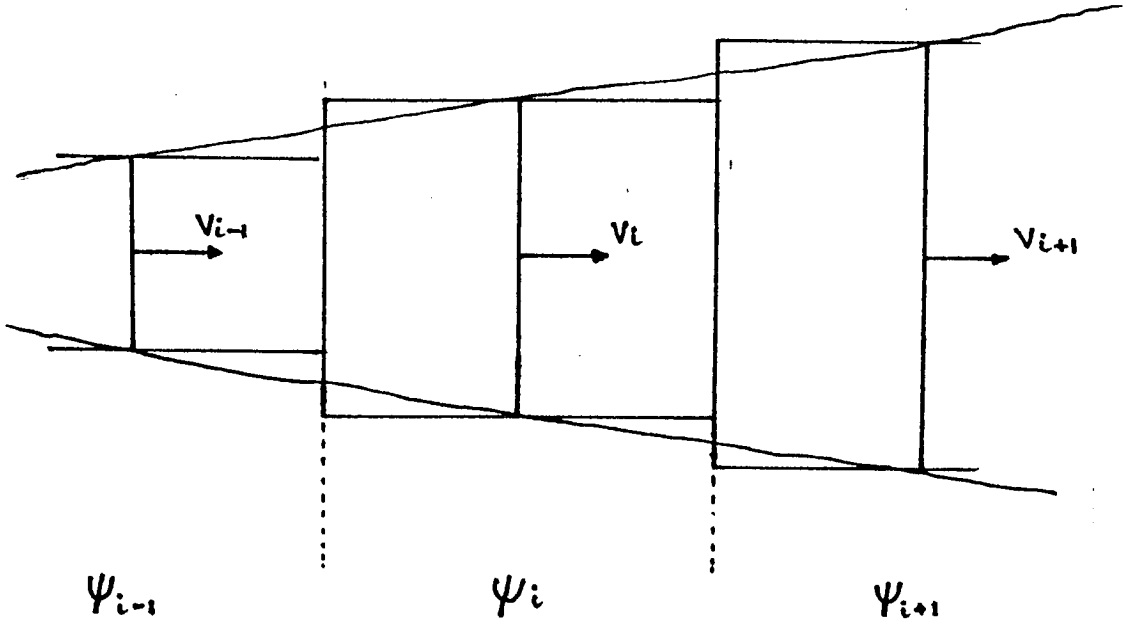

where $V_B = \frac{\pi}{6} d_B^3$

and ρ_{O_2} is the oxygen density.

The surface area flux, S_o, generated by the bubbles is then given by

$$S_o = N_o S_B \qquad 5.5.5$$

where $S_B = \pi d_B^2$

(4) Neglecting the effects of hydrostatic head and mass transfer on bubble size, and assuming the gas is in plug flow, the surface area flux, S_o, will be constant through each ψ_i. The interfacial area, a_i, in ψ_i will therefore be given by

$$a_i = S_o t_i \qquad 5.5.6$$

where t_i is the time taken by the gas to flow through ψ_i.

(5) The gas is carried through ψ_i by the velocity of the liquid flow. Approximately half the volume of flowing mixture travels at less than half the centre-line velocity, $\bar{v}_x$ (centre), and half at a velocity greater than $\frac{1}{2}\bar{v}_x$ (centre). Consequently, the average liquid flow velocity at x is $\frac{1}{2}\bar{v}_x$ (centre) and the average liquid velocity, $\bar{v}_i$, in ψ_i is assumed constant with

$$\bar{v}_i = \frac{v_n x_{uo}}{(x_i + x_{i-1})} \qquad 5.5.7$$

and $$t_i = \frac{x_i - x_{i-1}}{\bar{v}_i} \qquad 5.5.8$$

(6) Two-phase flow through a region ψ_i is illustrated in Fig. 5.5.5. A liquid flow-rate, V_{i-1}, with a dissolved oxygen concentration, $C_{O_2,i-1}$, passing into a region, ψ_i, entrains a second liquid flow-rate, V_{e_i}, with a dissolved oxygen concentration, $C_{O_2,T}$, from the surrounding liquid. Oxygen and nitrogen are carried into the region, ψ_i, and mix with the entrained liquid. Oxygen is dissolved and nitrogen desorbed, and the combined liquid flow-rate, V_i, with a dissolved oxygen concentration, $C_{O_2,i}$, then flows in to ψ_{i+1}, carrying undissolved oxygen and desorbed nitrogen with it.

(7) The mass of oxygen flowing into ψ_i is $R_{O_2,i-1}$ and the mass of nitrogen is $R_{N_2,i-1}$. The respective volumes of oxygen and nitrogen are $R_{O_2,i-1}/\rho_{O_2}$ and $R_{N_2,i-1}/\rho_{N_2}$, where ρ_{O_2} is the density of oxygen and ρ_{N_2} that of nitrogen. The partial pressure of oxygen, $P_{O_2,i}$, is given by

$$P_{O_2,i} = \left\{ \frac{R_{O_2,i-1}}{\rho_{O_2}} \div \left(\frac{R_{O_2,i-1}}{\rho_{O_2}} + \frac{R_{N_2,i-1}}{\rho_{N_2}} \right) \right\} P_B \qquad 5.5.9$$

where P_B is the gas bubble pressure

and similarly, the nitrogen partial pressure is given by

Fig. 5.5.5 Mass Transfer in a Jet Region, ψ_i

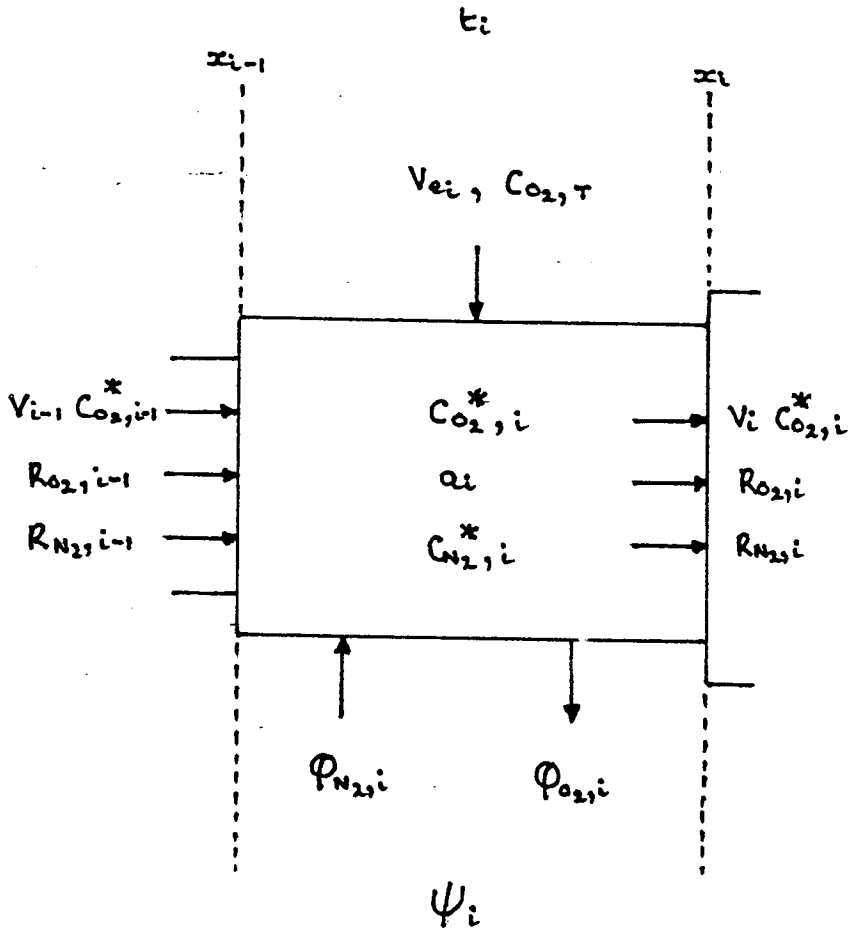

$$P_{N_2,i} = \left\{ \frac{R_{N_2,i-1}}{\ell_{N_2}} \div \left(\frac{R_{O_2,i-1}}{\ell_{O_2}} + \frac{R_{N_2,i-1}}{\ell_{N_2}} \right) \right\} P_B \qquad 5.5.10$$

These are both assumed constant in ψ_i.

$$C^*_{O_2,i} = P_{O_2,i}\, C^*_{O_2} \qquad 5.5.11$$

and

$$C^*_{N_2,i} = P_{N_2,i}\, C^*_{N_2} \qquad 5.5.12$$

where $C^*_{O_2}$ and $C^*_{N_2}$ are, respectively, the equilibrium concentrations of dissolved oxygen and nitrogen at a gas pressure of 1 atm. $C^*_{O_2,i}$ and $C^*_{N_2,i}$ are the equilibrium concentrations of the gas bubbles in ψ_i, therefore.

(8) Then in ψ_i, the oxygen mass transfer rate, $\varphi_{O_2,i}$, is governed by

$$\varphi_{O_2,i} = k_L a_i \left(C^*_{O_2,i} - C_{O_2,i} \right) \qquad 5.5.13$$

Now the gas is in plug flow over the jet length, but is dispersed by the entrainment of surrounding liquid. The entrained liquid flow-rate is far greater than the contribution from the nozzle. For example, at $x = 100 d_n$, the liquid flow-rate is 23 times greater than the initial flow-rate. The liquid phase is assumed to be well mixed in each ψ_i, therefore, and

$$\varphi_{O_2,i} = V_i\, C_{O_2,i} - V_{e_i}\, C_{O_2,\bar{T}} - V_{i-1}\, C_{O_2,i-1}$$

where V_{e_i} is the liquid flow-rate entrained in ψ_i and $C_{O_2,\bar{T}}$ is the dissolved oxygen concentration of the entrained liquid.

This simplifies to

$$\varphi_{O_2,i} = V_i (C_{O_2,i} - C_{O_2,T}) - V_{i-1} (C_{O_2,i-1} - C_{O_2,T}) \quad 5.5.14$$

with $V_o = V_n$ and $C_{O_2,o} = C_{O_2,T}$

Oxygen transfer in the whole jet region

$\Psi = \sum_{i=1}^{m} \psi_i$ is then given by

$$\varphi_{O_2} = \sum_{i=1}^{m} \varphi_{O_2,i}$$

Similarly for nitrogen transfer:

$$\varphi_{N_2} = k_{L,N_2} a_l \left(C_{N_2} - C^*_{N_2,i}\right) \quad 5.5.15$$

and $\varphi_{N_2} = V_i (C_{N_2,T} - C_{N_2,i}) - V_{i-1} (C_{N_2,T} - C_{N_2,i-1}) \quad 5.5.16$

with $C_{N_2,o} = C_{N_2,T}$

(9) $k_L \propto \sqrt{(\text{Diffusivity})}$ and so k_{L,N_2} can be calculated from

$$\frac{k_L}{k_{L,N_2}} = \frac{\sqrt{(O_2 \text{ Diffusivity})}}{\sqrt{(N_2 \text{ Diffusivity})}}$$ (Ellis & Boyes, 1976)

The values of k_L used are those collected by Motarjemi (1978).

(10) As a result of oxygen transfer into the liquid phase,

$$R_{O_2,i} = R_{O_2,i-1} - \varphi_{O_2,i} \quad 5.5.17$$

and, due to nitrogen transfer into the gas phase,

$$R_{N_2,i} = R_{N_2,i-1} + \varphi_{N_2,i} \quad 5.5.18$$

(11) Bubbles are generated at a depth, H, and the rise velocity of bubbles of diameter, d_B, is $v_{B\infty}$. The contact time is, therefore, $H/v_{B\infty}$ before the bubbles reach the liquid surface. The time taken by the liquid phase to flow through the jet region, ψ, is T where $T = \sum_{i=1}^{m} t_i$. If $H/v_{B\infty} < T$, then gas bubbles will reach the liquid surface within the jet region and no more dissolution can occur. Therefore $H/v_{B\infty}$ places a limit on $A = \sum_{i=1}^{m} a_i$ (see Fig. 5.5.6).

If $H/v_{B\infty} > T$, then gas bubbles will continue to dissolve beyond the jet region, ψ, (that is, where $x > x_m$) and will be carried along by the circulation of the water in the tank (see Fig. 5.5.7).

(12) Outside the jet region, no further entrainment can take place so both phases will be in plug flow. The liquid volumetric flow-rate, V_q, in the quiescent region, q, is given by

$$V_q = 0{\cdot}23 \frac{x_m}{d_n} V_n \qquad 5.5.19$$

and the interfacial area, in this region, a_q, is given by

$$a_q = \left(H/v_{B\infty} - T\right) S_o \qquad 5.5.20$$

Also $$P_{O_2,q} = \left\{ \frac{R_{O_2,m}}{e_{O_2}} \div \left(\frac{R_{O_2,m}}{e_{O_2}} + \frac{R_{N_2,m}}{e_{N_2}} \right) \right\} P_B \qquad 5.5.21$$

Fig. 5.5.6 Two-phase Flow Patterns - Short Contact Time

$(H/v_{g\infty} < T)$

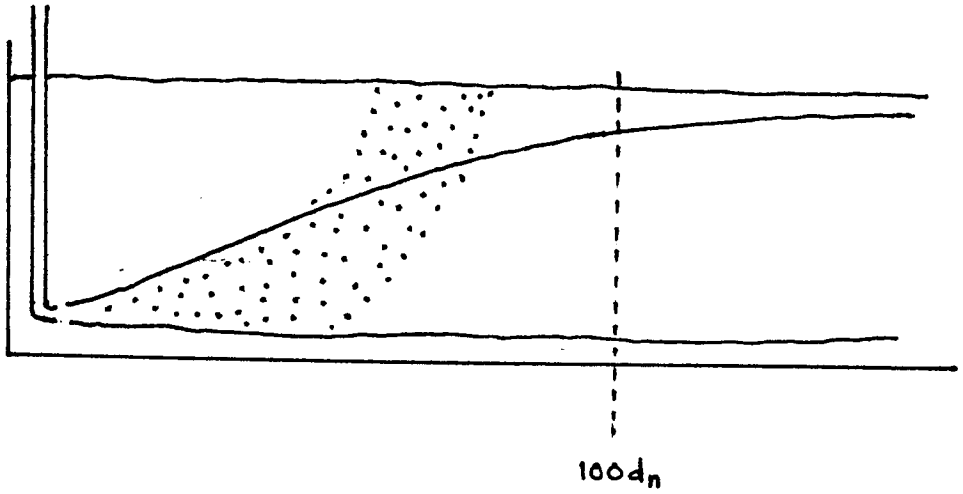

Fig. 5.5.7 Two-phase Flow Patterns - Long Contact Time

$(H/v_{g\infty} > T)$

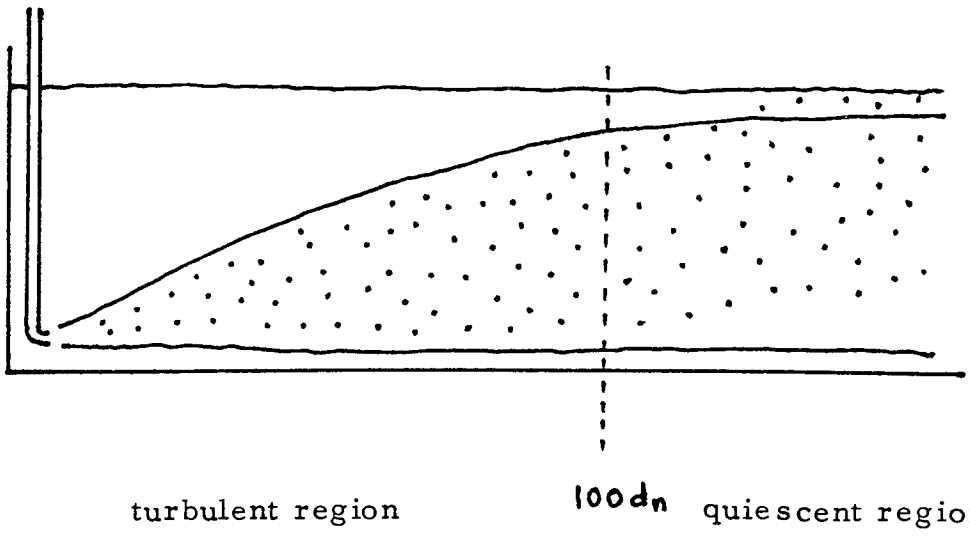

$$C^*_{O_2,q} = P_{O_2,q}\, C^*_{O_2} \qquad 5.5.22$$

and $$\varphi_{O_2,q} = k_L a_q \left(C^*_{O_2,q} - C_{O_2,q}\right), \qquad 5.5.23$$

for which a solution is

$$\ln\left(\frac{C^*_{O_2,q} - C_{O_2,m}}{C^*_{O_2,q} - C_{O_2,q}}\right) = \frac{k_L a_q}{V_q} \qquad 5.5.24$$

Similar equations can be written for nitrogen transfer.

Total oxygen transfer from the bubbles generated by the submerged jet can now be explored under various conditions of liquid flow-rate, oxygen flow-rate, nozzle diameter and bubble size or salinity.

5.5.6 Sample Calculation based on Experimental Data

The following data based on experimental results are used in the sample calculation to determine oxygen transfer rates.

Data

(1) Liquid volumetric flow-rate at nozzle, $V_n = 40 m^3/h$
$= 0.0111\ m^3/s$

Operating pressure, $h = 1.68$ atm $= 7$ m WG

(2) Oxygen flow-rate, $R_{O_2,0} = 2$ kg/h $= 0.55$ g/s

Oxygen density, $\rho_{O_2} = 1.38 \times 10^3$ g/m^3 at 1 atm and 10° C

(3) No nitrogen present in gas bubbles initially, $R_{N_2,0} = 0$

Nitrogen density, $\rho_{N_2} = 1.21 \times 10^3$ g/m^3 at 1 atm and 10°C

(4) Water salinity = 35 ppt

Observed bubble diameter, $d_B = 0.5 \times 10^{-3}$ m

The oxygen mass transfer coefficient for bubbles of this size, $k_L = 0.15 \times 10^{-3}$ m/s

and for nitrogen, $k_{L,N_2} = 0.12 \times 10^{-3}$ m/s

The rise velocity of 0.5 mm bubbles, $v_{B\infty} = 0.07$ m/s

(5) $Co_2^* = 54$ ppm dO_2, $Co_{2,T} = 10$ ppm dO_2;

$C_{N_2}^* = 24$ ppm dN_2, $C_{N_2,T} = 19$ ppm dN_2.

(6) The depth of jet nozzle below water surface, $H = 1.4$ m.

However, the bubbles are assumed to be created at 1 atm pressure, that is, $P_B = 1$.

Calculation

From equations 5.5.1 and 5.5.2, $d_n = 0.044$m

and $v_n = 7.5$ m/s.

For the sample calculation the two phase jet region is divided into four regions, ψ_i $(i = 1....4)$ with $x_i - x_{i-1} = 25 d_n$

It is considered that four steps will give a sufficiently accurate prediction of oxygen transfer and provide adequately detailed information about two-phase jet operation.

In ψ_1, the liquid volumetric flow-rate,

$$V_1 = 0.23\, V_n \left(\frac{x_1 + x_2}{2 d_n}\right) \qquad \text{from equ. 5.5.3}$$

$$= 0.032\ m^3/s$$

The volume of a 0.5 mm bubble,

$$V_B = 6.54 \times 10^{-11} \text{ m}^3.$$

Therefore, the number of bubbles generated by an oxygen flow-rate of 2 kg/h,

$$N_o = 6 \times 10^6 \text{ per second} \qquad \text{from equ. 5.5.4}$$

The surface area of a 0.5 mm bubble,

$$S_B = 7.85 \times 10^{-7} \text{ m}^2$$

and, therefore, the surface area generated by the oxygen flow-rate,

$$S_o = 4.7 \text{ m}^2 \text{ per second.} \qquad \text{from equ. 5.5.5}$$

The average liquid velocity in ψ_1 can be calculated from

$$\bar{v}_1 = v_n \frac{6.4 d_n}{x_1 + x_o} \qquad \text{from equ. 5.5.7}$$

$$= 1.92 \text{ m/s}$$

and, since the gas is carried through ψ_1 by the velocity of the liquid, the gas residence time in ψ_1,

$$t_1 = 0.52 \text{ s.} \qquad \text{from equ. 5.5.8}$$

Therefore the interfacial area in ψ_1,

$$a_1 = 2.44 \text{ m}^2. \qquad \text{from equ. 5.5.6}$$

Similarly, equations 5.5.1 - 5.5.6 can be used to estimate V_i and a_i in ψ_i for i = 2, 3, 4. These are summarised in Table 5.5.1.

TABLE 5.5.1 Liquid Flow-rate, V_i, Contact Time, t_i and Interfacial Area, a_i, in ψ_i $(i = 1 \ldots 4)$

Region ψ_i	Volumetric Flow-rate, V_i (m^3/s)	Contact Time t_i (s)	Interfacial Area, a_i (m^2)
ψ_1	0.032	0.52	2.44
ψ_2	0.096	1.56	7.34
ψ_3	0.160	2.60	12.24
ψ_4	0.223	3.65	17.14

With no nitrogen in the gas phase initially the oxygen and nitrogen partial pressures in ψ_1 are 1 atm and 0, respectively (from equations 5.5.9 and 5.5.10).

Then $C^*_{O_{2,1}} = 54$ ppm dO_2 from equ. 5.5.11

and $C^*_{N_{2,1}} = 0$ from equ. 5.5.12

Substituting in equations 5.5.13 and 5.5.14, the oxygen transfer rate in ψ_1,

$$\varphi_{O_{2,1}} = k_L a_1 (C^*_{O_{2,1}} - C_{O_{2,1}})$$
$$= V_1 (C_{O_{2,1}} - C_{O_{2,T}})$$

from which, $C_{O_{2,1}} = 10.49$ ppm dO_2

and $\varphi_{O_{2,1}} = 0.016$ g/s.

Similarly, the nitrogen transfer rate in ψ_1, is obtained from equations 5.5.15 and 5.5.16.

$$\varphi_{N_{2,1}} = k_{L,N_2} a_1 (C_{N_{2,1}} - C^*_{N_{2,1}})$$
$$= V_1 (C_{N_{2,T}} - C_{N_{2,1}})$$

from which, $C_{N_{2,1}} = 18.83$ ppm dN_2

and $\varphi_{N_{2,1}} = 5.5 \times 10^{-3}$ g/s.

Therefore $R_{O_2,1} = 0.54$ g/s from equ. 5.5.17

and $R_{N_2,1} = 5.5 \times 10^{-3}$ g/s. from equ. 5.5.18

Mass transfer rates can now be calculated in ψ_2 and hence, ψ_3 and ψ_4. The results are summarised in Tables 5.5.2 and 5.5.3.

TABLE 5.5.2 Oxygen Mass Transfer in ψ_i ($i = 1....4$)

Region ψ_i	$C^*_{O_2,i}$ ppm dO_2	$C_{O_2,i}$ ppm dO_2	$\Phi_{O_2,i}$ g/s	$R_{O_2,i}$ g/s
ψ_1	54.0	10.50	0.016	0.540
ψ_2	53.4	10.66	0.047	0.493
ψ_3	51.4	10.86	0.074	0.419
ψ_4	47.8	11.04	0.095	0.324

TABLE 5.5.3 Nitrogen Mass Transfer in ψ_i ($i = 1....4$)

Region ψ_i	$C^*_{N_2,i}$ ppm dN_2	$C_{N_2,i}$ ppm dN_2	$\Phi_{N_2,i}$ g/s	$R_{N_2,i}$ g/s
ψ_1	0	18.83	5.5×10^{-3}	5.5×10^{-3}
ψ_2	0.28	18.77	0.016	0.022
ψ_3	1.17	18.70	0.026	0.048
ψ_4	2.77	18.64	0.032	0.080

Now the contact time of gas bubbles rising to the surface,

$$H/v_{B\infty} \simeq 20\,s.$$

Contact time in the jet region ψ ,

$$T = \sum_{i=1}^{4} t_i = 8.33\,s.$$

Gas bubbles will therefore continue to dissolve beyond the jet region, ψ . The interfacial area in the quiescent region,

$a_q = 54.85\ m^2.$ from equ. 5.5.20

$C^*_{O_2,q} = 42.3$ ppm dO_2 from equ. 5.5.21 and 5.5.22

and similarly $C^*_{N_2,q} = 5.2$ ppm dN_2.

$V_q = 0.255\ m^3/s,$ from equ. 5.5.19

$C_{O_2,q} = 12$ ppm dO_2 from equ. 5.5.24

and $\varphi_{O_2,q} = 0.249$ g/s. from equ. 5.5.23

Therefore, the total mass transfer from the submerged jet,

$$\sum_{i=1}^{4} \varphi_{O_2,i} + \varphi_{O_2,q} = 0.48\ g/s.$$

This result is equivalent to $\simeq$ 1700 g/h.

The total nitrogen transfer into the gas bubbles,

$$\sum_{i=1}^{4} \varphi_{N_2,i} + \varphi_{N_2,q} = 0.166\ g/s.$$

5.6 Discussion

The result predicted above compares favourably with that deduced from experimental results (see Fig. 5.4.1). However, the model developed will

produce enhanced transfer rates for two reasons. Firstly, the volume of gas flowing at t = 0 is twice the volume which reaches the water surface and hence the surface area reduces to about 60% of its original value during bubble dissolution. However, this may be counteracted by an increased gas-liquid contact time, due to the reduction in the bubble rise velocity, $v_{B\infty}$, with bubble diameter.

Secondly, in this particular example, about 50% of the oxygen transfer occurs in the quiescent region, q. A constant oxygen concentration, $C^*_{O_2,q}$ is assumed for gas bubbles in this quiescent region, based on the value at the exit from the jet region, ψ. In practice, a reduction in oxygen concentration would be expected as gas bubbles pass through the quiescent region, q, due to nitrogen desorption, and since the proportion of mass transfer is high in this region, the change may be considerable. To investigate this further, q can be divided into smaller regions, $q_j (j = 1 \ldots p)$, as ψ has been divided into ψ_i $(i = 1 \ldots m)$ and mass transfer rates recalculated (see Fig. 5.6.1). Details of the calculations are summarised in Tables 5.6.1 and 5.6.2 for $p = 2$. Two steps are considered sufficient to examine the significance of the change.

Fig. 5.6.1 Terminal Flow Region Subdivided into Regions, q_i

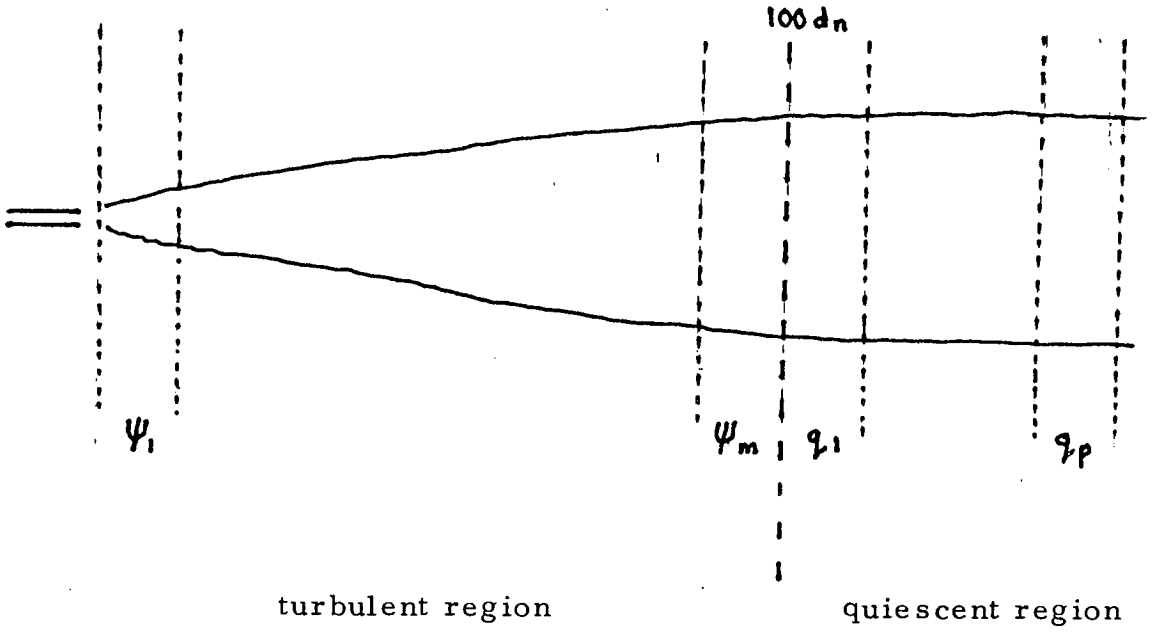

TABLE 5.6.1 Oxygen Mass Transfer in the Quiescent Region q_j ($j = 1,2$)

Region q_j	$C^*_{O_2,j}$ ppm dO_2	$C_{O_2,j}$ ppm dO_2	$\varphi_{O_2,j}$ g/s	$R_{O_2,j}$ g/s
q_1	42.3	11.50	0.117	0.207
q_2	32.4	11.83	0.084	0.123

TABLE 5.6.2 Nitrogen Mass Transfer in the Quiescent Region q_j ($j=1,2$)

Region q_j	$C^*_{N_2,j}$ ppm dN_2	$C_{N_2,j}$ ppm dN_2	$\varphi_{N_2,j}$ g/s	$R_{N_2,j}$ g/s
q_1	5.2	18.47	0.043	0.123
q_2	9.6	18.36	0.028	0.151

Total mass transfer from the jet oxygenator is estimated to be 1560 g/h, which represents only a relatively small reduction in overall transfer rate, and is still in reasonable agreement with observed results. Overall oxygen and nitrogen processes are illustrated graphically in Figs. 5.6.2 and 5.6.3.

Fig. 5.6.2 Oxygen Mass Transfer through Turbulent and Quiescent Regions.

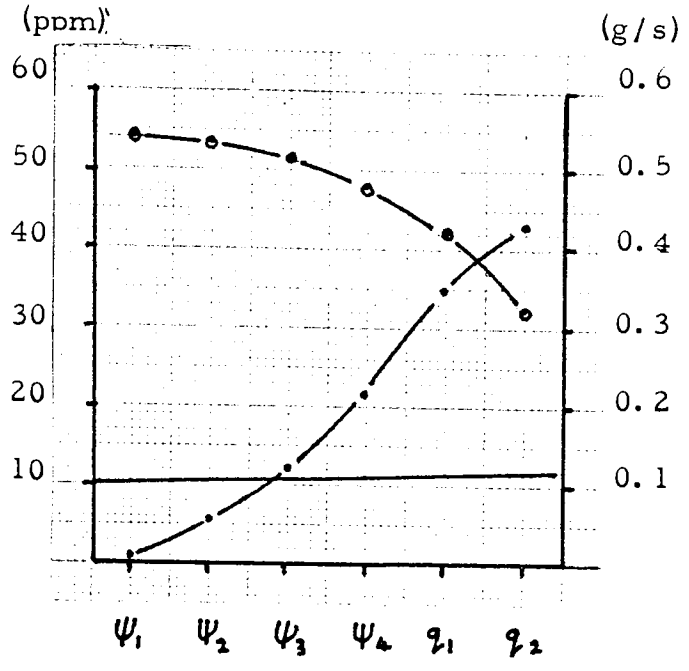

Equilibrium concentration dO_2 (ppm)

Total oxygen mass transfer (g/s)

dO_2 concentration in jet region (ppm)

Fig. 5.6.3 Nitrogen Mass Transfer through Turbulent and Quiescent Regions

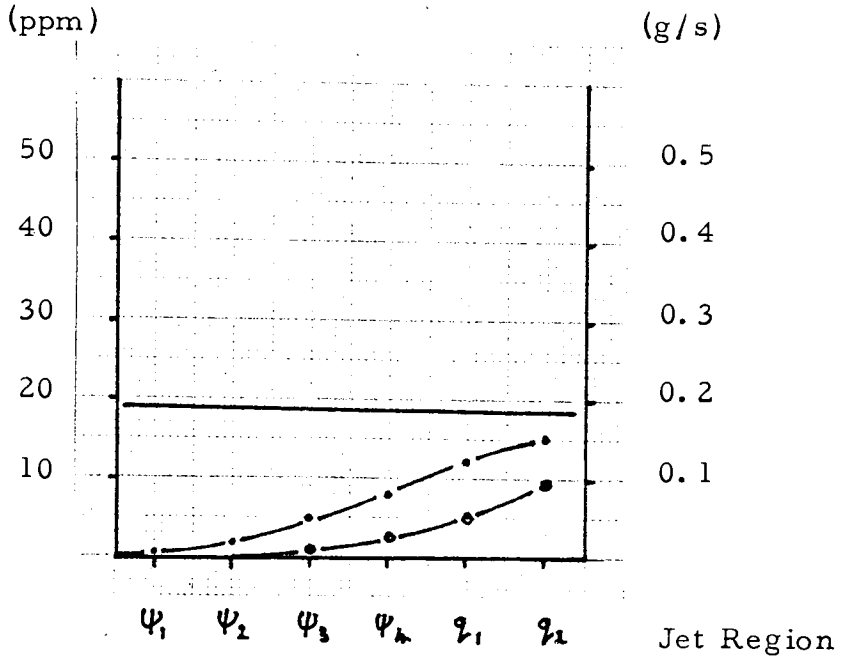

5.6.1 Effect of Salinity on ($k_L A$)

Bubble size is affected by salinity, ranging from 0.5mm diameter in seawater (35 ppt salinity) to 3-5mm in freshwater, and k_L varies with bubble size. Estimates of the variation in ($k_L A$) with bubble size are given in Fig. 5.6.4 using data from the sample calculation and by considering the path length of gas bubbles. Also shown is the recorded variation in dissolution efficiency with salinity of the production jet oxygenator (see section 5.4), operating with an oxygen flow-rate of 3 kg/h (Fig. 5.6.5).

Acceptable dissolution efficiencies can be expected in saline water down to between 10 and 15 ppt, but below this value considerably poorer performance will result. It should however be stressed that the bubble size and rise velocity are major determinants in the calculation of ($k_L A$) values and that estimates of bubble size were made by eye. A more systematic evaluation of the variation in bubble size with salinity is needed.

5.6.2 Effects of Pressure and Phase Flow-rates (see also Section 5.3.2)

Pressure

Examination of equations 5.5.1 and 5.5.2 suggests that increasing the operating pressure at a constant liquid flow-rate requires a reduction in nozzle diameter, d_n, and increases the water velocity at the nozzle, v_n. The liquid

Fig. 5.6.4 The Variation in ($k_L A$) with Bubble Size

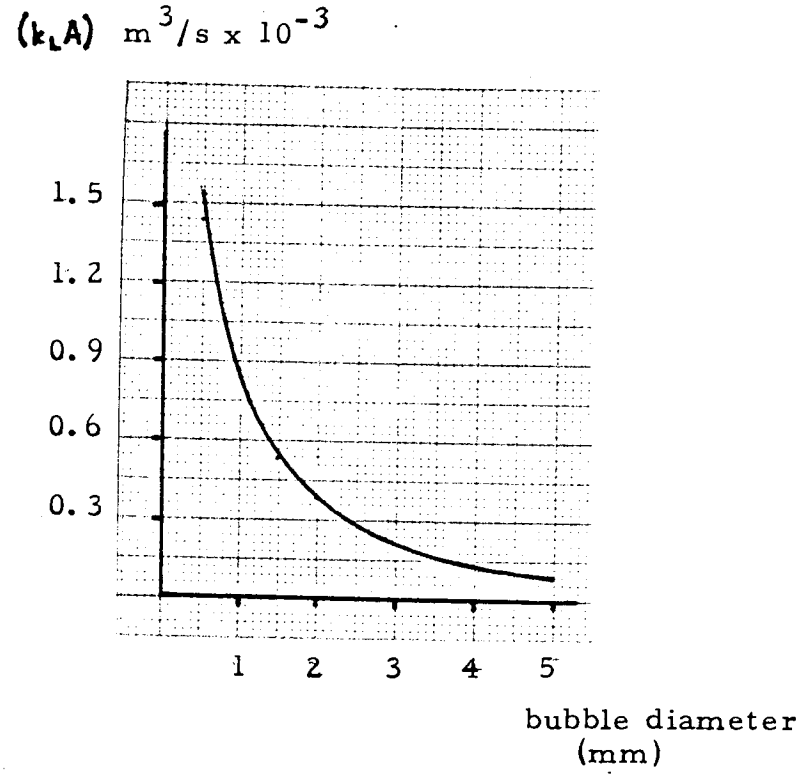

Fig. 5.6.5 Variation in Oxygenator Performance with Water Salinity

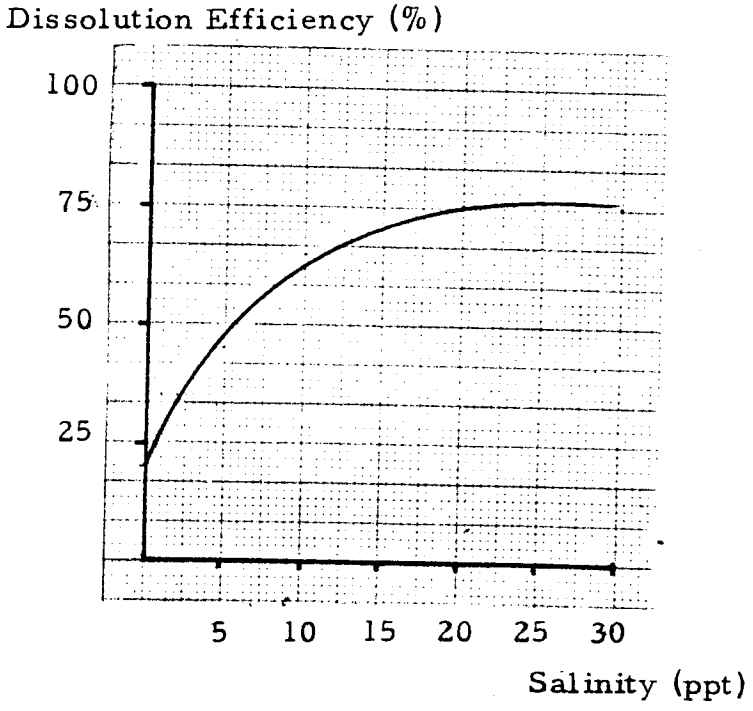

N.B. Bubbles formed in seawater (32 ppt) are 0.5mm in diameter; bubbles formed in freshwater (0 ppt) 3-5mm in diameter.

flow-rate, $V_x = 0.23 V_n \frac{x}{d_n}$, will be unchanged over the jet length $0 < x < 100\ d_n$, but since the velocity is increased, the gas residence time in the jet region, ψ, will be reduced and therefore oxygen transfer may be lower. However, the total contact time, $H/v_{B\infty}$, will be unchanged and hence the interfacial area remains constant. The gas residence time in the quiescent region, q, will therefore be increased, although the liquid flow-rate through this region will be unchanged. Increased oxygen transfer is likely in the quiescent region and consequently, the overall oxygen transfer rate may be changed very little by pressure (see Table 5.6.3).

One additional aspect is the possibility that the increased liquid velocity at the nozzle creates smaller bubbles, thereby increasing **A**, in a similar fashion to that of a venturi (Bayley and Wyatt, 1961). In the case of lower water salinities this is particularly likely and may explain the improvement in dissolution rate which can occur with increased pressure (see section 5.2.3). A better understanding of the effects of pressure on the bubble size produced by this type of oxygenator would be particularly useful to increase the effectiveness of the model.

Liquid Flow-rate

To increase the liquid flow-rate, V_n, whilst keeping the pressure (and hence v_n) constant, means that the nozzle diameter, d_n, must be increased. Since V_n increases with d_n^2

the liquid volumetric flow-rate, $V_x = 0.23\, V_n \frac{x}{d_n}$, will increase. Overall, this will result in an increased oxygen concentration gradient $(Co_2^* - Co_2)$, resulting in improved transfer rates and dissolution efficiencies despite the contact time and $k_L A$ remaining unchanged. However, as Co_2 approaches $Co_{2,T}$, no further improvement is found (see Table 5.6.3).

Oxygen Flow-rate

If the oxygen flow-rate is increased, the interfacial area will be increased (assuming no bubble coalescence) and the dissolved oxygen concentration, Co_2, in the two phase region will increase (provided the liquid flow-rate remains constant). Higher transfer rates can be expected due to an increase in **A** but, with a reduced concentration gradient $(Co_2^* - Co_2)$, the gas may take longer to dissolve. Since the overall contact time is unchanged, lower dissolution efficiencies may result (see Table 5.6.3).

Table 5.6.3 is a summary of predicted and observed results, for comparison. The results predicted using the model show the effects of increasing the pressure from 1.68 - 1.82 atm, the liquid flow-rate from 40 - 60 m^3/h and the oxygen flow-rate from 2 - 3 kg/h. The observed results are taken from the Yates' analyses (see Table 5.3.2) and show the average effects of increasing the pressure from 1.41 - 1.82 atm, the liquid flow-rate from 40 - 60 m^3/h and the oxygen flow-rate from 1 - 3 kg/h.

TABLE 5.6.3 Comparison of Predicted & Observed Results

	Predicted Values		Average Observed Values	
	Diss. Rate (g/h)	Diss. Efficiency (%)	Transfer Rate (g/h)	Diss. Efficiency (%)
	1560	78	1378	70
Pressure	+ 30	+ 2	+ 117	+ 5
Liquid	+ 30	+ 2	- 153	- 7
Oxygen	+780	0	+ 672	+ 1

The table shows that with inputs:

Pressure - 1.68 atm,

Liquid flow-rate - 40 m^3/h,

Oxygen flow-rate - 2 kg/h,

1560 g 0_2/h dissolved is predicted using the model. Increasing the pressure to 1.82 atm improves the dissolution rate by 30 g/h to 1590 g/h, for example, and increasing the oxygen flow-rate to 3 kg/h increases the dissolution rate by 780 g/h to 2340 g/h. By comparison, with inputs of

Pressure: 1.41 and 1.82 atm,

Liquid flow-rate: 40 and 60 m^3/h,

Oxygen flow-rate: 1·0 and 3·0 kg/h,

the average observed dissolution rate was 1378 g 0_2/h.

The average effect in all tests of increasing the pressure to 1.82 atm was an improvement in dissolution rate by 117 g 0_2/h to 1495 g/h. When the oxygen flow-rate was increased to 3 kg/h in the tests the average dissolution rate improved by 672 g/h to 2050 g/h.

5.6.3 Mixing in Tanks using Submerged Jets

In addition to the oxygenation capacity of jet oxygenators, the mixing ability of such devices should also be considered. The circulation rate of the liquid, the requirement for an even oxygen distribution and the mixing time are all important factors, although they are in fact, interrelated. Mixing in large reservoirs is often accomplished using submerged jets. Ali and Whittington (1979) found that mean circulation rate, $\bar{Q}_c$, could be estimated from the following equation:

$$\frac{\bar{Q}_c}{Q_o} = 4.3 \quad \frac{h}{b_o}\left(\frac{R}{d_o}\right)^{0.127}$$

where b_o is the height of the jet,

h is the reservoir depth,

R is the radius of the reservoir,

d_o is the width of the jet,

and Q_o is the jet discharge rate.

This suggests a value of 0.3 m/s for the mean circulation velocity.

The submerged jets used by Ali and Whittington (1979) issued tangentially to a curved wall. As the ratio of diameter to depth, (D/h), was reduced from 150 to 30, the circulation patterns became more symmetrical. In rearing tanks this effect is likely to cause a large oxygen gradient across the tanks, as (D/h) is typically 8 - 10. In other industries, mixing is often accomplished by directing

the jet radially across the tank. In fish tanks this would tend to oxygenate the effluent water and might also upset the self-cleaning action of tanks. Since neither of these approaches is satisfactory, the jet is directed at 45° to a tangent at the tank wall. This provides good circulation, an even oxygen distribution and good mixing. Mixing times can be estimated by

$$t_{mix} = \frac{h^{1/2} L^{3/2}}{Q_o v_n}$$ (Davies, 1972)

5.7 Conclusions

Jet oxygenators are an effective method of oxygenation in seawater and higher intermediate salinities. A unit has been designed to support Finnarts Bay rearing tanks and, with a liquid flow-rate of 40 m^3/h and an operating pressure of 1.68 atm, achieves transfer rates of up to the maximum requirement of 2 kg O_2/h with dissolution efficiencies of about 75%. The oxygenator has a transfer efficiency of about 1.7 kg O_2/kWh.

A model has been developed to predict performance which is in reasonable agreement with observed results over the range tested. However, the model depends on visual estimation of bubble sizes as little data is presently available relating to bubble sizes produced by this type of device. More accurate data would be particularly useful to increase the effectiveness of the model.

CHAPTER 6

U-TUBE OXYGENATION

6.1 Introduction

There is considerable potential in fish farming for an oxygenation device which can routinely increase production from a water supply for relatively low capital and running costs. Such a device would oxygenate the primary water source for simplicity.

The U-tube has long been used as an effective aeration device requiring only a low liquid head (Bruijn and Tuinzaad, 1958). High transfer rates are achieved as the gas is subjected to an increasing hydrostatic head within the U-tube.

This chapter describes the assessment of the U-tube as an oxygenation device. A maximum outlet concentration of 25 ppm dO_2 is specified which could allow up to a four-fold saving in water use. Dissolution efficiencies greater than 70% are desirable. Data taken from experimental observations and additional information relating to U-tube aeration are then used to model operation using oxygen.

6.2 Equipment and Experimental Programme

6.2.1 Equipment

The downflow pipe of the U-tube was a 6 m length of PVC pipe, 0.3 m in diameter. Five perspex windows were placed in each side, 1 m apart, to aid visual

observations. The upflow pipe was a length of 0.1 m diameter flexible hose, the height of which could be varied to keep the U-tube full. A vent pipe was attached to the top of the upflow pipe to prevent liquid syphoning out of the U-tube. Sampling points were installed at depths of 4 m and 6 m in the downflow pipe and at the top of the upflow pipe. Fig. 6.2.1 is a line diagram of the equipment.

Water was pumped from a 12 m diameter rearing tank, through a flow control valve, to the top of the downflow pipe. The water was discharged below the water level in the U-tube to prevent air entrainment and flowed through the U-tube, back to the rearing tank (see Fig. 6.2.2). Oxygen was introduced through a coiled diffuser suspended in the downflow pipe: the depth of the diffuser below the water surface could be adjusted (see Figs. 6.2.3 and 6.2.4). Oxygen flow-rate was controlled using a flow-meter, valve and pressure gauge.

6.2.2 Experimental Programme

Gas is carried along the downflow pipe by the velocity of the water, that is, cocurrent flow of the two phase fluid occurs in the U-tube. Since the rise velocity of 2 - 5 mm bubbles formed in freshwater is around 0.23 m/s, liquid flow-rates were specified so that superficial liquid velocities of 0.25 and 0.30 m/s occurred in the downflow pipe. Oxygen flow-rates of 0.5 kg/h and 1.5 kg/h were chosen since these

Fig. 6. 2. 1 The Prototype U-tube

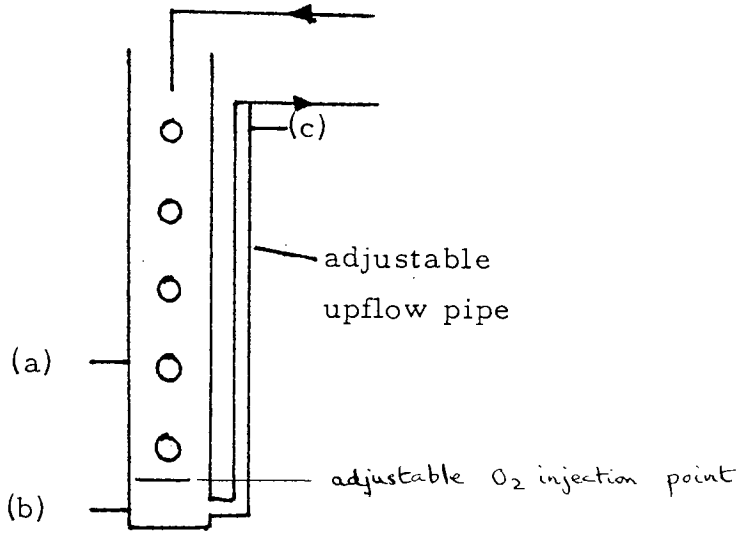

(a), (b), (c), (d) sample points

Fig. 6. 2. 2 The General Equipment Layout

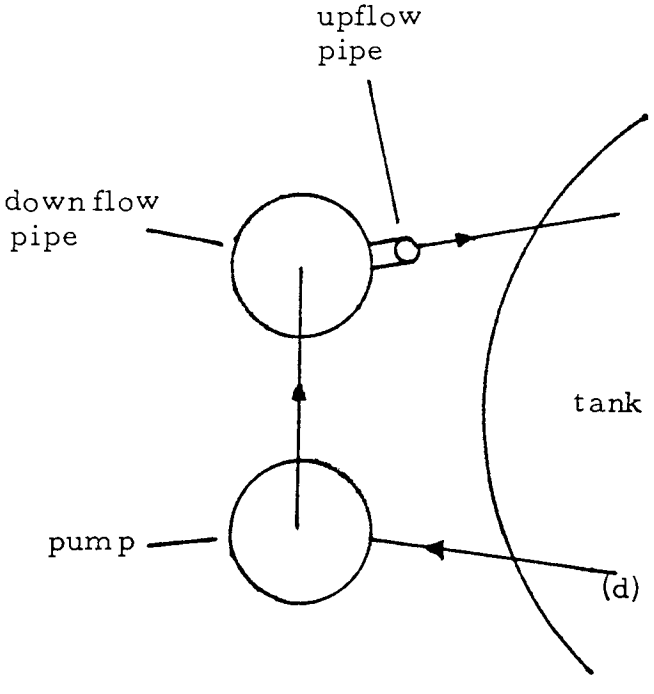

Fig. 6. 2. 3 The Coiled Oxygen Diffuser

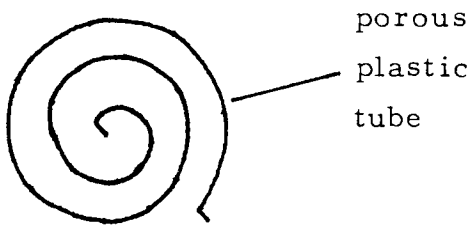

Fig. 6. 2. 4 The Diffuser Suspended in the Downflow Pipe

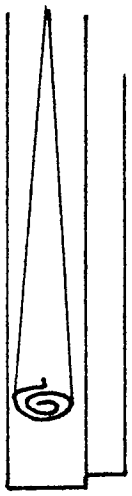

correspond to outlet concentrations of 15 and 25 ppm dO_2 at the higher liquid flow-rate, assuming an inlet dissolved oxygen concentration of 10 ppm and 80% dissolution efficiency. Oxygen diffuser depths of 2 m and 5 m were selected to measure the change in performance with diffuser depth. In all, eight tests were completed.

For each test, the water flow-rate was set with the column purged of all gas. The height of the upflow pipe was adjusted so that the water level in the downflow pipe was about 0.4 m below the top. Oxygen was then introduced and the system left for half an hour to stabilise. The gas bubbles in the system caused an increase in the water level in the downflow pipe and the change in height was taken to be an estimate of the gas hold-up. Samples were taken from the sample points and incoming water was sampled in the rearing tank near the pump inlet. Dissolved oxygen levels were determined by the Winkler method (APHA, 1971).

Yates' method of analysis was used to assess the importance of:

superficial liquid velocity,

oxygen flow-rate,

diffuser depth,

on the two response variables:

change in dissolved oxygen concentration

and oxygen absorption efficiency.

The method of analysis is given in Appendix 1.

6.3 Results and Observations

6.3.1 Results Summary

Untreated data and the results of the Yates analyses are given in Tables 6.3.1 and 6.3.2.

The maximum dissolved oxygen concentration achieved was around 20 ppm which seems to be an upper limit for the system throughout the range of conditions tested. Performance was consistently better with the diffuser at 2 m depth than at 5 m depth and, at 2 m depth, the transfer rate and dissolution efficiency improved further with the liquid flow-rate. However, two further tests conducted with a superficial liquid velocity of 0.35 m/s and oxygen inputs of 0.5 and 1.5 kg/h, demonstrated that this trend does not continue. The results of these tests are given in Table 6.3.3 and are combined with previous results in Fig. 6.3.1.

The Yates' analysis has been extended to study the relative importance of the downflow and upflow pipes in raising the dissolved oxygen levels. The results which are summarised in Table 6.3.4, show that a large proportion of total oxygen transfer must occur between 2 m and 4 m depth in the downflow pipe. Overall dissolution improved with path length but the rate of dissolution decreased along the length of the U-tube.

TABLE 6.3.1 Untreated Data

Superficial Liquid Velocity (m/s)	Oxygen Flow-rate (kg/h)	Diffuser Depth (m)	Dissolved Oxygen Oxygen Con. (ppm) 4m	6m	0/let	Dissolved Oxygen Change (ppm)	Dissolution Efficiency (%)
0.30	1.5	5	9.7	14.7	15.6	7.1	37
0.25	1.5	5	14.5	19.0	20.4	12.1	53
0.30	0.5	5	9.2	11.0	11.9	3.1	49
0.25	0.5	5	11.0	13.3	13.5	4.5	60
0.30	1.5	2	15.3	18.1	19.9	12.3	65
0.25	1.5	2	18.8	21.2	21.3	12.6	55
0.30	0.5	2	12.7	14.0	15.4	4.8	76
0.25	0.5	2	12.7	13.0	13.1	5.4	71

TABLE 6.3.2 Results of Yates' Analyses

	Change in dO_2 (ppm)	Dissolution Efficiency (%)
Average Effect	7.7	58
Liquid Flow-rate	-0.9	- 2
Oxygen Flow-rate	3.3	- 6
Liquid/Oxygen	-0.4	0
Diffuser Depth	-1.0	- 9
Diffuser/Liquid	-0.7	- 5
Diffuser/Oxygen	-0.4	1
D/O/L	-0.5	- 1

D/O/L is the combined diffuser depth, oxygen flow-rate and liquid flow-rate interaction.

TABLE 6.3.3 Results of Tests at 0.35 m/s Superficial Liquid Velocity

Superficial Liquid Velocity (m/s)	Oxygen Flow-rate (kg/h)	Diffuser Depth (m)	Dissolved Oxygen Oxygen Con. (ppm) 4m	6m	0/let	Dissolved Oxygen Change (ppm)	Dissolution Efficiency (%)
0.35	1.5	2	16.0	18.1	18.8	9.0	55
0.35	0.5	2	11.1	11.4	11.8	3.0	55

Fig. 6. 3. 1 The Effect of Superficial Liquid Velocity on Oxygen Dissolution Efficiency - Diffuser Depth 2m

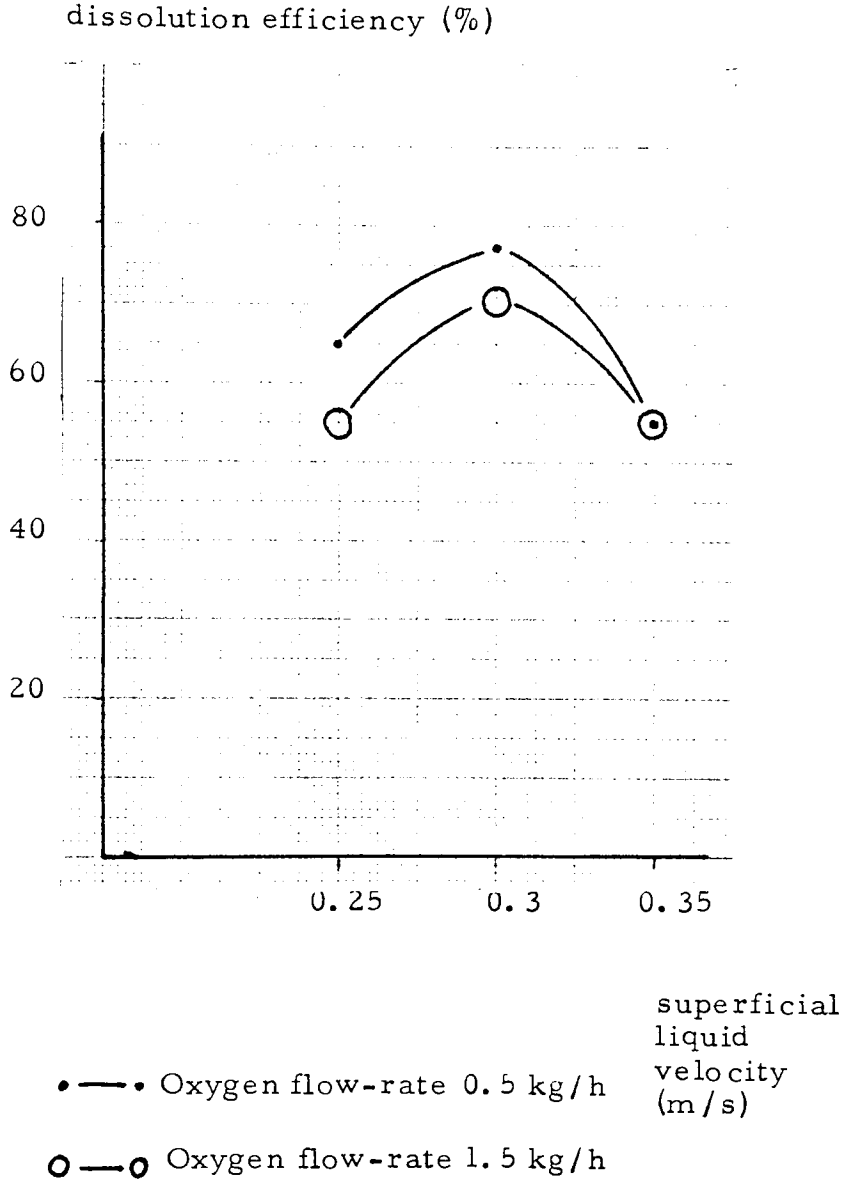

TABLE 6.3.4 The Change in Dissolved Oxygen Level with Path Length

	Change in Dissolved Oxygen Level (ppm)		
U-tube region (m)	0 - 4	4 - 6	6 - 0
Average	6.2	1.7	0.85
Liquid Flow-rate	-1.3	0.3	0.75
Oxygen Flow-rate	2.7	0.9	0.1
Liquid/Oxygen	0.1	-0.1	0.1

6.3.2 Visual Observations

Estimates of bubble size and gas hold-up were made by eye. With the diffuser at 5 m depth, two-phase flow existed throughout the downflow pipe and bubbles up to 5 mm in diameter were observed. Some gas escaped as slugs from the top of the downflow pipe (see Fig. 6.3.2). As the liquid flow-rate was increased, large 5 - 10 mm diameter bubbles remained in the downflow pipe but the gas hold-up in this region was very low (<1%). Smaller bubbles were swept below the diffuser where a dense bubble regime occurred with bubbles up to 5 mm in diameter (see Fig. 6.3.3).

Fig. 6. 3. 2 Observed Flow in the U-tube

Diffuser Depth - 5m; Superficial Liquid Velocity - 0. 25 m/s

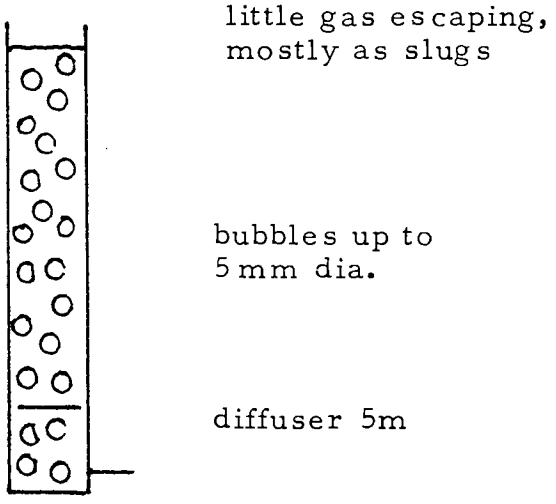

Fig. 6. 3. 3 Observed Flow in the U-tube

Diffuser Depth - 5m; Superficial Liquid Velocity - 0. 3 m/s

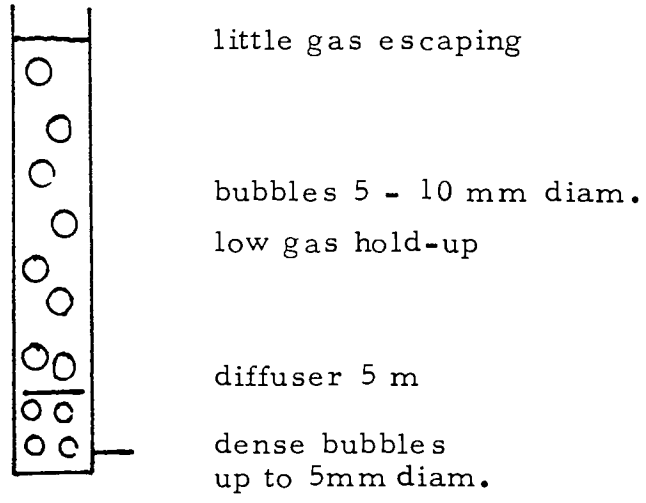

With the diffuser at 2 m depth, the bubble regime in the downflow pipe was very similar to that with the diffuser at 5 m depth, when operated at a lower liquid velocity (see Fig. 6.3.4). However, as the liquid flow-rate was increased, less gas was lost from the top of the downflow pipe and occurred only as small bubbles. Two-phase flow was observed in the entire U-tube below the diffuser, with bubbles up to 5 mm in diameter (see Fig. 6.3.5).

At the lower liquid velocity, more gas escaped from the top of the downflow-pipe as the oxygen flow-rate was increased, but at the higher liquid flow-rate, the oxygen flow-rate had little effect on gas loss. Gas hold-up increased with oxygen flow-rate but was estimated to be less than 5% in all tests.

The loss of gas slugs from the top of the downflow pipe, when the superficial liquid velocity was 0.25 m/s, suggests that the liquid flow-rate was not high enough to carry all the gas bubbles down through the U-tube. At the higher flow-rate all the gas is swept along the length of the tube, and optimum performance is obtained when the gas bubbles have the longest path length, that is with the diffuser at 2 m depth. Even so, the performance of the U-tube is not considered to be particularly good. However, the gas residence time is only about a minute under these conditions (assuming an average bubble rise velocity of 0.23 m/s),

Fig. 6. 3. 4 Observed Flow in the U-tube

Diffuser Depth - 2m; Superficial Liquid Velocity - 0. 25m/s

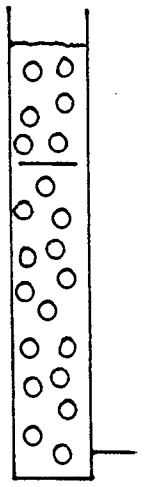

Fig. 6. 3. 5 Observed Flow in the U-tube

Diffuser Depth - 2m; Superficial Liquid Velocity - 0. 3m/s

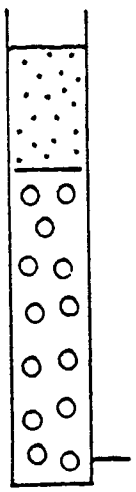

compared with a minimum dissolution time of two minutes recommended in section 1.8. When the superficial liquid velocity in the downflow pipe is increased to 0.35 m/s, gas is swept through the column more quickly and undissolved gas is lost from the top of the upflow pipe. Under these conditions the gas residence time is only about 30 secs., which explains the decline in performance.

6.4 Theory of U-tube Oxygenator

6.4.1 Modelling of U-tube Operation

Gas bubbles generated at the top of the downflow pipe are carried down to the bottom of the U-tube by the velocity of the water (see Fig. 6.4.1). The increasing hydrostatic head in the U-tube affects the transfer rate as the gas bubbles descend, changing both the interfacial area, A, and the equilibrium concentration, Co_2^*. These variables are also affected by the rate of nitrogen desorption into the gas bubbles. The process continues in the upflow pipe, except that the gas bubble pressure reduces to 1 atm again.

Published modelling procedures divide the U-tube into short incremental steps, to allow for internal changes, and in each step calculate the following: (1) mass of oxygen in bubbles, (2) mass of nitrogen in bubbles, (3) gas composition (4) hydrostatic pressure, (5) interfacial area, (6) dissolved oxygen deficit, (7) dissolved nitrogen deficit, (8) oxygen

Fig. 6. 4. 1 U-tube Operation

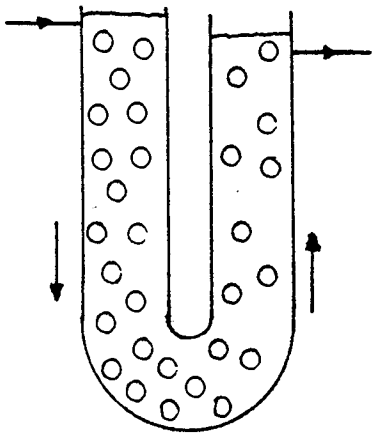

Gas bubbles are carried to the bottom of the U-tube by the liquid velocity, and are subjected to an increasing hydrostatic head.

Bubble size is affected by the pressure and by the exchange of gases. The process continues in the upflow pipe but the pressure of the bubbles reduces to 1 atm.

transferred and (9) nitrogen transferred. This procedure has been used to determine ($k_L A$) values which would predict observed outlet concentrations (Speece, 1970). A similar process has been used to predict oxygen transfer in an ICI "Deep Shaft", but this method also estimates power consumption under various conditions (Hosono et al, 1979). Both models consider mass transfer using air as a source of oxygen and also require the use of computer facilities.

6.4.2 U-tube Operation Using Pure Oxygen

A simplified incremental step model is developed to predict outlet concentrations in U-tube operation using pure oxygen. Initially, only mass transfer in the downflow pipe is considered. The assumptions and principles used in developing the theory are given below.

(1) The two-phase flow can be divided into regions, ψ_i defined by $\alpha(h_i - h_{i-1})$ for $i = 1 \ldots n$, where α is the cross-sectional area of the U-tube. $\sum_{i=1}^{n} (h_i - h_{i-1}) = h_n - h_o$ where h_n is the depth of the U-tube and h_o is the depth of oxygen injection.

Gas is carried through ψ_i by the velocity of the liquid phase. Two-phase flow through ψ_i is illustrated in Fig. 6.4.2.

Fig. 6.4.2. Two-phase Flow Through a Region, ψ_i, in the U-tube

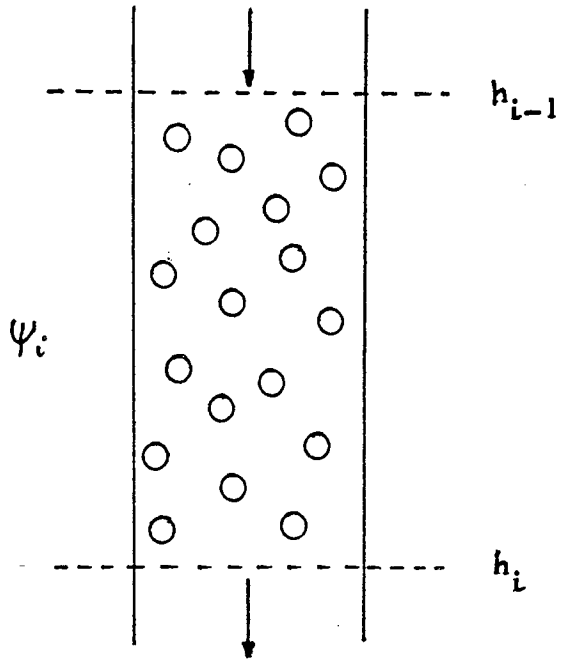

Interfacial area in ψ_i - a_i

Gas hold-up in ψ_i - ϵ_i

Total pressure in ψ_i - p_i

(2) The pressure, P_i, in each ψ_i is constant

with $P_i = 1 + \frac{h_i + h_{i-1}}{2h_A}$ 6.4.1

where h_A is the water gauge equivalent of 1 atm pressure

and $P_o = 1 + \frac{h_o}{h_A}$.

(3) The liquid flow-rate in the U-tube

$$Q_L = \alpha v_{SL} \quad 6.4.2$$

with v_{SL} = the superficial liquid velocity .

The initial superficial gas velocity in the U-tube,

$$v_{SG} = R_{O_2,o} / \rho_{O_2} P_o \alpha \quad 6.4.3$$

where $R_{O_2,o}$ = the initial oxygen flow-rate

and ρ_{O_2} = oxygen density at 1 atm pressure.

(4) The initial gas hold-up, ε_o, can be estimated from a consideration of the slip velocity, defined by

$$U_S = \frac{v_{SG}}{\varepsilon} - \frac{v_{SL}}{(1-\varepsilon)} \quad 6.4.4$$

In addition, for air-water systems, experimental results suggest that

$$U_S = v_{B\infty} (1-\varepsilon) \quad 6.4.5$$

where $v_{B\infty}$ is the single-bubble rise velocity for bubbles of diameter d_B (Wallis, 1969).

Values of $v_{B\infty}$ used are those proposed by Motarjemi (1978).

A solution of equations 6.4.4 and 6.4.5 is, therefore, given by

$$v_{sg}(1-\varepsilon) - v_{sL}\varepsilon = v_{B\infty}\varepsilon(1-\varepsilon)^2 \qquad 6.4.6$$

Behaviour over a range of operating conditions can be studied from graphical considerations of equ. 6.4.6. An example is given in Fig. 6.4.3 for cocurrent downward flow such as would be found in a U-tube (that is with $v_{sg}, v_{sL} < 0$)

(5) The oxygen flow-rate in ψ_i is $R_{O_2,i-1}$ and the nitrogen flow-rate is $R_{N_2,i-1}$. The volumetric flow-rates corrected to 1 atm pressure are $\frac{R_{O_2,i-1}}{\rho_{O_2}}$ and $\frac{R_{N_2,i-1}}{\rho_{N_2}}$, where ρ_{O_2} and ρ_{N_2} are the oxygen and nitrogen densities at 1 atm pressure. As the gas descends in the U-tube, the interfacial area changes due to the increasing hydrostatic head and due to oxygen and nitrogen transfer. The bubble size remains constant but the number of bubbles reduces due to bubble coalescence (Speece, 1970). The gas hold-up, ε_i, therefore varies with depth, but is assumed constant in each ψ_i, with

$$\varepsilon_i = \left\{\left(\frac{R_{O_2,i-1}}{\rho_{O_2}} + \frac{R_{N_2,i-1}}{\rho_{N_2}}\right) \div \left(\frac{R_{O_2,0}}{\rho_{O_2}}\right)\right\} \frac{P_0}{P_i}\varepsilon_0 \qquad 6.4.7$$

Fig. 6.4.3 Graphical Estimation of ε_o

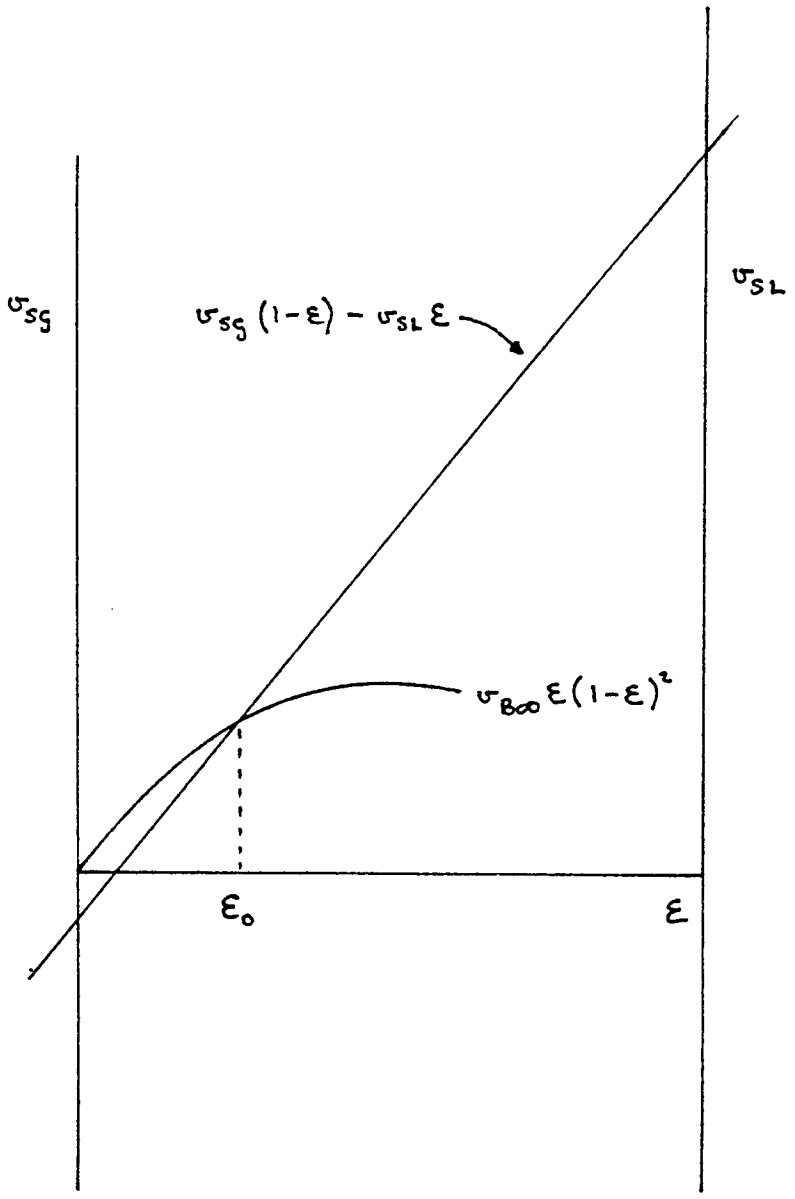

Solution of $v_{sg}(1-\varepsilon) - v_{sL}\varepsilon = v_{B\infty}\varepsilon(1-\varepsilon)^2$

for $v_{sg} < 0$, $v_{sL} < 0$ i.e. cocurrent downward flow

Estimates of the interfacial area can then be found from,

$$a_i = 6 \frac{\varepsilon_i}{d_B} \psi_i \qquad 6.4.8$$

where a_i is the interfacial area in ψ_i .

(6) Then, the oxygen and nitrogen partial pressures in ψ_i are given by

$$P_{O_2,i} = \left\{ \frac{R_{O_2,i-1}}{e_{O_2}} \div \left(\frac{R_{O_2,i-1}}{e_{O_2}} + \frac{R_{N_2,i-1}}{e_{N_2}} \right) \right\} P_i \qquad 6.4.9$$

and $$P_{N_2,i} = \left\{ \frac{R_{N_2,i-1}}{e_{N_2}} \div \left(\frac{R_{O_2,i-1}}{e_{O_2}} + \frac{R_{N_2,i-1}}{e_{N_2}} \right) \right\} P_i \qquad 6.4.10$$

Then $$C^*_{O_2,i} = P_{O_2,i} C^*_{O_2} \qquad 6.4.11$$

and $$C^*_{N_2,i} = P_{N_2,i} C^*_{N_2} \qquad 6.4.12$$

where $C^*_{O_2,i}$ and $C^*_{N_2,i}$ are the equilibrium dissolved oxygen concentrations in ψ_i, and $C^*_{O_2}$ and $C^*_{N_2}$ are the corresponding values for 1 atm oxygen and nitrogen respectively.

(7) Plug flow of both gas and liquid phases through ψ_i is assumed and the rate of oxygen transfer, $\varphi_{O_2,i}$, can be derived from

$$\ln \left(\frac{C^*_{O_2,i} - C_{O_2,i-1}}{C^*_{O_2,i} - C_{O_2,i}} \right) = \frac{k_L a_i t}{V} \qquad 6.4.13$$

where $\frac{V}{t} = Q_L$, the liquid flow-rate,
$C_{O_2,i-1}$ = the initial dissolved oxygen concentration in ψ_i
and $C_{O_2,i}$ = the final dissolved oxygen concentration in ψ_i
Similarly, the rate of nitrogen transfer, $\varphi_{N_2,i}$,

can be deduced from

$$\ln\left(\frac{C_{N_2,i-1} - C^*_{N_2,i}}{C_{N_2,i} - C^*_{N_2,i}}\right) = \frac{k_{L,N_2}\, a_i}{Q_L} \qquad 6.4.14$$

(8) $k_L \propto \sqrt{(\text{Diffusivity})}$, so k_{L,N_2} can be calculated from

$$\frac{k_L}{k_{L,N_2}} = \frac{\sqrt{(O_2 \text{ Diffusivity})}}{\sqrt{(N_2 \text{ Diffusivity})}}$$ (Boyes and Ellis, 1976)

Values of k_L used are those collected by Motarjemi (1978)

(9) Finally, $R_{O_2,i} = R_{O_2,i-1} - \Phi_{O_2,i}$ 6.4.15

and $R_{N_2,i} = R_{N_2,i-1} + \Phi_{N_2,i}$ 6.4.16

6.4.3 Sample Calculation from Experimental Data

The assumptions and principles used above are sufficient for the calculation of the dissolved oxygen concentration $C_{O_2,i}$ for i = 1 ... n. The following data, based on experimental results, will be used to find the concentration $C_{O_2,n}$ at the bottom of the U-tube.

Data

(1) The superficial liquid velocity, $v_{SL} = 0.3$ m/s

(2) The U-tube diameter is 0.3 m and

$$\alpha = 0.073 \text{ m}^2$$

(3) The oxygen flow-rate, $R_{O_2,0} = 1.5$ kg/h
$= 0.417$ g/s

(4) The depth of oxygen injection, $h_o = 2$ m

and the depth of the U-tube, $h_n = 6$ m

(5) h_A = 10 m WG for 1 atm pr.

(6) Bubble sizes of up to 10 mm were observed in experiments, so an average bubble diameter, d_B = 5 mm is used in the calculations. k_L for bubbles of this size is 0.34×10^{-3} m/s and $k_{L,N_2} = 0.3 \times 10^{-3}$ m/s. The rise velocity of 5mm diameter bubbles is 0.23 m/s.

(7) $Co_2^* = 54$ ppm dO_2, $Co_2 = 10$ ppm dO_2

$C_{N_2}^* = 24$ ppm dN_2, $C_{N_2} = 19$ ppm dN_2

(8) $\rho_{O_2} = 1.38 \times 10^3$ g/m^3 and $\rho_{N_2} = 1.21 \times 10^3$ g/m^3 at 1 atm pressure and 10° C.

Calculation

No nitrogen is present in the gas initially, so $R_{N_2,0} = 0$

For the sample calculation $n = 2$ with $h_2 - h_1 = h_1 - h_0 = 2$m. This allows a comparison with experimental results since oxygen concentrations were sampled at 4 m and 6 m depth. The liquid flow-rate in the U-tube,

$Q_L = 0.022$ m^3/s from equ. 6.4.2

Now $p_o = 1.2$ atm

and $v_{sg} = 3.45 \times 10^{-3}$ m/s from equ. 6.4.3

Fig. 6.4.4 is a graphical solution of equation 6.4.6 which gives a solution of $\varepsilon_o = 0.038$. Only part of the graph is shown on an expanded scale for detail. Substitution in the equation shows that the estimate is accurate enough for the sample calculation.

Fig. 6.4.4 Graphical Estimation of ε_o for the Sample Calculation

$v_{sL} = -0.3$ m/s

$v_{sg} = -3.45 \times 10^{-3}$ m/s

(shown on an expanded scale - see Fig. 6.4.3)

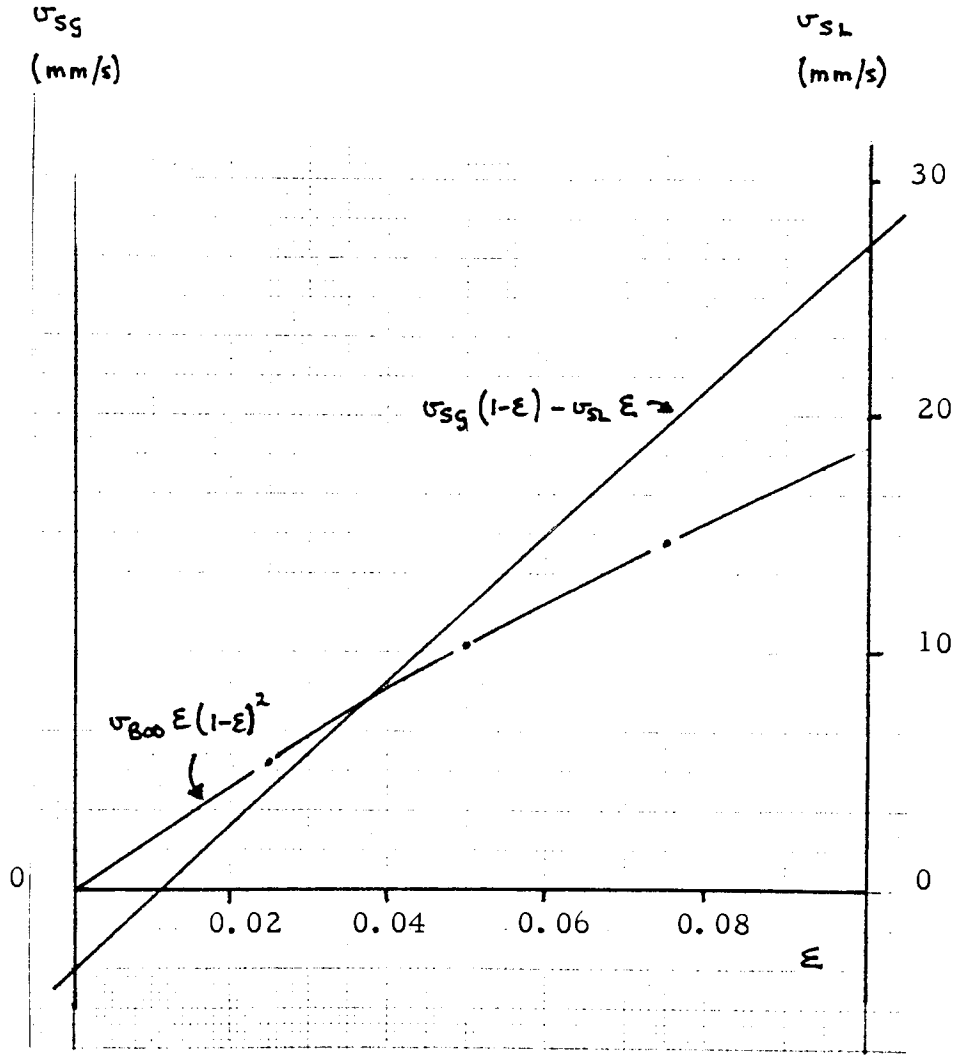

Solution of $v_{sg}(1-\varepsilon) - v_{sL}\varepsilon = v_{B\infty}\varepsilon(1-\varepsilon)^2$
shown over range $0 < \varepsilon < 0.1$

NB $v_{sg} < 0$, $v_{sL} < 0$ i.e. cocurrent downward flow.

In ψ_1,

$P_1 = 1.3$ atm — from equ. 6.4.1

so $\varepsilon_1 = 0.035$ — from equ. 6.4.7

and $a_1 = 6.15\ m^2$ — from equ. 6.4.8

$P_{O_2,1} = 1.3$ atm — from equ. 6.4.9

and $P_{N_2,1} = 0$

$C^*_{O_2,1} = 70.2$ ppm dO_2

and $C^*_{N_2,1} = 0$

Substituting in equation 6.4.13,

$$\ln\left(\frac{C^*_{O_2,1} - C_{O_2,0}}{C^*_{O_2,1} - C_{O_2,1}}\right) = \frac{k_L a_1}{Q_L}$$ from which $C_{O_2,1} = 15.5$ ppm dO_2

and $\Phi_{O_2,1} = 0.114$ g/s

Similarly, from equation 6.5.14, $C_{N_2,1} = 17.5$ ppm dN_2

and $\Phi_{N_2,1} = 0.032$ g/s

Therefore $R_{O_2,1} = 0.303$ g/s — from equ. 6.4.15

and $R_{N_2,1} = 0.032$ g/s. — from equ. 6.4.16

In ψ_2,

$P_2 = 1.5$ atm — from equ. 6.4.1

and $\varepsilon_2 = 0.025$, — from equ. 6.4.7

so $a_2 = 4.38\ m^2$. — from equ. 6.4.8

Now $P_{O_2,2} = 1.34$ atm — from equ. 6.4.9

and $P_{N_2,2} = 0.16$ atm, — from equ. 6.4.10

so $C^*_{O_2,2} = 72.3$ ppm dO_2 — from equ. 6.4.11

and $C^*_{N_2,2} = 3.9$ ppm dN_2. — from equ. 6.4.12

$Co_{2',2}$ = 19.2 ppm dO_2 from equ. 6.4.13

and $\Phi_{O_{2,2}}$ = 0.079 g/s.

$C_{N_{2,2}}$ = 16.7 ppm dN_2 from equ. 6.4.14

and $\Phi_{N_{2,2}}$ = 0.017 g/s.

$R_{O_{2,2}}$ = 0.224 g/s from equ. 6.4.15

and $R_{N_{2,2}}$ = 0.049 g/s. from equ. 6.4.16

The dissolution efficiency is therefore 46%.

6.5 Discussion

Overall, the model provides a useful insight into U-tube operation, illustrating the high initial transfer rate, the increase in dissolution with path length and the decreasing transfer rate along the length of the U-tube. However, in detail, certain errors are highlighted in comparison with experimental results (see Table 6.5.1).

TABLE 6.5.1 Comparison of Predicted and Observed Results

Region (Ψi)	Ψ_1		Ψ_2
Dissolved Oxygen Level (ppm)	$Co_{2,0}$	$Co_{2',1}$	$Co_{2',2}$
Predicted	10	15.5	19.2
Observed	7.6	15.3	18.1

In ψ_1, the predicted dissolved oxygen concentration, $Co_{2,1}$, is fairly accurate despite the difference between observed and estimated values of $Co_{2,0}$. This suggests that oxygen transfer is underestimated in ψ_1 using the model. However, the predicted dissolved oxygen concentration, $Co_{2,2}$ is higher than the observed value which suggests that oxygen transfer is overestimated in ψ_2. The most likely sources of error are the estimates of gas hold-up and bubble size in each region. The graphical solution of equation 6.4.6 must be accurately interpreted, since errors can occur when the gas hold-up is low. All estimates of gas hold-up confirm visual observations, however.

The model is considered sufficiently accurate to explore theoretically some of the variables measured in experiments.

6.5.1 Effects of Depth and Phase Flow-rates

Depth

The effects of increased depth can be calculated using equations 6.4.1 - 6.4.16 in additional regions, ψ_i, for $i=n+1,\ldots,m$. A higher final dissolved oxygen concentration $Co_{2,m}$ is likely and, in addition, a longer contact time will result in improved dissolution efficiency. The result below has been estimated using the data from section 6.4.3 but

with $m = 3$ and $h_m = 8$ m. A final dissolved oxygen concentration of 21.8 ppm is predicted which gives a dissolution efficiency of 60%.

One interesting aspect of increasing the U-tube depth is the effect of hydrostatic head on the nitrogen which is desorbed into the gas phase. A depth will be reached at which the equilibrium concentration is greater than the dissolved nitrogen concentration in the liquid and nitrogen will be re-absorbed into the liquid. The modelling procedure will take this into account since nitrogen absorption will be shown by a negative nitrogen desorption rate, $\Phi_{N_2,i}$. Care must therefore be exercised when using the model to predict oxygen transfer in deep U-tubes. If the U-tube is sufficiently deep, all the gas will be dissolved ultimately. It should also be remembered that, in the case when nitrogen is re-absorbed, the nitrogen partial pressure can never be greater than 0.8 atm and hence nitrogen supersaturation cannot occur.

Oxygen Flow-rate

Increasing the gas flow-rate produces a higher superficial gas velocity, v_{sg}. Examination of Fig. 6.4.3 shows that this will increase the gas hold-up and hence higher transfer rates will be achieved through an enlarged interfacial area. However, this will result in higher values of $Co_{2,i}$ and so the driving force $(Co_2^*,_i - Co_{2,i})$ will be lower. There-

fore, the gas will take longer to dissolve and lower dissolution efficiencies can be expected. Using the data in section 6.4.3 but with an oxygen flow-rate of 2 kg/h a concentration of 21.1 ppm dO_2 is predicted which is equivalent to 42% dissolution efficiency.

Liquid Flow-rate

As a result of increasing the liquid flow-rate the superficial liquid velocity, v_{SL}, will be increased and the gas hold-up will be reduced, assuming the gas flow-rate remains constant (see Fig. 6.4.3). Lower dissolved oxygen concentrations can be expected, therefore. In addition, since the gas and liquid are both in plug flow, the increased liquid flow-rate will sweep gas bubbles out of the U-tube more quickly. The contact time will be reduced, and lower dissolution efficiencies will be achieved. These trends are demonstrated using the model, but when results are compared with experimental observations, the predicted results are considerably lower than observed values. With a liquid flow-rate of 0.0255 m^3/s, equivalent to a superficial velocity of 0.35 m/s, a dissolved oxygen concentration of 16.0 ppm is predicted using the model whereas a concentration of 18.1 ppm dO_2 was observed in tests.

6.5.2 Mass Transfer in the Upflow Pipe

So far the theory has been concerned with mass transfer in the downflow pipe. In the upflow pipe, the preceding equations, 6.4.1 - 6.4.16 will apply, except that the hydrostatic head is reduced as the gas bubbles rise. The gas hold-up will change due to oxygen and nitrogen exchange and due to the reduction in hydrostatic head. An initial value can be deduced from a solution of equation 6.4.6 which is estimated graphically in Fig. 6.5.1 assuming v_{sL} in the upflow pipe is the same as that in the downflow pipe; the data from the sample calculation in section 6.4.3 are used. The initial estimate of 0.5%, together with the reducing oxygen partial pressure, means that only a low transfer rate can be expected in the upflow pipe. Using air, 25% of the total transfer has been estimated to occur in the upflow pipe (Speece, 1970).

If the U-tube is sufficiently deep, the dissolved gas concentrations may exceed the respective equilibrium concentrations in the upflow pipe, as the hydrostatic pressure on the gas bubbles reduces, and so, oxygen and nitrogen may be desorbed. Careful interpretation of the results is necessary in deep U-tubes, therefore. However, if the gas is completely dissolved under the hydrostatic head, then degassing may occur as the pressure is reduced. The extent of degassing depends on many factors, including the rate of pressure reduction (determined by v_{sL}), the depth of the

Fig. 6.5.1 Graphical Estimation of ε_o in the Upflow Pipe

$v_{sL} = 0.3$ m/s

$v_{sg} = 2.03 \times 10^{-3}$ m/s

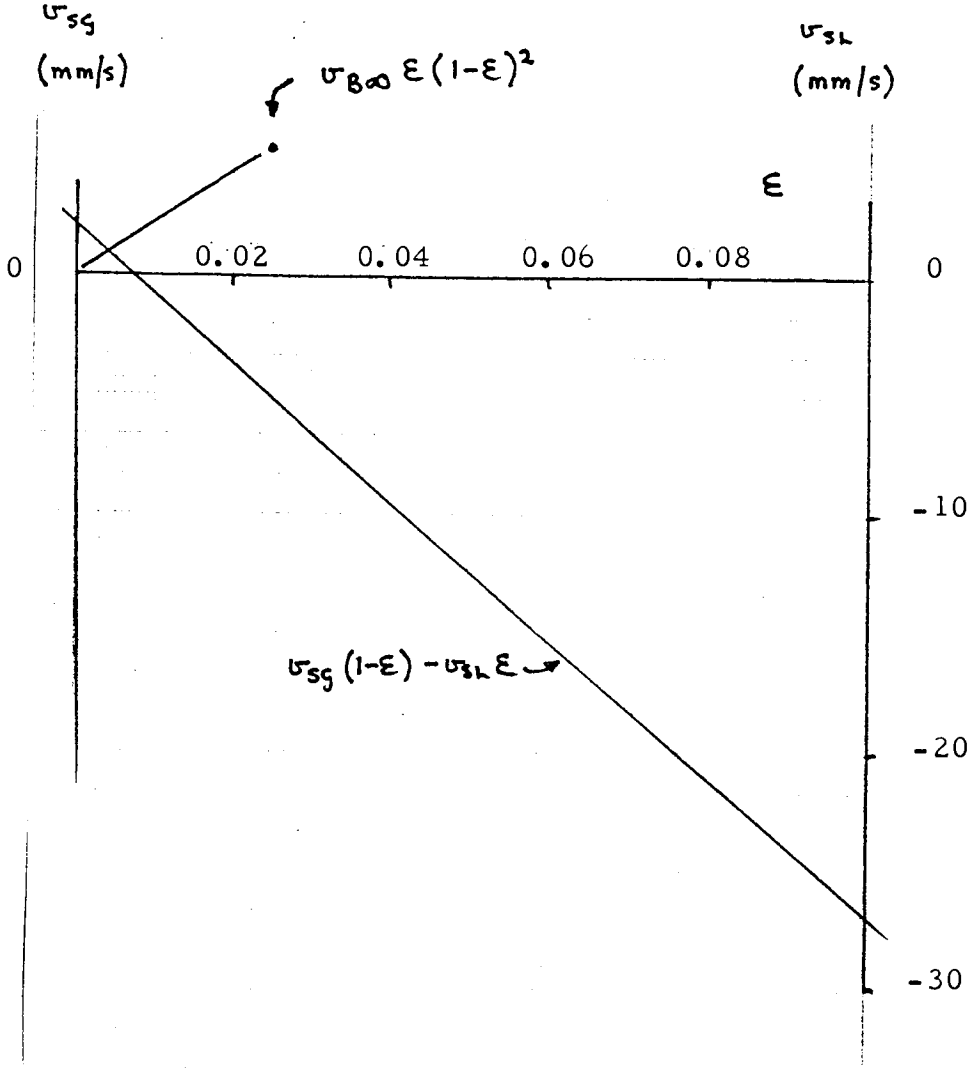

Solution of $v_{sg}(1-\varepsilon) - v_{sL}\varepsilon = v_{B\infty}\varepsilon(1-\varepsilon)^2$

shown over range $0 < \varepsilon < 0.1$

NB $v_{sg} > 0$, $v_{sL} > 0$ i.e. cocurrent upward flow

U-tube, the dissolved gas concentrations, and the physical and chemical properties of the water. The model does not take account of this effect.

6.6 Conclusions

The U-tube is a suitable method for oxygenating fish farms due to its ability to oxygenate large volumes of water and, with its low operating head, to achieve this for relatively low operating costs.

The maximum dissolution efficiency of a 6 m deep U-tube was over 70% and occurred with a superficial liquid velocity of 0.3 m/s and a change in dissolved oxygen level of 5 ppm. Attempts to increase this change to 10 ppm dO_2 resulted in a reduction in absorption efficiency. It would seem that the only way to increase the outlet concentration to the specified level of 25 ppm dO_2 is to increase the depth of the U-tube. This would increase the gas residence time and also the hydrostatic head within the U-tube.

A model has been developed to study U-tube oxygenation. The model is useful for both prediction and analysis over a limited range of operation, but needs further development to increase its potential.

CHAPTER 7

OXYGENATION THROUGH DIFFUSER ELEMENTS

7.1 Introduction

Diffuser elements are used on Shearwater's fish farms as a standby method of oxygenation involving no external power source. When operating in freshwater tanks of only one metre depth, oxygen dissolution efficiencies are poor, but the system is acceptable for back-up purposes. In seawater, smaller bubbles are formed which dissolve more quickly and so using diffuser systems may lead to acceptable dissolution efficiencies (say 60%). This would allow the continuous support of fish stocks without any additional power requirements.

In this chapter, the performance of a diffuser system is evaluated with particular attention being given to the effects of oxygen flow-rate and depth. Preliminary ideas for modelling oxygen transfer are also presented.

7.2 Equipment and Experimental Programme

7.2.1 Equipment

The diffuser tube is made of low density poly ethylene of 50% porosity and 12 mm in diameter. It is supplied by Spline Gauges Ltd of Tamworth, Staffordshire, who recommend flow-rates of 0.3 m^3/h per metre length for aeration, with the air supplied at a pressure of 0.5 atm. Elements are constructed to Shearwater's own design and each consists of a one metre length of tube. A brass rod is inserted in the

tube for rigidity and the ends are capped and clamped. Oxygen is supplied to one end of the element. Fig. 7.2.1 is a diagram of a diffuser element.

In the experimental runs, eight one-metre elements were placed radially in pairs around the fish tank as shown in Fig. 7.2.2. Oxygen flow to each pair of diffusers was controlled independently with a valve, flowmeter and pressure gauge. Oxygen flow-rates of 1 kg/h and 2 kg/h were used to meet a typical tank oxygen demand of 1 kg/h at assumed dissolution efficiencies of 100% and 50% respectively: the corresponding volumetric flow-rates were 0.09 and 0.18 m^3/h per metre of diffuser.

Water circulation in the 12 m diameter fish tank was maintained by the inlet water flow. The water depth was controlled using standpipes of different heights in the outflow, which discharged effluent water drawn from the centre of the tank. Water depths of 1.0 and 1.5 m were used in the tests since these are convenient for husbandry purposes.

7.2.2 Experimental Programme

The water flow-rate to the tank was constant throughout tests and the salinity and temperature of the water were measured daily. The methods used to determine oxygen transfer rate and oxygen dissolution efficiency are given in Appendix 2.

Fig. 7.2.1 Oxygen Diffuser Element

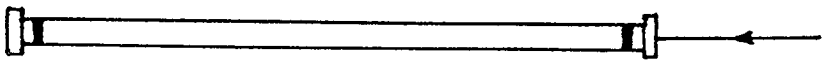

porous plastic tube

Fig. 7.2.2 General Equipment Layout

(a) diffuser elements

(b) standpipe for water level control

(c) water inlet

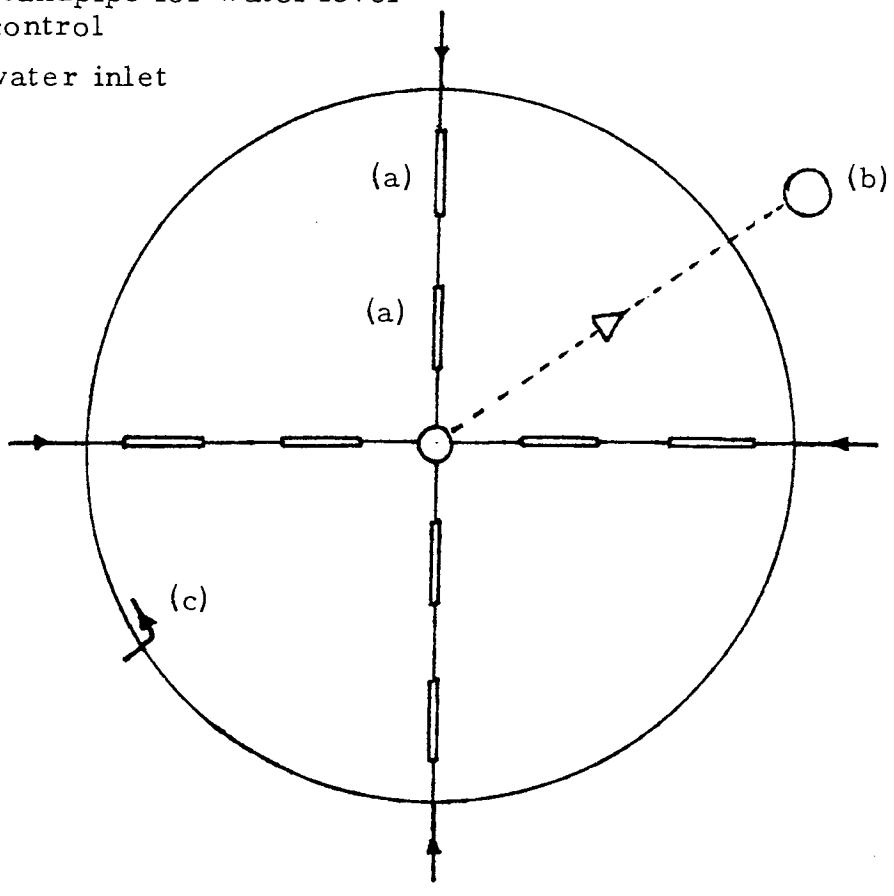

Four tests were conducted in all: these involved the combinations of the two values for oxygen flow-rate and those for water depth. Yates' method of analysis was used to assess the importance of the oxygen flow-rate and the water depth on the two response variables, oxygen transfer rate and oxygen dissolution efficiency. The method of analysis is given in Appendix 1.

7.3 Results and Observations

7.3.1 Results Summary

The results of the tests are summarised in Tables 7.3.1 - 7.3.3.

TABLE 7.3.1 Dissolution Efficiency (%)

	Water Depth (m)		
		1	1.5
Oxygen Input (kg/h)	1	41	63
	2	49	70

TABLE 7.3.2 Dissolution Rate (gO_2/h)

	Water Depth (m)		
		1	1.5
Oxygen Input (kg/h)	1	407	627
	2	980	1403

TABLE 7.3.3 Results of Yates' Analysis

	Oxygen Dissolution Efficiency (%)	Oxygen Dissolution Rate (g/h)
Ave effect	56	854
Depth	8	161
Oxygen	4	337
Depth/Oxygen	0	51

Water Temperature 11.5 - 13° C Salinity 30 - 32 ppt

Oxygen transfer rate improved significantly with oxygen flow-rate. The oxygen dissolution efficiency also improved slightly, which was not expected. These results suggest that there is scope for increasing the oxygen flow-rate through each diffuser, which would increase the "active" surface area of the element.

The oxygen absorption rate and dissolution efficiency both improved with increased depth, but the required minimum dissolution efficiency was only achieved at the greater depth.

7.3.2 Visual Observations

At the water surface only very small bubbles, less than 0.5 mm in diameter were observed in the region of the diffuser elements. The number of these bubbles increased with the oxygen flow-rate but a change in water depth made no observable difference.

Detailed observation of the elements showed that oxygen bubbles were not produced evenly across the surface of the porous tube, but were seen streaming from particular "active" areas. This in part, is thought to promote bubble coalescence which can occur in freshwater even at low oxygen flow-rates (see Figs. 7.3.1 and 7.3.2).

7.4 Theory of Diffuser Systems

7.4.1 Modelling of System Operation

Diffusers operate as an oxygen transfer device by creating a stream of gas bubbles which rise to the liquid surface (see Fig. 7.4.1). As the bubbles rise, oxygen and nitrogen are transferred between the phases, at rates described by the mass transfer equations. Motarjemi and Jameson (1978) have undertaken some of the most recent work concerning bubbles rising in liquids. Their results are summarised in Fig. 7.4.2 which shows the dissolution efficiency of oxygen bubbles of various initial

Fig. 7.3.1 Bubble Formation in Seawater at the Diffuser Element

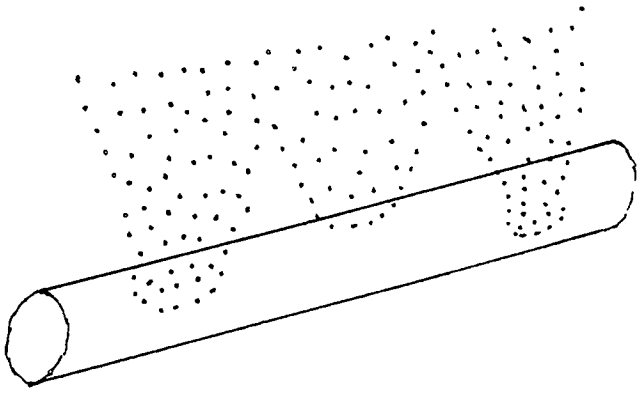

Bubbles formed at certain "active" areas.

Fig. 7.3.2 Bubble Formation in Freshwater at the Diffuser Element

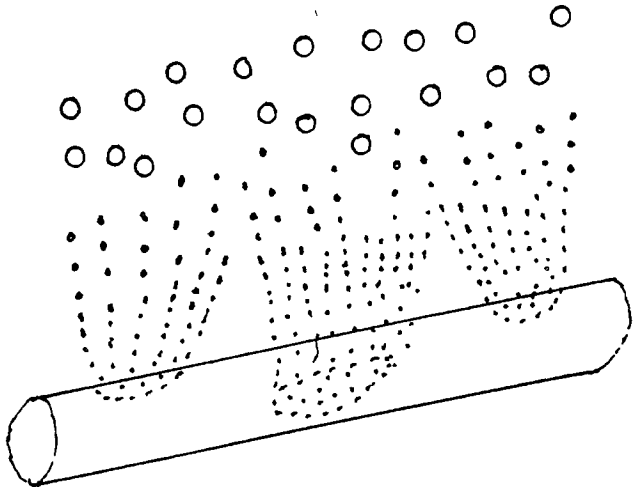

In freshwater, bubble streams coalesce forming large bubbles.

Fig. 7.4.1 Two-phase flow Above a Diffuser Element

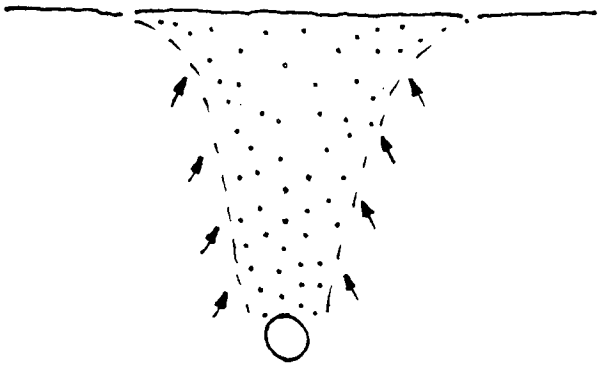

Fig. 7.4.2 The Dissolution Efficiency of Oxygen Bubbles Rising in Tap Water (Motarjemi and Jameson, 1978).

Oxygen Dissolved (%)
100

Aston University

Content has been removed for copyright reasons

Release Depth (m)

diameters released at a depth, H, below the surface of water containing no oxygen or nitrogen, although similar trends are suggested for water saturated with nitrogen. However, these results are based on the assumption that a bubble rises through stationary liquid whereas, in fact, gas bubbles created by the diffuser elements cause liquid circulation by transporting liquid in their wakes. The results obtained in the author's tests are in reasonable agreement with those of Motarjemi (1978) which suggests that the rate of liquid circulation was relatively small under the conditions employed (see Table 7.4.1). However, the degree of liquid circulation may be responsible, in part, for determining the limits of acceptable operation, and so, it has been considered in developing the model.

TABLE 7.4.1 Comparison of Observed and Theoretical Dissolution Efficiencies of Rising Bubbles

Depth (m)	Dissolution Efficiency (%)	
	Observed	Theoretical (Motarjemi, 1978)
1	41 - 49	56
1.5	63 - 70	73

7.4.2 Liquid Flow in a Bubble Stream

Assume that the liquid in wake flow provides an estimate of liquid circulation and that spherical bubbles are symmetrically arranged within the two phase region, forming a cubic pattern as shown in Fig. 7.4.3. The gas hold-up, ε, is then given by

$$\varepsilon = \frac{\pi}{6} d_B^3 \Big/ d_c^3$$

where d_B = bubble diameter

and d_c = width of unit cell.

Rearranging this relationship,

$$\frac{d_c}{d_B} = \left(\frac{\pi}{6\varepsilon}\right)^{1/3}$$

The "wake" is taken to be that liquid trapped between two gas bubbles (as shown in Fig. 7.4.4), although it should be noted that interchange between the trapped liquid and the bulk liquid can occur.

The volume of liquid, V_W, trapped between gas bubbles is given by

$$V_W = \frac{\pi}{4} d_B^2 d_c - \frac{\pi}{6} d_B^3$$

$$= \frac{\pi}{6} d_B^3 \left(\frac{3}{2} \cdot \frac{d_c}{d_B} - 1\right)$$

Hence

$$\frac{V_W}{V_B} = \frac{3}{2}\left(\frac{\pi}{6\varepsilon}\right)^{1/3} - 1 \qquad 7.4.1$$

Fig. 7.4.3 Hypothetical Arrangement of Bubbles Produced by a Diffuser Element

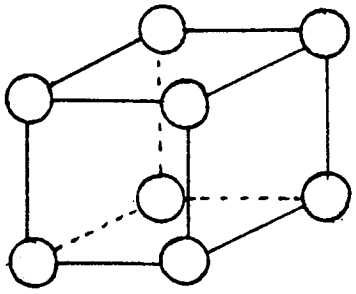

bubble diameter, d_B

unit cell width, d_c

Fig. 7.4.4 Trapped Liquid in a Bubble Stream

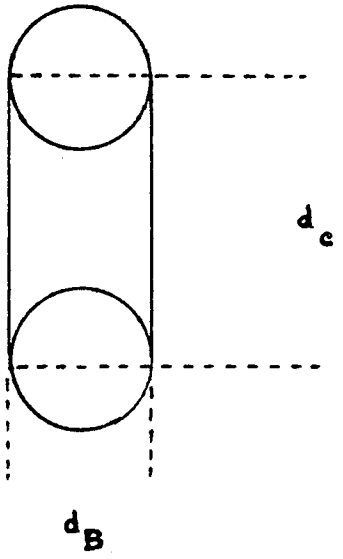

Therefore, the liquid volume in the wake of a bubble can be estimated from the gas hold-up and the bubble volume, and in turn, the liquid flow-rate, Q_L, can be estimated from the gas flow-rate.

The above analysis is used to estimate the initial flow of liquid at the diffuser surface. Plane jet theory can be used to assess the increase in liquid flow-rate above the diffuser, caused by entrainment as gas bubbles rise to the surface.

7.4.3 Two-Phase Flow above a Diffuser Element

Consider the flow of gas bubbles from a diffuser element of length, ℓ, and diameter, $\mathcal{D}$, through a liquid of depth H. In developing the theory the following assumptions are made. (1) The oxygen flowing through each diffuser element is broken down into bubbles, diameter d_B, at the surface of the element. The number of bubbles produced in unit time, N_0, is given by

$$N_0 = \frac{R_{O_2}}{V_B \rho_{O_2}} , \qquad 7.4.2$$

where $V_B = \frac{\pi}{6} d_B^3$,

ρ_{O_2} = the oxygen density

and R_{O_2} = the oxygen flow-rate through each diffuser.

The gas-liquid interfacial area, S_o, generated in unit time is then given by

$$S_o = N_o S_B \qquad 7.4.3$$

where $S_B = \pi d_B^2$

(2) The bubbles rise with a velocity equal to that for a single bubble in an infinite liquid, $v_{B\infty}$, and so the contact time, t, is given by

$$t = \frac{H}{v_{B\infty}} \qquad 7.4.4$$

Thus, the total interfacial area, A, is given by

$$A = S_o t \qquad 7.4.5$$

neglecting the effects of hydrostatic pressure and mass transfer on bubble size.

(3) The rising bubbles initially draw liquid into their wakes from a distance, D, either side of the diffuser element (Fig. 7.4.5). Therefore the volume of the two phase region generated in unit time is initially,

$$3 D \rho v_{B\infty}$$

The initial gas hold-up, ε, is then obtained from the identity,

$$S_o = \frac{6\varepsilon}{d_B} \left(3 D \rho v_{B\infty}\right) \qquad 7.4.6$$

Fig. 7.4.5 The Generation of Two-phase Flow Around the Diffuser

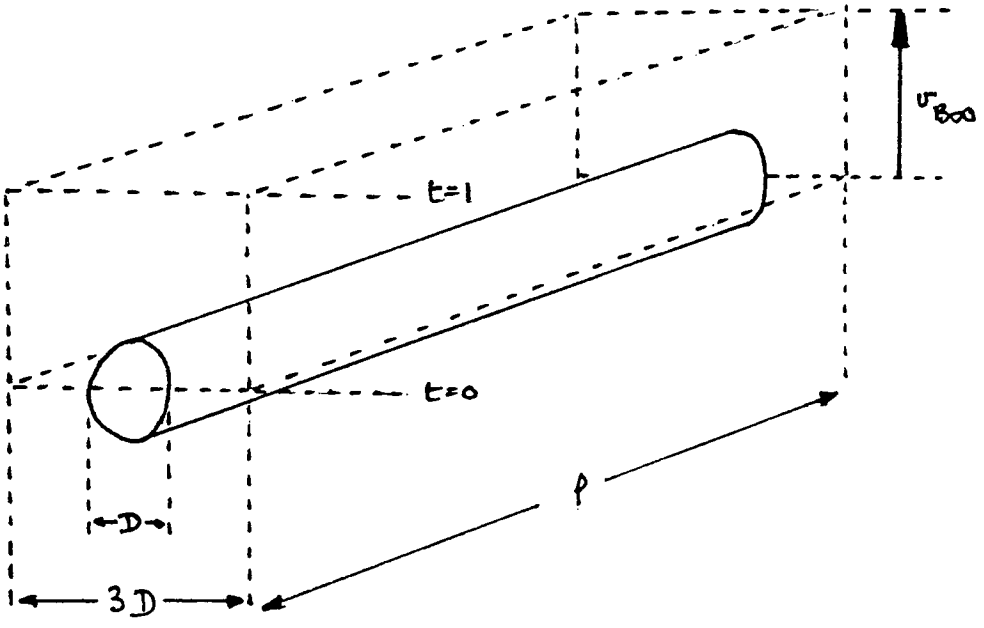

Using this value of ε in equation 7.4.1 provides an estimate of the initial liquid flow-rate, Q_L, in the two-phase region.

(4) As the liquid rises in the wakes of gas bubbles, it will entrain further liquid according to plane jet theory (see also section 5.5.3). The total volumetric liquid flow-rate at a point x is

$$0.625\ V_{ns} \sqrt{\left(\frac{x}{w}\right)}$$

where V_{ns} = the liquid flow-rate at the nozzle

and w = slot width.

In this case the slot width is taken to be 3D so that, the flow is $0.625\ Q_L \sqrt{\left(\frac{H}{3D}\right)}$ at the surface.

Therefore, the average liquid flow-rate within the two-phase region, $\bar{Q}_L$, is

$$\frac{Q_L}{2}\left\{1 + 0.625 \sqrt{\left(\frac{H}{3D}\right)}\right\} \qquad 7.4.7$$

(5) The oxygen transfer rate, ϕ, is given by

$$\phi = k_L A \left(C_{O_2}^* - C_{O_2}\right) \qquad 7.4.8$$

where $C_{O_2}^*$, the equilibrium dissolved oxygen concentration, is assumed constant by neglecting the effects of hydrostatic head on $C_{O_2}^*$: the effects of nitrogen desorption on $C_{O_2}^*$ can also be ignored (Motarjemi, 1978). Values of k_L are based on those reported by Motarjemi (1978).

Oxygen transfer can then be explored for a range of oxygen flow-rates and water depth.

7.4.4 Sample Calculation based on Experimental Data

The following data based on experimental results have been used in the sample calculation.

Data

(1) Oxygen flow-rate = 2 kg/h and so with eight diffuser elements the flow-rate through each = 0.694 g/s

Oxygen density = 1.38×10^3 g/m^3 at 1 atm and 10°C.

(2) For each diffuser element ℓ = 1 m, D = 0.012 m.

(3) Water depth, H = 1 m.

(4) Co_2^* = 54 ppm dO_2, Co_2, = 10 ppm dO_2.

(5) Observed bubble size, d_B = 0.5 mm.

The rise velocity, v_{bo}, for bubbles of this size is 0.07 m/s and $k_L = 0.15 \times 10^{-3}$ m/s.

The number of bubbles produced,

N_o = 774,000 per second, from equ. 7.4.2

assuming the gas bubbles are produced at a pressure of 1 atm. The interfacial area generated by these bubbles is

S_o = 0.61 m^2/s from equ. 7.4.3

and since the contact time

t = 14.3 s, from equ. 7.4.4

the total interfacial area = 8.7 m^2 from equ. 7.4.5

Now, the initial gas hold-up

$$\varepsilon = 0.02 \qquad \text{from equ. 7.4.6}$$

and substituting in equation 7.5.1,

$$\frac{V_W}{V_B} = 3.45 ,$$

Hence, the initial liquid flow-rate

$$Q_L = 1.74 \times 10^{-4} \ m^3/s .$$

So the average liquid flow-rate in the two phase region

$$\bar{Q}_L = 3.74 \times 10^{-4} \ m^3/s . \qquad \text{from equ. 7.4.7}$$

The quantity of two phase fluid in motion amounts to less than 16% of the two-phase region since the average liquid flow-rate is only about eight times that of the initial gas flow-rate and the initial gas hold up is only 2%. Therefore, the region is unlikely to be well-mixed and the appropriate solution for plug flow using equation 7.4.3 is

$$\ln \left(\frac{C_{O_2}^* - C_{O_2,T}}{C_{O_2}^* - C_{O_2,t}} \right) = \frac{k_L A}{V} t$$

where $C_{O_2,T}$ is the initial dissolved oxygen concentration,

$C_{O_2,t}$ is the final dissolved oxygen concentration, C_{O_2},

and $\frac{V}{t} = \bar{Q}_L$, the average liquid flow-rate.

$C_{O_2} = 52.7$ ppm dO_2 ,

from which $\varphi = 1.75 \times 10^{-3}$ g/s (50 g/h through all diffusers)

Missing page(s) from the bound copy

7.5 Discussion

The above result is far lower than that found by experiment corresponding to a dissolution efficiency of only 2.5%. The high value of Co_2 relative to Co_2^* suggests that mass transfer is restricted by the low predicted liquid flow-rate. A liquid flow-rate of about seven times that suggested by the theory developed would be needed to be in agreement with experimental observations. It is well known that significant volumes of liquid circulate due to the motion of rising bubbles, but actual quantities are difficult to assess. Bulk liquid circulation within the tank may also aid two-phase mixing, but again the extent and importance of this effect is difficult to judge. Further research is obviously required in this area, although the benefit in fish farming may be small due to the limited scope for the use of diffuser elements, other than as a stand-by measure.

7.6 Conclusions

Diffuser elements are in general an inefficient method of oxygenation but their use in conjunction with a liquid oxygen store can be justified for stand-by since oxygen can be dissolved independently of any external power source.

In seawater, acceptable dissolution efficiencies can be achieved provided the water depth is at least 1.5 m. The

Missing page(s) from the bound copy

gas flow-rate must also be low enough to inhibit bubble coalescence. For the porous plastic tube used in the author's tests, a gas flow-rate of 0.18 m^3/h per metre length of diffuser element was found to be satisfactory, although optimum flow-rates will vary with the type of element used.

Dissolution efficiencies using diffuser element systems can be estimated by considering oxygen transfer from bubbles rising in a stationary liquid. Predicted results compare favourably with observed results at low gas-flow-rates, but estimates are likely to be in error as flow-rates are increased due to the effects of liquid circulation. At the present time, insufficient data are available about the rate of liquid circulation to explore performance limits.

CHAPTER 8

COMMERCIAL-SCALE OXYGENATION COSTS

8.1 Introduction

A major factor in economising on water use is, of course, the cost of a reoxygenation system. In section 1.6, various factors were described which might influence the choice of method and the cost of operation, and it was concluded that accurate estimates can only be derived for each individual site.

In this chapter, the costs of oxygenating both the Low Plains and Finnarts Bay sites are estimated, to provide some insight into typical costs of achieving high degrees of water economy. In addition, an estimate is also derived for achieving somewhat lower savings in water use, by considering an example of U-tube oxygenation. These are then compared with budget figures developed for aeration methods.

8.2 Equipment and Estimation of Oxygen Requirements

8.2.1 Equipment

Individual tank oxygenators require a three-phase electricity supply to each production unit, and a single-phase supply for the oxygen control system, which is coupled to a central alarm system warning of low oxygen levels.

Oxygen is supplied from one of a pair of liquid storage tanks (VIE) and distributed through a copper ring main to

each tank. In addition, each tank has an independent oxygen supply to a diffuser element for standby use.

8.2.2 Estimation of Oxygen Requirements

Production from the Low Plains site can be nearly constant throughout the year, due to the constant water temperature, and adequate stocks of fish in intermediate size ranges are maintained to achieve this. Food rations are allocated according to Shearwater's own feeding levels, which are adapted from the feeding tables produced by BP Nutrition Ltd., who supply the food (see Appendix 3). By considering the food ration to each tank, oxygen consumptions can be calculated since, for rainbow trout under intensive conditions, 1 kg oxygen is required to metabolise 2.5 kg food (Harman, 1978).

Peak oxygen consumption can be used for equipment specification and can be calculated from the maximum daily oxygen demand per tank. An additional 33% oxygenation capacity is specified to allow for diurnal variations in oxygen demand.

The annual oxygen use can be estimated from the average daily requirements and the performance data of the oxygenation equipment. Average daily requirements are taken to be the oxygen requirements of the average weight of fish in each size range.

At the Finnarts Bay site the situation is more complex because the temperature regime affects both growth rates and production targets. However, it is assumed that the distribution of stocks in intermediate size ranges is the same proportionately as that at Low Plains.

Peak oxygen consumption can then be derived from the maximum daily oxygen demand at the highest recorded water temperature, and equipment specified with an additional 33% capacity.

Average recorded monthly water temperatures are used to predict average daily oxygen consumption which can then be used with oxygenator performance data to estimate annual oxygen use.

8.3 Low Plains Costs

8.3.1 Equipment Specification

Maximum stock levels, food ration and daily oxygen consumption per tank for the Low Plains site are summarised in Table 8.3.1. The table shows a maximum oxygen demand of 10.7 kg/day, or 450 g/h. Peak oxygen demand is estimated to be 600 g/h which was the design specification for the oxygenation system at Low Plains.

TABLE 8.3.1 Maximum Tank Stock Levels, Food Ration and Oxygen Consumption for the Low Plains Site

Wt. Range (g)	5-20	20-80	80-180	180-250
Tanks Allocated	2	5	8	5
Max Wt. (g)	20	80	180	250
Max. Biomass (kg)	936	2064	2268	2475
Max Food Ration (kg/day)	18.3	26.8	25.0	24.8
Max Oxygen Cons. (kg/day)	7.3	10.7	10.0	10.0

8.3.2 Running Costs

Average stock levels, food ration and oxygen consumption per tank are summarised in Table 8.3.2.

TABLE 8.3.2 Average Tank Stock Levels, Food Ration and Oxygen Consumption for the Low Plains Site

Wt. Range (g)	5-20	20-80	80-180	180-250
Ave. Wt (g)	15	50	130	220
Ave. Biomass (kg)	702	1290	1638	2178
Ave. Food Ration (kg/day)	15.4	19.4	18.8	21.8
Ave. Oxygen Cons. (kg/day)	6.2	7.8	7.5	8.7

The average hourly tank oxygen consumption can be deduced and using the performance data given in Fig.8.3.1, the total annual oxygen use can be estimated (see Table 8.3.3).

Fig. 8.3.1 Column Oxygenator Performance Data

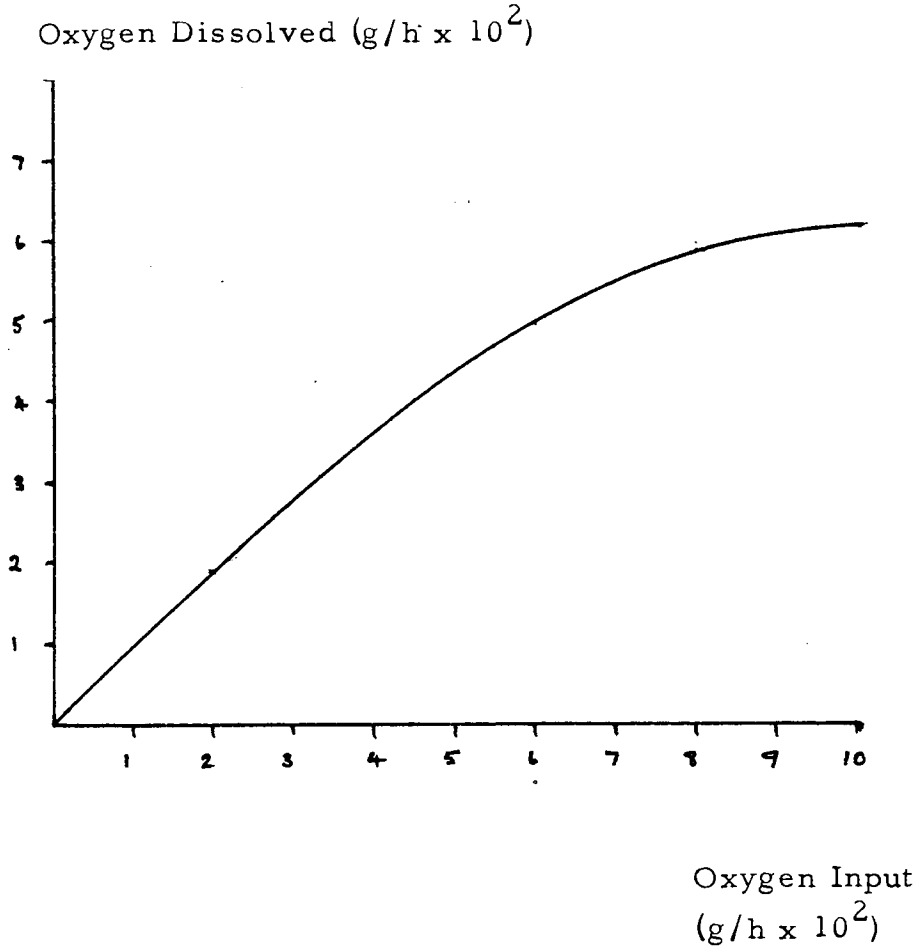

TABLE 8.3.3 Summary of Oxygen Use at the Low Plains Site.

Wt. Range (g)	5-20	20-80	80-180	180-250
Tanks Allocated	2	5	8	5
Oxygen Consumption (kg/h/tank)	0.26	0.33	0.31	0.36
Oxygenator Efficiency (%)	90	87	88	85
Oxygen Use (kg/h/tank)	0.29	0.38	0.35	0.42
Total Oxygen Use (tonnes/yr)	5.1	16.6	24.5	18.4

Annual oxygen use for the twenty production tanks amounts to 64.6 tonnes/yr. With a unit oxygen cost of £41.24 per tonne (Jan. 1978) the annual oxygen costs of about £2,700 are estimated.

The oxygen is stored in two liquid containers (although only one is essential) and the total rental on these at Low Plains is about £5,500.

Each oxygenator operates with a 0.75 kW pump and the manufacturer's data suggests that the power consumed is 0.7 kW. The total power requirements for the twenty tanks is 14 kW, therefore, and with a unit cost of 1.9p per kW h, (Jan. 1978) the total electricity costs amount to £2,330 per annum.

In all, the total annual running cost is estimated to be £10,500. A production of 80 tonnes per annum is therefore achieved with an overall conversion ratio (including

mortalities) of 1.7:1, based on the oxygen consumption, from which a running cost of 13.1 p per kg output can be deduced.

8.3.3 Capital Costs

Table 8.3.4 is an analysis of the capital costs involved in installing an oxygenation system. The figures given are budget figures, based on suppliers' estimates where possible. The total capital cost, depreciated over 10 years (flat-rate), amounts to £2,060 per annum, or 2.6 p per kg product.

Total operating costs of 15.7 p per kg output are estimated assuming 80 tonnes per annum production.

TABLE 8.3.4 Capital Costs of the Low Plains Oxygenation System.

Item	Unit Cost (£)	Total Cost (£)
VIE installation*	1000	2000
Column oxygenator	400	8000
Oxygen ring main	2000	2000
Electricity ring main	3000	3000
Diffuser element	30	600
Alarm system	5000	5000
Total Capital		£20,600
Depreciation over 10 yrs (flat-rate)		£ 2,060

*VIE stands for Vacuum Insulated Evaporator and refers to the liquid oxygen storage tank

8.4 Finnarts Bay Costs

8.4.1 Equipment Specification

The average monthly seawater temperatures recorded during 1976-7 varied from 6-16°C with a minimum of 4°C and a maximum of 17°C. The maximum water temperature and estimated stock levels have been used to calculate the maximum food ration and oxygen requirements for Finnarts Bay tanks. These are summarised in Table 8.4.1. From the table, a maximum oxygen demand of 36 kg/day is expected, or 1.5 kgO_2/h. Peak oxygen demand is estimated to be 2 kg/h, which was the design specification for the oxygenation system at Finnarts Bay.

TABLE 8.4.1 Maximum Tank Stock Levels, Food Ration and Oxygen Consumption for the Finnarts Bay Site (17°C)

Wt. Range (g)	5-20	20-80	80-180	180-250
Tanks Allocated	3	8	11	8
Max. Wt. (g)	20	80	180	250
Max. Biomass (kg)	1663	3670	4040	4400
Max. Food Ration (kg/day)	63	90	85	88
Max. Oxygen Cons. (kg/day)	25.2	36.0	34.0	35.2

8.4.2 Running Costs

The final design for the jet oxygenator used at the Finnarts Bay site was based on an estimate of the annual running costs. Experimental results showed that oxygen dissolution efficiency increased with operating pressure, but pumping costs will increase similarly. Oxygenation costs have been evaluated at three operating pressures, using the mean monthly recorded seawater temperatures to decide daily food rations and oxygen consumption. The three operating pressures were 1.54 atm, 1.68 atm and 1.82 atm. Average stock levels are given in Table 8.4.2.

TABLE 8.4.2 Average Tank Stock Levels for the Finnarts Bay Site

Wt. Range (g)	5-20	20-80	80-180	180-250
Ave. Wt. (g)	15	50	130	220
Ave. Biomass (kg)	1250	2300	2900	3900

Experimental results also showed that dissolution efficiency did not vary significantly with oxygen flow-rate, and so for ease of calculation flat-rate dissolution efficiencies were used to estimate the annual oxygen use. Oxygen dissolution efficiencies of 68%, 78% and 92% were derived from the performance data (see Fig. 5.3.4) with the jet oxygenators operating at 1.54, 1.68 and 1.82 atm respectively. Average

annual oxygen use is summarised in Table 8.4.3, together with the annual oxygen costs, assuming a unit oxygen cost of £48.37 per tonne (Jan. 1979). A detailed analysis of oxygen consumption is given in Appendix 4.

TABLE 8.4.3 Summary of Annual Oxygen Use and Costs at the Finnarts Bay Site

Oxygenator Pressure (atm)	Oxygen Use (tonnes)	Oxygen Cost (£)
1.54	257	12450
1.68	224	10850
1.82	190	9200

Power costs are summarised in Table 8.4.4 with a unit electricity cost of 2.16 p per kWh (Jan. 1979), using the pump manufacturers' data to derive the power consumed by the oxygenators.

TABLE 8.4.4. Power Consumption and Costs at the Finnarts Bay Site.

Oxygenator Pressure (atm)	Nominal Power (kW)	Power Consumed (kW)	Total Cost (£)
1.54	1.1	1.1	6240
1.68	1.5	1.3	7380
1.82	2.2	2.1	11910

Total running costs are summarised in Table 8.4.5 and show that the estimated lowest operating cost is likely to be achieved with an oxygenator operating at 1.68 atm pressure,

which was specified in the oxygenator design.

TABLE 8.4.5 Total Running Costs of Finnarts Bay Oxygenators

Oxygenator Pressure (atm)	Oxygen Cost (£)	Power Cost (£)	Total Cost (£)
1.54	12450	6240	18690
1.68	10850	7380	18230
1.82	9200	11910	21110

The liquid oxygen is supplied from two liquid oxygen stores and the total rental on these is about £15,000.

Running costs for the oxygenation system at the Finnarts Bay site amount to about £33,000. Assuming an overall conversion ratio of 1.7:1 annual production is estimated to be 257 tonnes, from which a production cost of 12.8 p per kg output can be deduced.

8.4.3 Capital Costs

Capital costs for oxygenation at the Finnarts Bay site are summarised in Table 8.4.6. These costs are budget figures based on suppliers' quotations where possible. The total capital cost depreciated over 10 years (flat-rate) amounts to £4,540 per annum or 1.8 p per kg product.

Total operating costs of 14.6p per kg output are estimated assuming 257 tonnes per annum production.

TABLE 8.4.6 Capital Costs of the Finnarts Bay Oxygenation System

Item	Unit Cost (£)	Total Cost (£)
VIE* installation	1500	3000
Jet Oxygenator	600	18000
Oxygen Ring Main	6000	6000
Electricity Ring Main	10000	10000
Diffuser Elements	30	900
Alarm System	7500	7500
Total Capital		£25,400
Depreciation of 10 years (flat-rate)		£ 4,540

8.5 Oxygenation Costs - High Levels of Water Economy

Low Plains oxygenation costs were based on Jan. 1978 prices. Since then, the cost of liquid oxygen has increased by about 50% which is equivalent to another £1,300 p.a. Electricity costs have risen by about 10% and all other costs by about 20%. Finnarts Bay costs were based on Jan. 1979 prices, since when overall prices have risen by about 10%. However, if the additional rental on the second liquid oxygen store is omitted in both estimates, since only one is essential, then operating costs of about 15 p/kg product are still fairly accurate.

*VIE is the liquid oxygen storage tank

Both farms are economising on water by a factor of about eight through oxygenation, and hence for highly intensive fish farming using individual tank oxygenators, the cost of oxygenation is approximately 15 p/kg output. This figure is of course subject to fluctuations of scale and local costs, but it is interesting to note that the costs of each site are similar despite the differences in size and operating conditions.

8.6 Oxygenation Costs - Low Levels of Water Economy

Oxygenation costs can also be estimated for achieving up to a four times saving in water economy, for example by using a U-tube oxygenator. A typical case might be a fish farm with a variable temperature water source supplied under a natural head which can produce 80 tonnes per year using oxygenation methods. Due to the temperature regime, most of the supplemental oxygen would be required in the summer months when the water temperature may reach 20°C. In winter little oxygen would be necessary. If it is assumed that, overall, 50% of the oxygen is supplied by the water but that oxygenation may supply up to 70% of the peak summer oxygen demand then oxygenation costs of 8.9 p per kg output are estimated. Details of the running costs are given in Table 8.6.1. Capital costs are summarised in Table 8.6.2. U-tube construction costs (1970) have been estimated to range from £300 in soil to £1500 in rock for a depth of 12 m (Speece, 1970).

TABLE 8.6.1 Summary of U-tube Running Costs

Production	80 tonnes
Conversion Ratio	1:7:1
Food Fed	136 tonnes
Oxygen Required	54 tonnes
Oxygen from Water	27 tonnes
U-tube Dissolution Efficiency	70%
Liquid Oxygen Required	39 tonnes
Unit Oxygen Cost	£70/tonne

	(£) pa
Liquid Oxygen	2700
VIE Storage Tank Rental	3500
Power Cost	0
Total	6200

TABLE 8.6.2 Summary of Capital Costs

Item	Cost (£)
VIE Installation	1000
U-tube Installation	5000
Oxygen Ring Main	2000
Diffuser Elements	600
Alarm System	500
Total Capital	9100

Depreciation over 10 years (flat-rate) £910

Operating costs of oxygenation system £7100 p.a.

8.7 Aeration Costs

The costs of an oxygenation system must be compared with those for aeration. Aeration costs for both the Low Plains and Finnarts Bay site are estimated, and are based on the maintenance of minimum dissolved oxygen levels of 70% saturation, although aeration capacity is based on the peak oxygen demand. Typical aeration costs for achieving lower levels of water economy from a variable temperature water source are also given.

Running costs can be derived from the performance data given in Fig. 8.7.1 which shows the power requirements necessary to supply 1kg O_2/h at various dissolved oxygen levels. Maximum stock levels are used to assess daily oxygen demand and an additional 33% capacity is specified to meet peak oxygen demand.

Capital costs will of course vary greatly with scale, location of farm and type of equipment used. Colt (1979) estimates the total capital cost of supplying 1kg O_2/h, including freight and electrical installation, to be £750-1000 using mechanical aerators. Mitchell and Kirby (1976) found that the capital cost required to dissolve 1.15 kg O_2/h was £300-1100 for mechanical aerators and £2500 for a diffused air system. Capital costs given below are budget figures for diffused air systems which are more suitable for use in rearing tanks.

8.7.1 Low Plains Site

Examination of Fig. 8.7.1 shows that 2.78 kW is required to supply 1 kg O_2/h at 70% saturation and 10°C. Maximum daily oxygen demand is estimated to be 198 kg (see Table 8.3.1) which will therefore require 23 kW of power. An additional 33% capacity for peak oxygen demand boosts the total power requirement to 31 kW, which gives an annual running cost of £5100 or 6.4p per kg produced. Capital costs (summarised in Table 8.7.1) depreciated over 10 years, amount to £2,300 or 2.9p per kg output.

Total operating costs, therefore, amount to 9.3p per kg produced.

TABLE 8.7.1 Summary of Capital Costs for Aeration at the Low Plains Site

Item	Unit Cost (£)	Cost (£)
Aerators	500	10000
Fan Blower	3000	6000
Air Distribution	1000	1000
Electricity Supply	1000	1000
Alarm System	5000	5000

Total Capital £23,000

Depreciation over 10 years (flat-rate) £2,300

Fig. 8.7.1 Power Requirements to Dissolve 1 kg O_2/h

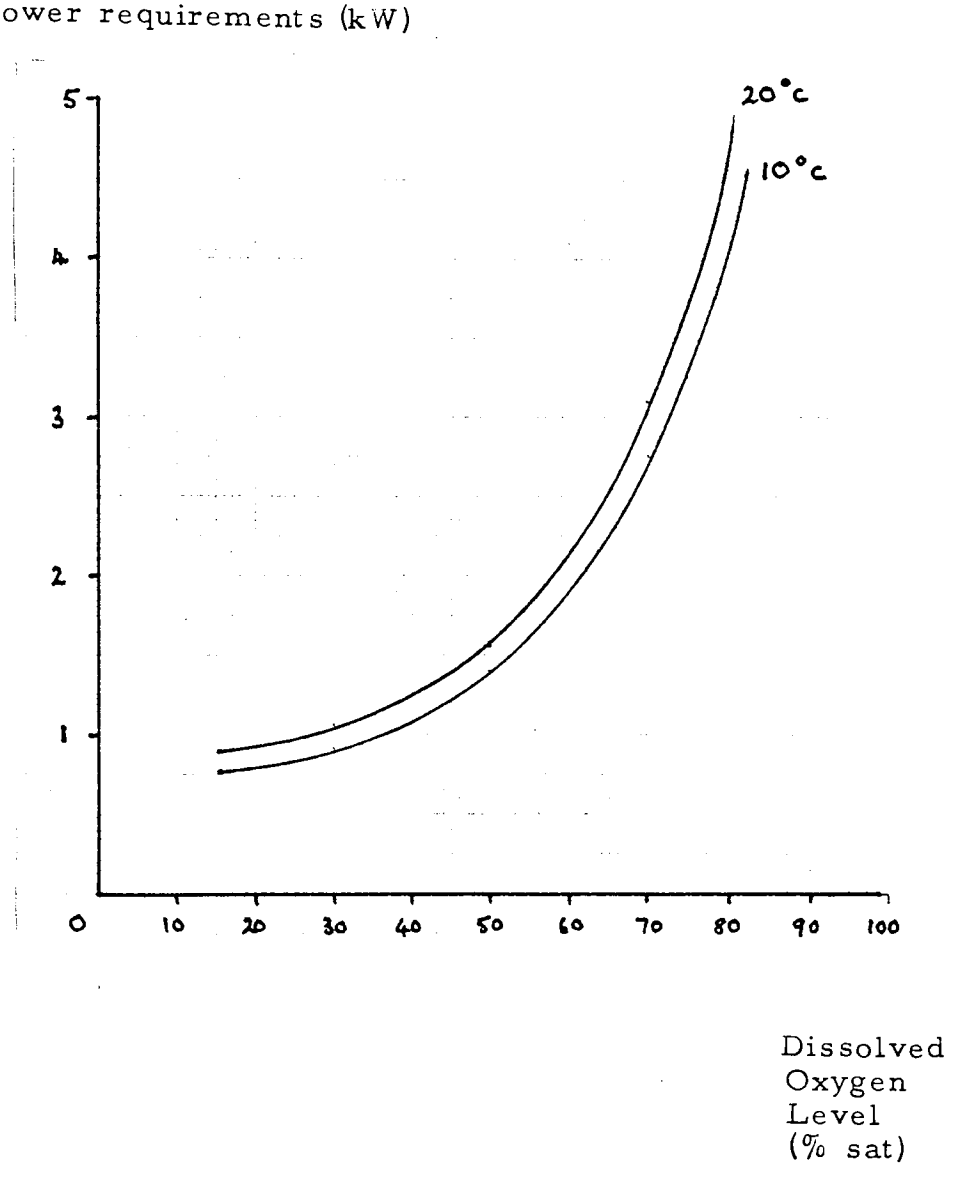

Derived from equation 2.3.1 (see also section 2.5)

8.7.2 Finnarts Bay Site

Examination of Fig. 8.7.1 shows that 3.15 kW is required to supply 1 kg O_2/h at 70% saturation and 17°C. Maximum daily oxygen demand is estimated to be 1020 kg (see Table 8.4.1) which will therefore require 134 kW of power. Total power requirement allowing for excess capacity to meet peak demands amounts to 178 kW. It is assumed that 50% of the aeration capacity can be turned off for the six cooler months which gives an annual running cost of £25,000, or 9.8p per kg produced. Capital costs are summarised in Table 8.7.2 and depreciated over 10 years, amount to £7350, or 2.9p per kg produced.

Total operating costs, therefore amount to 12.7p per kg output.

TABLE 8.7.2 Summary of Capital Costs for Aeration at the Finnarts Bay Site.

Item	Unit Cost (£)	Total Cost (£)
Aerators	1000	30000
Fan Blower	10000	30000
Air Distribution	3000	3000
Electricity Supply	3000	3000
Alarm System	7500	7500

Total Capital £73,500

Depreciation over 10 years flat-rate £7,350

8.7.3 Aeration Costs at Lower Levels of Water Economy

Aeration costs can be estimated for the situation outlined in section 8.5.2 where 80 tonnes p.a. are produced from a variable temperature water supply with the water providing 50% of the overall oxygen requirements but where 70% of the peak summer oxygen demand is supplied by aeration. Maximum stock levels will be similar to those at Low Plains but maximum oxygen requirements will be boosted by maximum summer temperatures of say 20°C. Details of the maximum stock levels, food ration and oxygen requirements are given in Table 8.7.3.

TABLE 8.7.3 Maximum Stock Levels, Food Ration and Oxygen Consumption (20°C)

Wt. range (g)	5-20	20-80	80-180	180-250
Tanks allocated	2	5	8	5
Max. wt. (g)	20	80	180	250
Max. biomass (kg)	936	2064	2268	2475
Max. food ration (kg/day)	43.0	49.5	52.2	56.9
Max. oxygen cons. (kg/day)	17.2	19.8	20.9	22.8

Examination of Fig. 8.7.1 shows that 3.15 kW is required to supply 1 kg oxygen per hour at 70% saturation and 20°C. Maximum daily oxygen demand is estimated to be 414.6 kg and if 70% of this is supplied by aeration then 38 kW will be required. An additional 33%

capacity for peak oxygen demands increases the power requirement to 51 kW. It is assumed that aeration continues for 50% of the year, so running costs (at 2p per kWh) amount to £4,500 p.a. or 5.6p per kg produced. Capital costs amount to about £3,090 depreciated over 10 years or 3.9p per kg of product (see Table 8.7.4).

Total operating costs, therefore, amount to 9.5p per kg output.

TABLE 8.7.4 Capital Cost of an Aeration System Supplying 70% of Peak Summer Oxygen Demand

Item	Cost (£)
Aerators	17000
Fan Blowers (2)	10000
Air Distribution	1700
Electricity Supply	1700
Alarm System	500

Total Capital £30,900

Depreciation over 10 years (flat-rate) £3,090

8.8 Discussion of Results

8.8.1 Comparison of Oxygenation and Aeration Costs

Estimated operating costs for aeration methods in intensive systems are lower than oxygenation systems, particularly so in the case where water temperatures are constant. However, it

should be remembered that aeration costs were based on maintaining minimum dissolved oxygen levels of 70% saturation. In the case of the Finnarts Bay site, 70% saturation is only 5.5 ppm dO_2, which is close to the acceptable minimum for salmonids. Capital costs are high for both systems but higher using aeration methods, particularly in situations where the water temperature is variable and equipment must be specified for the maximum demand.

It is worthwhile considering an extreme case where summer temperatures may exceed the anticipated maximum. Since aeration may not cope with the increased oxygen demand, reduced feeding would be necessary. With oxygenation, it is simple to increase the oxygen flow-rate (accepting a lower dissolution efficiency) to meet the increased demand, thereby increasing overall production.

One further point is that a generator was not included in the capital costs. This is absolutely essential to ensure continuous aeration. In the case of electrically-powered oxygenation methods, short-term cover can be provided by diffuser elements, although a generator is advisable.

At lower levels of water economy, the operating costs of the two systems are approximately the same. This is mainly due to the reduction in overall efficiency of aerations systems caused by the variable oxygen demand and is exaggerated by significantly higher capital costs. With the simplicity of just

one oxygenation point, control of oxygen supply to meet demand and the stand-by support afforded by diffuser elements, oxygenation has many advantages in this situation.

The clear financial benefits of oxygenation become apparent when dissolved oxygen levels are maintained above 70% saturation. Examination of Fig. 8. 7. 1 shows that power requirements for aeration (and hence capital costs and overall operating costs) increase significantly if dissolved oxygen levels of 80% are specified. Dissolved oxygen concentrations of 90% are practically impossible to achieve. With oxygenation methods there is little or no cost penalty in maintaining 100% saturation.

The whole question of what constitutes an optimum dissolved oxygen level is of major importance in maximising production from a water source and may have a significant effect on production costs, taking into account that a 0. 1 improvement in conversion rate is worth 3 p / kg reduction in production costs, with food at £300 per tonne (1980). However, this major area for study is outside the scope of this thesis, although it is understood that the work is to be undertaken by another IHD student.

In any analysis of the costs of economising on water use, it should be remembered that 60-75% of aeration costs are attributable to power requirements and 65-90% of oxygenation costs are in respect of liquid oxygen storage and use. Operating costs for such systems can therefore only be accurately predicted for each individual site. However, in general, aeration and oxygenation can account for up to 20% of total production costs.

8.8.2 Maintenance

Operating experience over the last two years has shown that in general, maintenance requirements at the Low Plains and Finnarts Bay sites are low, especially when compared with overall running costs. At the Low Plains site, the most significant problem has been fouling of the oxygenator pipework and pumps by "sewage fungus". This, however, has been overcome by routine cleaning. The major maintenance problem at the Finnarts Bay site has been corrosion of the pumps caused by the action of seawater on the stainless steel shafts. Careful pump selection is therefore essential for marine sites. More than the cost of maintenance, however, these problems are important since lack of attention reduces overall operating efficiency which increases oxygen use.

With the U-tube, particularly in situations where no power is required, maintenance requirements are likely to be minimal.

Maintenance requirements for aeration will depend largely on the type of aerator chosen and the local availability of spare parts and service will be an important consideration in selecting aerators (Colt, 1979). The intermittent use of diffused aeration systems, especially the fine-bubble type, can result in the diffuser elements clogging (Mitchell and Kirby, 1976). Overall reliability of any aeration system will depend on its care and maintenance (Colt, 1979).

8.8.3 Additional Pumped Water

Pumping additional water can be an effective alternative to reoxygenation methods. In the case of both the Low Plains and Finnarts Bay site, this is not possible due to the prohibitive cost of abstraction at Low Plains and the lack of additional freshwater at Finnarts Bay. However, in many cases pumping is feasible and should always be considered as an alternative.

8.9 Conclusions

Oxygenation costs of about 15 p per kg product are estimated for both the Low Plains and Finnarts Bay sites which are economising on water use by a factor of about eight. Comparative aeration costs for the two sites are 9.3 p and 12.7 p respectively, the latter figure reflecting a reduced overall efficiency caused by the variable temperature water source. Oxygenation methods are, however, extremely flexible compared with aeration methods, and have the benefit of a stand-by system which has proved exceptionally useful during grading, cropping and when transporting fish, as well as during power loss and equipment failure. Even so, these benefits do not easily justify the additional operating cost. Capital costs for aeration methods are higher, however, and significantly so where equipment must be specified to meet peak summer oxygen requirements.

With lower degrees of water economy, the operating costs of both oxygenation and aeration methods are similar. Oxygenation is simple requiring only one point of introduction and also has significantly lower capital costs. Together with the general benefits of oxygenation systems and minimal maintenance requirements the use of oxygen has significant advantages over aeration at this level of water saving.

In all cases, there will be a clear financial advantage in favour of oxygenation methods if dissolved oxygen levels above 70% saturation are specified. However, it must be remembered that 60-75% of aeration costs are for power and 65-90% of oxygenation costs are for liquid oxygen storage and use, so the local costs of power and oxygen are important determinants of operating cost.

CHAPTER 9

GENERAL CONCLUSIONS AND COMMENTS

9. General Conclusions and Comments

A major constraint to the development of the fish farming industry is the need to acquire massive water supplies to meet the oxygen requirements of the fish, since natural air-saturated waters contain little dissolved oxygen. Water requirements can be reduced significantly by artificially replenishing the oxygen which the fish consume. The source of oxygen may be either air (aeration) or pure oxygen or a mixture of the two (oxygenation).

Aerator methods have been reviewed in Chapter 2. The principal advantage of such methods is the universal availability of air. However, the nitrogen in air reduces its effectiveness as a source of oxygen. Aeration methods can at best only re-saturate water and, in general, excessive power requirements are necessary to maintain dissolved oxygen levels above 70% saturation. As a result capital expenditure on aeration equipment can be high. In addition, aeration capacity cannot easily be controlled to meet oxygen demand which will tend to reduce overall operating efficiency. However, aeration methods have much merit in removing carbon dioxide which is produced by the fish as a waste product of metabolism.

Using pure oxygen,high transfer rates are possible since (1) the solubility of oxygen is approximately five times that of oxygen in air and (2) pressurisation is possible without any risk of nitrogen supersaturation. As a result of these high transfer rates capital costs for oxygenation are generally lower than those for aeration. However, since pure oxygen gas is expensive, it is necessary not only to dissolve a high proportion of the gas but also to control the dissolution rate so that it matches oxygen demand. In addition the high efficiencies required mean that there is little scope for stripping other gases and, in particular, for removing carbon dioxide. Higher levels of dissolved carbon dioxide can be expected, therefore.

Four oxygenation methods have been described by the author, each based on a different mode of operation. The column oxygenator was designed with inlet and outlet superficial liquid velocities such that the 2-5 mm diameter bubbles formed in freshwater are trapped within the column. The column is pressurised slightly to enhance transfer rates but, in addition, purged nitrogen is replaced by oxygen to increase transfer rates further. A fundamental characteristic of this method of oxygenation is the creation of a plunging jet, which maintains gas-liquid contact. This jet has been

acknowledged to be one of the more efficient aeration processes and, in the column oxygenator, the process occurs in an oxygen-enriched atmosphere. However, the independent parameters affecting the efficiency of the jet are still not fully understood, and this is reflected in the limited progress made in developing a model to analyse column performance.

In marine applications, an important consideration is the small bubbles which are generated in seawater and waters of high intermediate salinities. These bubbles dissolve relatively quickly and, since they have lower rise velocities than bubbles formed in freshwater, dissolution is possible within the rearing tank. Liquid flow within a submerged jet is well-documented and the jet oxygenator utilises the characteristics of the submerged jet (1) to provide gas bubbles with the required path length for dissolution and (2) to disperse the oxygen within the rearing tank. A model has been developed which can be used to analyse many variables affecting the operation of the jet oxygenator.

In the case of the U-tube oxygenator, the liquid velocity in the downflow pipe is specified so that all gas bubbles are carried to the bottom of the "U", thereby achieving a sufficiently long path length for efficient dissolution. As the gas bubbles descend they are subjected to an increasing hydrostatic head which enables

high overall transfer rates to be achieved. In addition, power requirements are low so very high transfer rates per unit of energy consumed are possible. This, together with a relatively low initial cost and the capacity to oxygenate large volumes of water, make the U-tube suitable for oxygenation of the primary water source. The approach developed to model U-tube performance can be used for both system analysis and design.

If the depth of water in a rearing tank could be made equal to the minimum path length for bubble dissolution, then continuous support of fish stocks would be possible using only the pressure available from a liquid oxygen storage vessel. However, consideration of bubbles rising in a stationary liquid suggests that this can only be achieved in seawater or at high intermediate salinities and, even then, the water depth must be at least 1.5 m. Such depths will generally make fish husbandry difficult. However, this technique is invaluable as a standby measure, when lower dissolution efficiencies are acceptable.

A variety of techniques now exist for economising on water use using either pure oxygen or air. Knowledge of these methods is now approaching the point where design specifications can be tailored to meet the requirements of individual fish farms. However, a detailed analysis of each specific site is required to determine the most cost-effective system for increasing production.

ACKNOWLEDGEMENTS

I would like to thank Dr Eric Smith (Main Supervisor) and Dr John Forster (Industrial Supervisor) for all their assistance and encouragement with all aspects of this project. I would also like to thank Dr Niall Bromage (Associate Supervisor) and Dr David van Rest for their constructive input.

Finally I would like to thank the staff of Shearwater Fish Farming Ltd for their assistance with all the work conducted there.

REFERENCES

REFERENCES

Ali, K.H.M. and R.B. Whittington. 1979. Liquid - liquid mixing in tanks and reservoirs. Proc. 3rd European Conference on Mixing. BHRA Bedford, Vol. 1 - A3 37-60 pp.

Ambromovich, G.N. 1963. The theory of turbulent jets. M.I.T. Press Massachusetts 670 pp.

APHA. 1971. Standard methods for the examination of water and wastewater. American Public Health Association, Washington D.C. 875 pp.

Aston, R.J. 1981. The availability and quality of power station cooling water for aquaculture. Aquaculture in Heated Effluents and Recirculation Systems, Vol. 1, ed. Tiews K. Heenemann Verlagsgesellsch aft mbH, Berlin 513 pp.

Barret, M.J., A.L.H. Gameson, and C.G. Ogden. 1960. Aeration studies at four weir systems. Wat. and Wat.Eng. 64:407-413.

Bayley, R.W. and K. Wyatt. 1961. Aeration of effluents by venturi tubes. Wat. Waste Treat. J. 8(10):498-500.

Bin, A. 1979. Mass motion in a jet absorber. Int. Chem. Eng. 19(2):227-235.

Boon, A.G. 1976. Technical review of the use of oxygen in the treatment of wastewater. Wat. Pollut. Contr. 75:206-213.

Boyes, A.P. and S.R.M. Ellis. 1976. An investigation into the oxygenation of water for use in B.O.C. fish farms. Shearwater Technical Report no. 0105 76.

Brett, J.R. 1970. Fish. The energy cost of living. Marine Aquaculture, ed. McNeil, W.J. Oregon State University Press. 37-51 pp.

Brodkey, R.S. 1975. Turbulence in mixing operations: theory and application to mixing and reaction. Academic Press, London, 339 pp.

Bruijn, J., and H. Tuinzaad. 1958. The relationship between depth of U-tubes and the aeration process. Journ. A.W.W.A. 50:879.

Bruun de Neergaard, J. 1978. Pure oxygen in trout production. Danish Fish Farms Research Institute. Tech. Report no.60, 22 pp.

Burgess, J.M. et al. 1972. A note on the plunging liquid jet reactor. Chem. Eng. Sci. 27:442-445.

Busch, C.D., J.L. Koon and K.R. Allison. 1974. Aeration, water quality and catfish production. Trans. Am. Soc. Agr. Eng. 17(3):433-435.

Calderbank, P.H. 1958. Physical rate processes in industrial fermentation. Trans. I. Chem. E. 36:443.

Campbell, H.J. and R.F. Rocheleau. 1976. Waste treatment at a complex plastics manufacturing plant. J. Wat. Pollut. Contr. Fed. 48(2):256-273.

Chessness, J.L., L.J. Fussell and T.K. Hill. 1973. Mechanical efficiency of a nozzle aerator. Trans. Am. Soc. Agr. Eng. 16(1):67-68.

Chessness, J.L. and J.L. Stevens. 1971. A model study of gravity flow aerators catfish raceway systems. Trans. Am. Soc. Agr. Eng. 14(6):1167-1169.

Colt, J. and G. Tchobanoglous. 1979. Design of aeration systems for aquaculture. Bio-engineering Symposium, Culture Section of the American Fisheries Soc. Traverse City, Michigan. 15-19 Oct.

Davies, J.T. 1972. Turbulence phenomena. Academic Press, London, 412 pp.

Degrémont . 1979. Water treatment handbook. Ed. Barraqué, C. et al, Wiley and Sons, New York, 1186 pp.

Downing, A.L. and G.A. Truesdale. 1955. Some factors affecting the rate of solution of oxygen in water. J. Appl. Chem. 5:570-581.

Eckenfelder, W.W. 1956. Process design of aeration systems for biological wastewater treatment. Chem. Eng. Prog. 52(7):286.

Forster, J.R.M. and G.R. Smart. 1979. Water economy in aquaculture. Power Plant Waste Heat Utilisation in Aquaculture, Workshop II, eds. Godfriaux, B.L. et al. Allenheld Osman and Co., N.J. 97-207 pp.

Harman, J.P. 1978. Characterisation, treatment and utilisation of the effluent from an intensive fish farm. Ph.D. Thesis, University of Aston in Birmingham, U.K.

Harman, J.P. 1975. Oxygen dissolving trials at Hunterston. Shearwater Technical Report no. STR 010975.

Hemming, M.L. et al. 1977. "Deep shaft" - latest postion. Wat. Pollut. Contr. 76(4):441-458.

Hinze, J.O. 1975. Turbulence. McGraw-Hill, New York, 790 pp.

Hood, T. 1976. Experimental evaluations of the Birmingham oxygenation rigs under normal operating conditions at Low Plains. 55 pp. Shearwater Tech. Rep. no. STR 010876.

Hosono, Y., K. Fujie and H. Kubota. 1979. Operational characteristic evaluation of a liquid pump type deep shaft aerator. J. Chem. Eng. Japan, 12(2):136-141.

Ippen, A. T. et al. 1952. The determination of oxygen absorption in aeration processes. Mass. Inst. Technol. Hydrodyn. Lab. Tech. Report no. 7.

Jones, A. 1976. Oxygen dissolving trials - seawater. Shearwater Tech. Report no. STR 010276, 3 pp.

Jones, J.R. 1964. Fish and river pollution. Butterworths, London.

Joshi, J.B. and M.M. Sharma. 1979. A circulation cell model for bubble columns. Trans. I. Chem. E., 57 T244.

Koide, K. et al. 1968. Bubbles generated from a porous plate. J. Chem. Eng. Japan, 1(1):51-56.

Larmoyeux, J.D. and R.G. Piper. 1973. Effects of water reuse on rainbow trout in hatcheries. Prog. Fish-Cult. 35(1):2-8.

Leary RDet al. 1969. Full scale oxygen transfer studies of seven diffuser systems. J. Wat. Pollut. Contr. Fed., 41:461-473.

Lee, J.C. and D.L. Meyrick. 1970. Gas-liquid interfacial areas in salt solutions in an agitated tank. Trans. I. Chem. E. (48) T 37.

Lewis, W.K. and W.G. Whitman. 1924. Principles of gas absorption. Ind. Eng. Chem. 16:1215-1220.

Liao, P.B. 1971. Water requirements of salmonids, Prog. Fish Cult., 33(4):210-215.

Lister, A.R. and A.G. Boon. 1977. Aeration in deep tanks - an evaluation of a fine bubble diffused air system. W.P.R.L. Tech. Report, A.I.D.T.575, 25 pp.

Mavanic, D.S. and J.K. Bewtra. 1974. Mass transfer of oxygen in diffused air systems. Can. J. Civ. Eng. 1:71-84.

Mertes, A.T. 1938. U.S. Patent no. 2128 311.

Mitchell, R.E. and A.M. Kirby Jr. 1976. Performance characteristics of pond aeration devices. In Proc. 7th ann. meeting of the World Maric. Soc. J.W. Avault, ed. Louisiana State University, Baton Rouge, 561-581 pp.

Motarjemi, M. and G.J. Jameson. 1978. Mass transfer from very small bubbles: the optimum size for aeration. Chem. Eng. Sci. 33:1415-1423.

Petit, J. and J.L. Ferron. 1975. Les problèmes de l'eau en pisciculture - l'oxygénation des eaux de pisciculture. Methods de choix d'un procédé. La Pisciculture Française 44(11)53-62.

Rappaport, A., S. Sarig and M. Marek. 1976. Results of tests of various aeration systems on the oxygen regime in the Genosar experimental ponds and growth of fish there in 1975. Bamidgeh 28(3):35-49.

Reid, G.K. 1961. Ecology of inland waters and estuaries. Reinhold, New York.

Rucher, R.R. 1972. Gas bubble disease of salmonids: a critical review. U.S. Dept. of Interior, Fish and Wildlife Service Tech. Paper Bureau of Sport Fisheries and Wildlife No. 58.

van de Sande, E. and J.M. Smith. 1973. Surface entrainment of air by high velocity water jets. Chem. Eng. Sci. 28: 1161-1168.

Schnurman, R. 1937. The size of bubbles in liquids. Kolloid Zeitschrift 80(2) 148-151.

Schügerl, K. et al. 1977. Comparison of bubble columns with air lift fermentors and mechanically agitated fermentors. Adv. in Biochem. Eng. 7(1):76.

Shabi, F.A. and R.L. Hibberd. 1977. U.K. patent no. 1476883.

Short, C.S. 1973. Removal of ammonia from river water. Water Research Association Tech. Paper. T.P. 101 40 pp.

Smart, G.R. 1975. The acute toxicity mechanism of ammonia to rainbow trout. PhD Thesis, University of Bristol, U.K.

Smart, G.R. et al. 1978. Nephrocalcinosis in fish reared at elevated carbon dioxide concentrations. J. Fish Diseases 2:279-289.

Smith, J.M. and E. van de Sande. 1974. Mass transfer in a pool with plunging liquid jets. Multi-phase flow systems symposium. University of Strathclyde, Vol. II 2-4 April. I. Chem. E. Symp. Series no. 38 J3.

Sneath, R.W. 1976. The performance of a plunging jet aerator and aerobic treatment of pig slurry. Wat. Pollut. Contr. 77(3) 408-414.

Sowerbutts, B.J. and J.R.M. Forster. 1981. Gases exchange and reoxygenation. In Aquaculture in Heated Effluents and Recirculation Systems, Vol. 1, ed. Tiews K, Heenemann Verlagsgesellsch aft mbH, Berlin 513 pp.

Speece, R.E. and M.J. Humenick. 1973. Carbon dioxide stripping from oxygen activated sludge systems. J. Wat. Pollut. Contr. Fed., 45(3):412-423.

Speece, R.E., M. Madrid and K. Needham. 1971. Downflow bubble contact aeration. J. Sanit. Eng. Div. Proc. Am. Soc. Civil Eng. 97(SA4), 433-441.

Speece, R.E. and R. Orosco. 1970. Design of U-tube aeration systems. J. Sanit. Eng. Div. Proc. Am. Soc. Civil Eng. 96(SA4) 715-725.

Speece, R.E., J.L. Adams and C.B. Woodridge. 1969. U-tube aeration operating characteristics. J. Sanit. Eng. Div. Proc. Am. Soc. Civil Eng. 95(SA3), 563-574.

Uhl, V.W. and J.B. Gray. 1966. Mixing: theory and practice Vol. 1. Academic Press, London, 340 pp.

USEPA. 1974. Process manual for upgrading existing wastewater treatment plants (Technology Transfer). U.S. Environmental Protection Agency, Washington D.C.

Wallis, G.B. 1969. One dimensional two-phase flow. McGraw-Hill, New York. 408 pp.

Warren, C.E., P. Douderoff and D.L. Shumway. 1973. Development of dissolved oxygen criteria for freshwater fish. Ecological Research Series, E.P.A.-R3-73-019, 121 pp.

WRC. 1977. Cost information for water supply and sewage disposal. Water Research Centre, Tech. Rep. TR61, Stevenage, U.K.

Yoshida, F. 1965. Performance of gas bubble columns. A.I.Ch.E.J. 11:9.

Zieminski, S.A. and R.C. Whittemore. 1971. Behaviour of gas bubbles in aqueous solutions. Chem. Eng. Sci. 26-509.

APPENDICES

Appendix 1 - Analysis of Experimental Results

Each series of tests was designed for factorial analysis. Yates' method of analysis was used to assess the importance of each factor on various response variables.

Yates' method of analysis is illustrated below, using the absorption rate data from tests with the column oxygenator.

First, the data are arranged in standard order

Run Number	Operating Pressure	Oxygen Flow-rate	Liquid Flow-rate
1	P	O	L
2	p	O	L
3	P	o	L
4	p	o	L
5	P	O	l
6	p	O	l
7	P	o	l
8	p	o	l

where P = 1.48 atm O = 600 g/h L = 30 m^3/h

p = 1.14 atm o = 200 g/h l = 10 m^3/h

The derivation of the results of the analysis is shown in Table A1.1.

TABLE A1.1 Derivation of Results of the Analysis - Oxygen Absorption Rate, Column Oxygenator.

Run No.	Oxygen Absorption Rate (g/h)	Col. (1)	Col. (2)	Col. (3)	Col. (3) ÷ 8	Effect
1	573	1034	1491	2220	278	Ave
2	461	457	729	232	29	Pressure
3	221	448	97	744	93	Oxygen
4	236	281	135	48	6	Pressure/O
5	238	112	577	762	95	Liquid
6	210	-15	167	-48	-6	Pressure/L
7	194	28	127	410	51	Oxygen/L
8	87	107	-79	206	26	Pressure/O/L

Pressure/O is Pressure/Oxygen Interaction
Pressure/L is Pressure/Liquid Interaction
Pressure/O/L is Pressure/Oxygen/Liquid Interaction

The figures in column (1) are generated in the following manner. The four pairs of results are added in sequence to form the first four numbers in column (1). The same four pairs of results are then subtracted to generate the last four numbers in column (1). For example:

Adding	Subtracting
573 + 461 = 1034	573 - 461 = 112
221 + 236 = 457	221 - 236 = -15
238 + 210 = 448	238 - 210 = 28
194 + 87 = 281	194 - 87 = 107

This procedure is used a total of three times in this case, since three factors were used in the 2^3 experimental programme.

Inspection shows that the first figure in column (3) denotes the total amount of oxygen dissolved in all eight tests. The second figure is derived in the following way

$$232 = 97 + 135$$
$$= 112 + (-15) + 28 + 107$$
$$= (573 - 461) + (221 - 236) + (238 - 210) + (194 - 87)$$

which is the combined effect of changing the operating pressure in tests. Altogether, therefore, 232 g/h more oxygen were dissolved in the four tests at the higher pressure than were dissolved at the lower pressure. Similarly, the third figure in column (3) represents the effect of increasing the oxygen flow-rate in all tests, and the fifth, the total effect of increasing the liquid flow-rate.

Rows 4, 6, and 7 in col (3) denote the interactions between pressure and oxygen flow-rate, pressure and liquid flow-rate, and liquid and oxygen flow-rates respectively. The last figure in col (3) represents the interaction between all three. The interactions are an important feature of the analysis and their significance is best illustrated by means of an example. Fig. A1. 1 shows how to interpret the oxygen flow-rate/liquid flow-rate interaction. It can be seen that increasing the oxygen flow-rate at a liquid flow-rate of 30 m^3/h has a greater effect than increasing the oxygen flow-rate by the same amount at a liquid flow-rate

Fig. A1.1 Yates' Analysis -
The Liquid Flow-rate/Oxygen Flow-rate Interaction

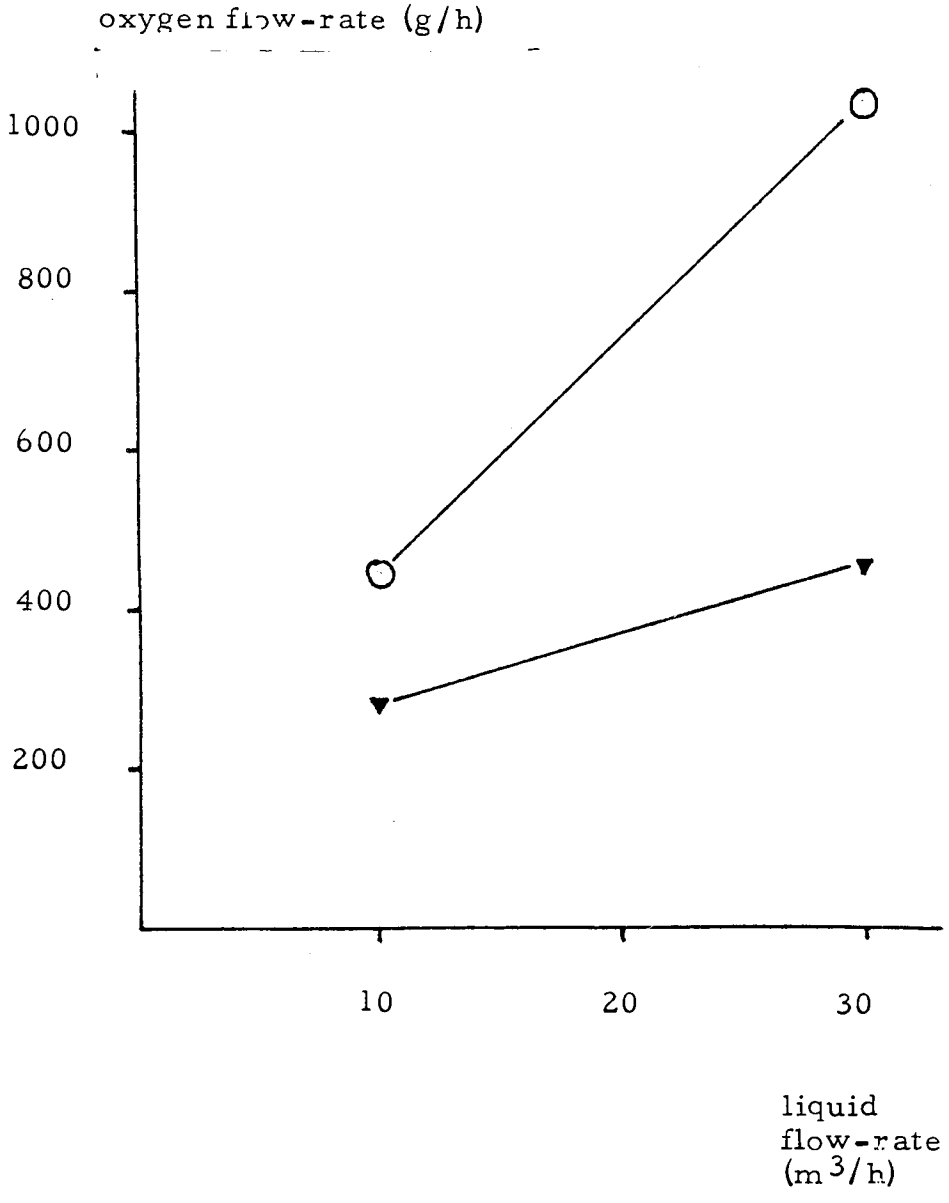

results at both pressures combined for each point

of 10 m^3/h. (Note that each point in the figure is achieved by combining results at both pressures). Altogether, 410 g/h more oxygen were dissolved when the oxygen flow-rate was increased at the higher liquid flow-rate than at the lower liquid flow-rate.

Dividing column (3) by eight, the average effects of each factor or interaction are obtained. The final column of figures can now be used to assess the average effect of each factor or interaction on oxygenator performance. The main effects show what happens when each factor is increased from the lower to the higher value, for example, on increasing the pressure from 1.14 atm to 1.48 atm. An interaction demonstrates how the effect of one factor may depend upon the level of another.

Appendix 2 - Absorption Rate Calculation for the Jet Oxygenator and for Oxygenation Using Diffuser Elements

At the Finnarts Bay site, stocking densities are high and the fish are dependent on the oxygenators to supply their oxygen requirements. If the oxygen supply is turned off, then the oxygen requirements are met by removing dissolved oxygen from the water, and the rate of fall of the dissolved oxygen concentration can be used to estimate fish oxygen consumption. In addition, by restoring the oxygen flow-rate to a known level, the rate of increase of the dissolved oxygen concentration and the fish oxygen consumption can be used to measure the dissolution rate (and hence the dissolution efficiency) of the oxygenation system. Dissolved oxygen concentrations are measured using a Phox dissolved oxygen meter with a Mackereth-type probe, placed in the outlet from the tank.

Consider a tank, volume V, with a flow-rate, Q_L, through the tank. The inlet dissolved oxygen concentration is $Co_{2,IN}$ and the effluent concentration $Co_{2,OUT}$. Go_2 is the fish oxygen consumption, and $F\,(Co_2^* - Co_{2,OUT})$ is a function describing oxygen transfer across the surface of the tank, which is related to the deficit between the equilibrium value (with respect to air), Co_2^*, and the dissolved oxygen concentration in the tank. It is necessary to assume that the tank is well-mixed, that is to say the oxygen concentration is uniform throughout the tank and always equals $Co_{2,OUT}$ (Fig. A2.1). Then with no oxygen input from the oxygenator, an oxygen mass balance gives

Fig. A2.1 Oxygen Balance in a Fish Tank

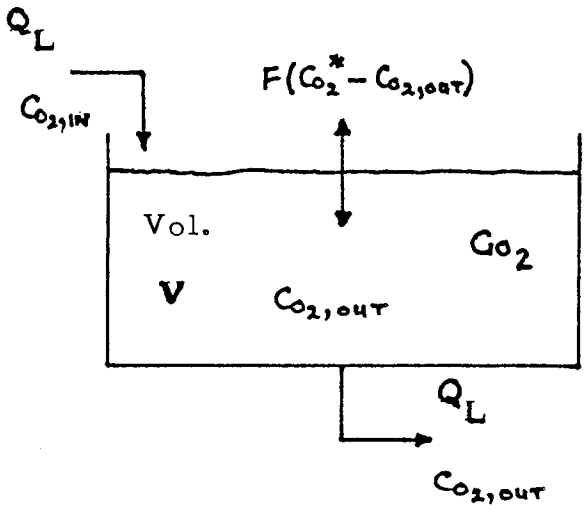

when $C_{O_2,OUT}$ = 100% saturation,

$C_{O_2,IN} - C_{O_2,OUT} = 0$, assuming inlet water is saturated,

and $F(C_{O_2}^* - C_{O_2,OUT}) = 0$, since equilibrium is achieved across the tank surface.

Then $$-G_{O_2} = V \frac{d C_{O_2,OUT}}{dt}\Bigg|_{C_{O_2,OUT} = 100\% \text{ sat.}}$$

Now, assuming the fish oxygen consumption remains constant, which can be justified provided the fish are not fed or placed under any new stress, a new oxygen balance can be achieved with an oxygen dissolution rate, φ_{O_2}, from the oxygenator.

$$\varphi_{O_2} + Q_L C_{O_2,IN} + F(C_{O_2}^* - C_{O_2,OUT}) - Q_L C_{O_2,OUT} - G_{O_2} = V \frac{dC'_{O_2,OUT}}{dt}$$

Then if $\frac{dC'_{O_2,OUT}}{dt}$ is measured when $C_{O_2,OUT}$ = 100%sat.

$$\varphi_{O_2} = V \frac{dC'_{O_2,OUT}}{dt}\Bigg|_{C'_{O_2,OUT} = 100\% \text{ sat.}} + R_{O_2}$$

$$= V \left(\frac{dC'_{O_2,OUT}}{dt} - \frac{dC_{O_2,OUT}}{dt} \right)\Bigg|_{C_{O_2,OUT} = 100\% \text{ sat.}}$$

Therefore, if $Co_{2',out}$ and $Co_{2',out}$ are plotted against time and the gradients of the curves measured at 100% saturation, the oxygen dissolution rate can be calculated from the difference between the gradients. The dissolution efficiency can then be calculated from the oxygen flow-rate.

Appendix 3 - Feeding Levels

Food is allocated according to the size and number of fish in each rearing tank and the water temperature. Table A3. 1 shows the daily food ration as a percentage of total biomass; it is adapted from feeding tables produced by BP Nutrition Ltd, the food suppliers.

TABLE A3.1 Daily Food Ration as a Percentage of Total Biomass for Rainbow Trout

Temp	Fish Size (g)													
oC	5	10	20	30	40	50	60	70	80	90	100	120	140	180+
4	1.90	1.65	1.35	1.20	1.10	1.00	0.95	0.85	0.80	0.75	0.75	0.70	0.70	0.65
6	2.25	1.45	1.60	1.45	1.35	1.25	1.15	1.05	1.00	1.00	0.95	0.90	0.85	0.8
8	2.60	2.20	1.80	1.60	1.50	1.40	1.30	1.25	1.20	1.15	1.15	1.10	1.05	0.95
10	3.10	2.70	2.15	1.90	1.75	1.65	1.55	1.45	1.40	1.40	1.35	1.25	1.25	1.15
12	3.45	2.95	2.45	2.20	2.05	1.90	1.80	1.75	1.70	1.65	1.60	1.50	1.45	1.30
14	4.05	3.50	2.85	2.50	2.30	2.20	2.10	2.00	1.95	1.85	1.80	1.70	1.65	1.55
16	4.80	4.10	3.30	2.95	2.70	2.50	2.40	2.30	2.20	2.10	2.05	2.00	1.95	1.85
18	5.50	4.70	3.90	3.30	3.00	2.80	2.70	2.60	2.50	2.40	2.30	2.20	2.10	2.00
20	6.10	5.30	4.50	3.60	3.30	3.10	3.00	2.90	2.80	2.70	2.55	2.40	2.25	2.15

Appendix 4 - An Estimate of Oxygen Use at the Finnarts Bay Site.

Fig. A4.1 is a histogram of average monthly seawater temperatures recorded at the Finnarts Bay site in 1977-1978. Using the average stocking level data (see Table A4.1) and the feeding tables given in Appendix 3, daily food rations (see Table A4.2) and oxygen consumption can be calculated (see Table A4.3). Assuming flat-rate oxygen dissolution efficiencies for the jet oxygenators and using the oxygenator performance curves (see Fig. A4.2), oxygen use can be estimated.

TABLE A4.1 Average Stock Levels at the Finnarts Bay Site.

Wt. Range (g)	5 - 20	20 - 80	80 - 180	180 - 250
Tanks Allocated	3	8	11	8
Ave. Wt. (g)	15	50	130	220
Ave. Biomass (kg)	1250	2300	2900	3900

Fig. A4.1 Average Monthly Seawater Temperatures at the Finnarts Bay Site (1977/78)

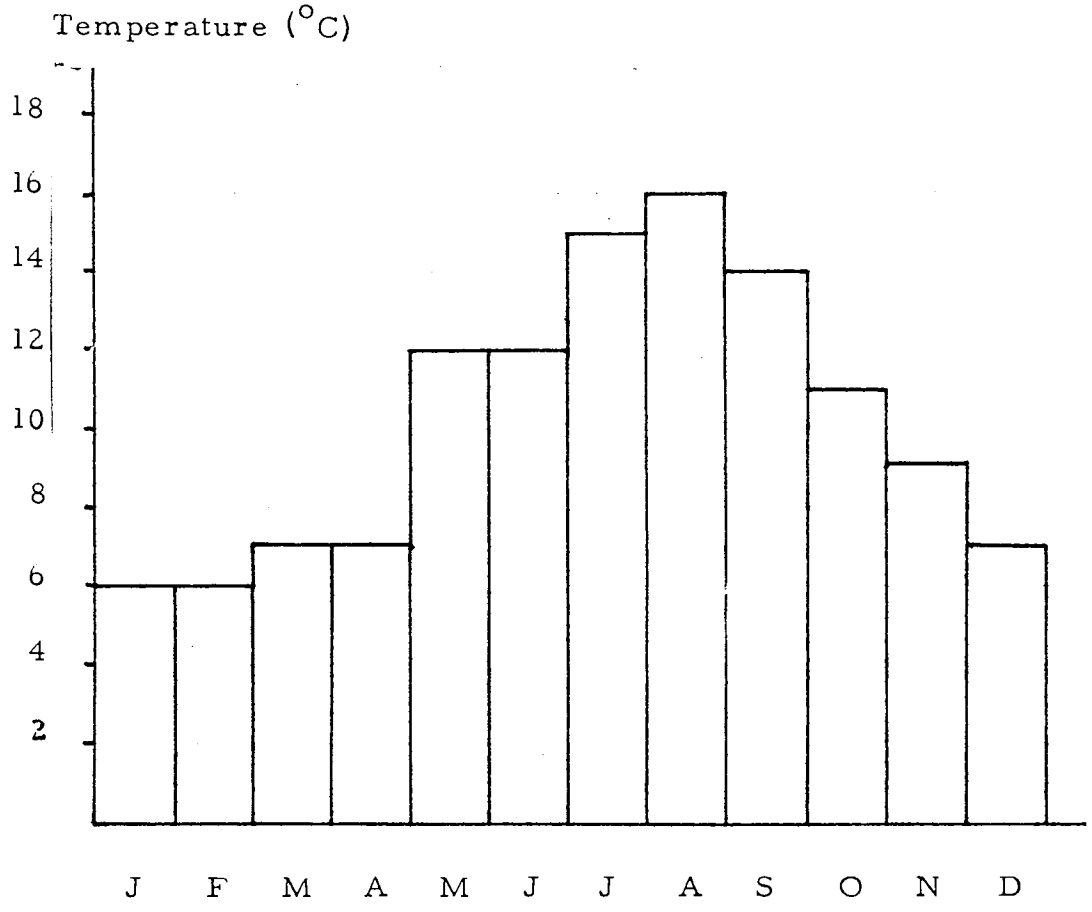

TABLE A4.2 Daily Food Rations

Month		J	F	M	A	M	J	J	A	S	O	N	D
Temp (°C)		6	6	7	7	12	12	15	16	14	11	9	7
		FOOD RATION (kg/day)											
Av. Wt. (g)	15	22	22	24	24	34	34	43	46	40	32	18	24
	50	29	29	31	31	44	44	54	58	51	41	35	31
	130	25	25	28	28	44	44	54	58	49	40	35	28
	220	31	31	33	33	51	51	66	72	60	49	39	33

TABLE A4.3 Daily Oxygen Consumption

Month		J	F	M	A	M	J	J	A	S	O	N	D
Temp (°C)		6	6	7	7	12	12	15	16	14	11	9	7
		OXYGEN CONSUMPTION (kg/day)											
Av. Wt. (g)	15	8.8	8.8	9.6	9.6	13.6	13.6	17.9	18.4	16.0	12.8	11.2	9.6
	50	11.6	11.6	12.4	12.4	17.6	17.6	21.6	23.2	20.4	16.4	14.0	12.4
	130	10.0	10.0	11.2	11.2	17.6	17.6	21.6	23.2	19.6	16.0	14.0	11.2
	220	12.4	12.4	13.2	13.2	20.4	20.4	26.4	28.8	24.0	19.6	15.6	13.2

Fig. A4.2 Jet Oxygenator Performance Data

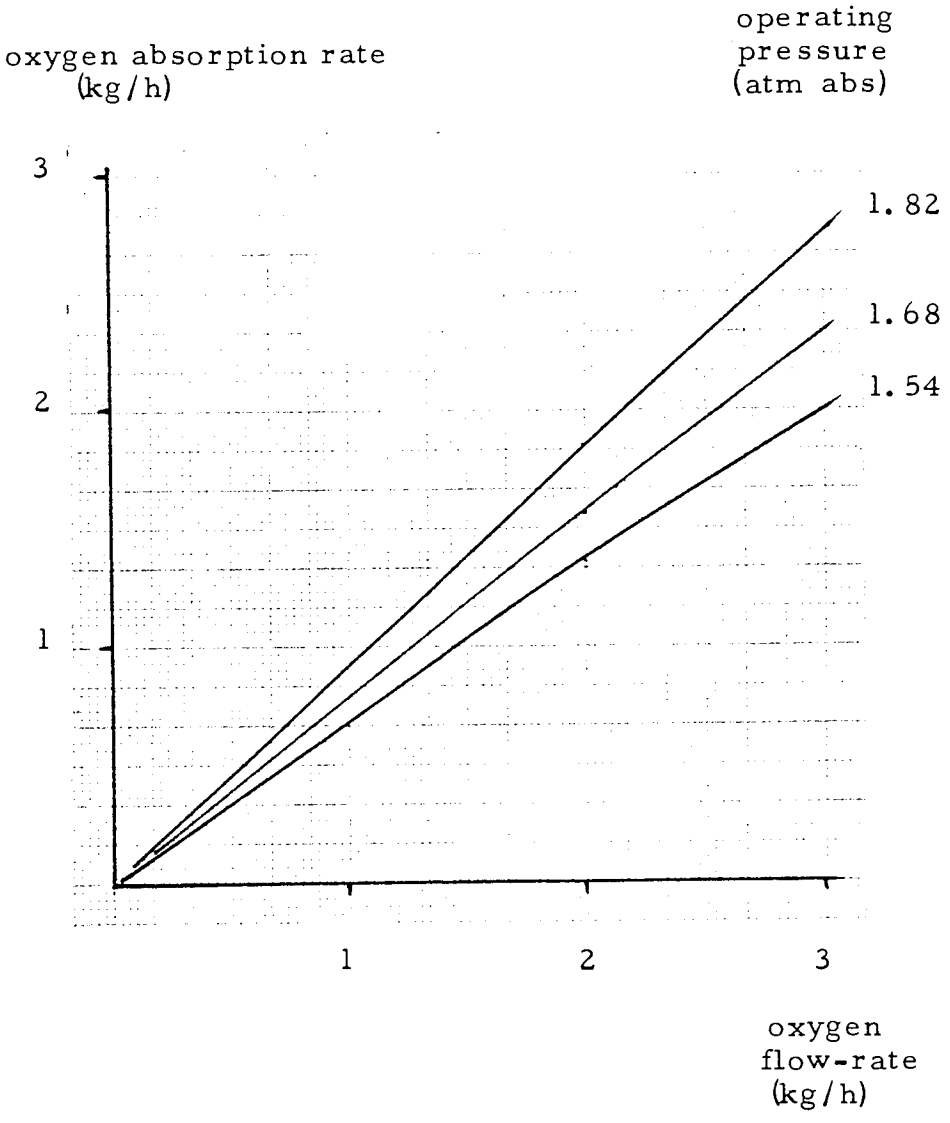

Total Food Consumed = 437 tonnes p. a.

Assuming 1.7:1 conversion rate

Total production = 257 tonnes p. a.

Oxygen consumption by fish = 175 tonnes p. a.

Total annual oxygen use is given in Table A4.4

TABLE A4.4 Oxygen Use at the Finnarts Bay Site

Oxygenator		Total Oxygen Use (tonnes p. a.)
Pressure (atm)	Diss. Efficiency (%)	
1.54	68	257
1.68	78	224
1.82	92	190